Colorado State University
Department of Soil and Crop Sciences,
Colorado State University,
Fort Collins,
Colorado 80523-1170
USA

3rd January 2019

Cover Letter and Responses to Reviewer Comments to accompany the manuscript:
"Unifying soil organic matter formation and persistence frameworks: the MEMS model"

Authors: Andy Robertson, Keith Paustian, Stephen Ogle, Matthew Wallenstein, Emanuele Lugato, and Francesca Cotrufo

Thank you for your correspondence concerning our manuscript and for giving us the opportunity to resubmit a revised version. All comments from the reviewers have been carefully considered and appropriate responses are made below.

Sincerely,

Andy Robertson

Responses to comments from Thomas Wutzler on "Unifying soil organic matter formation and persistence frameworks: the MEMS model" by Andy D. Robertson *et al.*

Reviewer comments in bold and our responses in normal text. Selected new text in the revised manuscript is pasted here in italics. Reference to the manuscript is given as new line number (L).

General comments

The study of Robertson *et al*. presents a first version of the MEMS model, a parsimonious dynamical model of soil organic carbon (SOC) development at ecosystem scale, together with a validation across many sites. I enjoyed reading the manuscript, which is well structured and succeeds in getting the fundamental ideas across in a concise way and provides the details in the appendix.

The proposed model is of similar complexity as classical pool-based models but better incorporates recent mechanistic understanding and is better comparable to measurable pools. Hence, it is of great interest to soil science, ecosystem research, and potentially also global change communities. It adds a complementary alternative in the suite of simple to much more detailed SOC models and the study should be published after revisions.

Many thanks for your comments and time spent reviewing our manuscript. We appreciate the detail and clarity of your suggested revisions – this certainly helps us to improve our manuscript. We are glad you enjoyed reading it and are excited to have an opportunity to publish the MEMS model. It is our hope that it can do just as you say and add to the suite of SOC models already available and stimulate discussion of how to advance this field.

Through the revisions described in detail below we hope to have addressed all your comments.

I liked the approach of directly modeling relevant quantities at the scale model purpose, the management scale. I liked the simulation time dependent sensitivity analysis, although Fig. 2 is hard to read.

I suspect part of the difficulty in reading the figure is because the submission guidelines are to embed the picture as a low-quality jpg. The original vectorized PDF is much clearer. However, we have also now hopefully made the figure easier to read by increasing the size of the text and limiting the colours to only the 4 most influential parameters. All other parameters are coloured in greyscale in order from top to bottom. The 'full colour' figure version is included as a supplementary figure and attached as a lossless vector PDF for detailed inspection if the reader wishes. For your reference we show the new figure below and have also attached the vectorized full-colour PDF version to this response (now Figure S5).

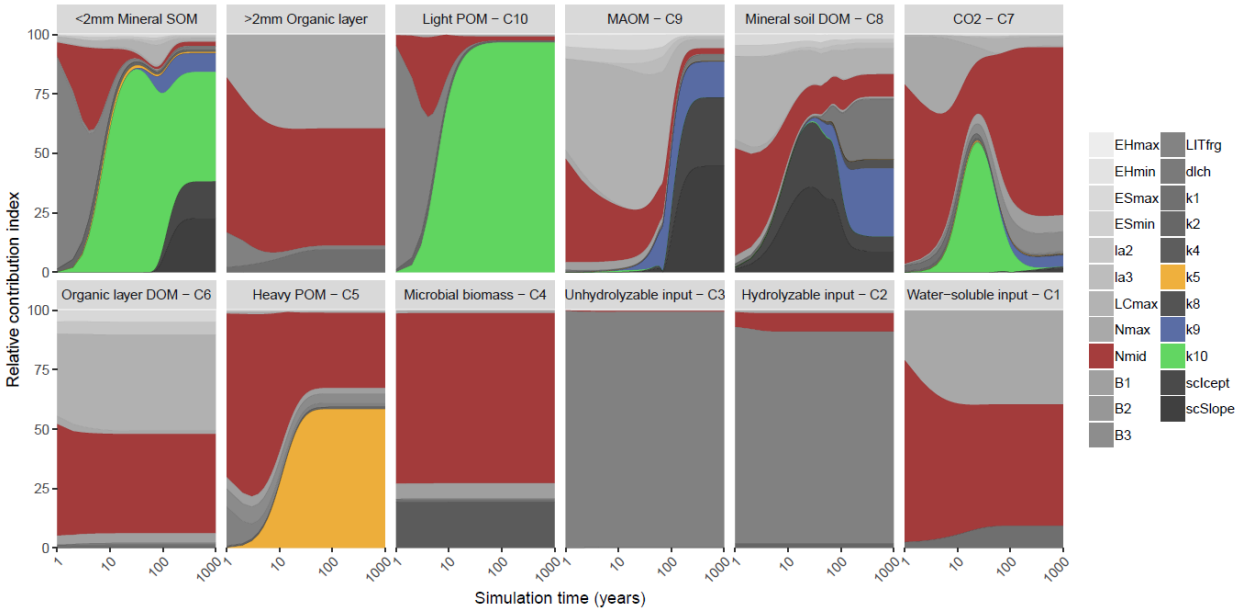

The supplementary is complicated by already anticipating several mineral soil layers and sometimes is inconsistent with the main text. For example, there is explicit microbial assimilation in mineral layers in the supplementary, but the main text states that microbes are implicit there. Please, provide a version that matches the main text and the presented model structure.

We apologise for this confusion – the microbial assimilation, as a process, is indeed 'explicit' in that it is represented by fluxes into a microbial pool. However, in this inaugural version of the model the use of a microbial pool is more one to help differentiate the direct *versus* microbially-processed flux of organic matter inputs (pools C1-C3) to the soil C pools, *sensu* Liang *et al*., 2017. Once these inputs are added to the soil pools belowground, then the microbial biomass and associated metabolic processes are implicit (i.e., we assume there is microbial activity and mineralization of the carbon within these soil pools, but we do not represent these processes with discrete pools or fluxes). We certainly appreciate the comment because on review this is an important point that needed to be made clearer. At different points in the main manuscript, we have added additional points as to why we have a distinct microbial pool at the point of entry of the C input, but not after it is processed and transformed into the SOC pools, which have microbes within them.

A large part of the confusion likely resulted from the 'microbial assimilation from litter' section of the supplementary and we can indeed understand why. The use of the layer superscript certainly made our descriptions less clear. Consequently, we have also removed the superscript notations for soil layers that created unnecessary confusion in the supplementary model description. There should now be no inconsistency between the main text and the supplementary materials.

Liang, C., *et al*. (2017). "The importance of anabolism in microbial control over soil carbon storage." *Nature Microbiology* 2: 17105.

L197-217:
Many of the biogeochemical processes represented by MEMS v1.0 are assumed to be microbially mediated (and therefore result in exo-enzyme breakdown and CO_2 production), but only two lead to C assimilation into a distinct microbial biomass pool – from the water-soluble and acid-soluble litter pools (C1 and C2, respectively). In the mineral soil (i.e., pools C5, C8, C9 and C10), microbial anabolism and catabolism are implicit and considered part of the turnover of each pool. This ensures parsimony and allows model parameters to represent the differences in microbial community for each pool, as opposed to the alternative of explicit microbial pools. The C transferred from the C1 and C2 litter pools into microbial biomass is defined by a dynamic CUE parameter controlled by the N content of the input material and the lignocellulose index (LCI; defined as the ratio between acid-insoluble to the sum of acid-soluble + acid-insoluble) of the litter layer (i.e., lower CUE results when a

higher proportion of the litter is acid-insoluble). Including microbially-explicit processes in the litter layer helps to determine the proportion of C inputs that result in MAOM vs POM formation (see Liang et al., 2017) and allows for future model versions to account for distinctions between different points of entry for inputs (Sokol et al., 2018). The lack of C transferred from other pools (e.g., C3) into microbial biomass implies their decay from co-metabolism with the more labile C sources (i.e., Klotzbucher et al., 2011; Moorhead et al., 2013). Once assimilated within microbial biomass, the anabolism of microbial activity results in generation of microbial products (i.e., necromass) that form tightly bound aggregates of biofilms and small litter fragments around sand-sized soil particles (Huang et al., 2006; Buks and Kaupenjohann, 2016), and dissolved organic matter (DOM). These contribute to the heavy POM (C5) and litter DOM (C6) pools, respectively. While these specific processes are well supported by relevant literature, to retain parsimony and the generalizable structure required by an ecosystem scale model MEMS v1.0 represents microbial metabolism processes more generally (i.e., by linking them to a dynamic microbial CUE rather than specific community traits).

The wording of "litter layer" and "mineral soil" are used in a fuzzy way. Also it did not became clear to me, how model-data comparison dealt with organic layers, which are neither part of the litter (in the model lacking particulate organic matter (POM) pools) nor the mineral soil (in the model simulating sorption to minerals). Maybe this partly causes the large model-data discrepancies for broadleaved sites with large POM stocks.

Thank you for raising this. Our categorization of the aboveground and belowground pools as litter layer and mineral soil, respectively, appear to have led to some confusion. We have changed the terminology throughout the manuscript to make clear that all belowground pools (all POM, pools C5 and C10; MAOM, pool C9 and soil DOC, pool C8) are operationally defined as < 2mm in size and sum to what we refer to as *total soil* (i.e., ***not*** that 'mineral soil' only refers to MAOM and that we are using the terms to differentiate between mineral and organic soil layers).

It is our intention that the sum of the C1/2/3 pools equal all the carbon inputs as above and below ground litter. However, we do not have any 'litter layer' measurements to provide us model-data comparisons. In fact, both above- and below-ground litter was removed during the LUCAS soil sampling and post-processing. We agree with you that the current model does not have the ability to simulate a specific organic horizon, and this is why we removed all organic soils (> 12% OC) from our analysis. Initially, simulating organic soil layers was not our initial priority but now after seeing the current model's results it has become a priority for our next steps in development. As a result, we are working to fractionate several soils with high OC content, so we can help parameterize a new model version that has a finer resolution of soil layers to depth. We are also adding an explicit hydrological submodel that will help to improve the model's capability to vary decomposition processes in different environmental conditions. Both should help reduce some of the large model-data discrepancies from this first version.

It is our belief that the model structure should not need to change to better represent an organic horizon (which will be dominated by litter and POM pools), but rather parameter values may differ to help represent how decomposer communities differ with depth/access to fresh inputs. Additionally, we are aware that if future model versions are to represent an organic horizon we would need to implement a mechanism that reduces sorption to mineral surfaces accordingly to account for large POM accrual (for example in anaerobic conditions). This will be a key feature when we look to test the model in peaty soils where the 'mineral layer' is moved further from the surface while POM (and associated organic layer) accumulates.

Detailed comments for model structure:

Could you, please, elaborate a bit more why you (as well as the LIDEL model) choose microbes to not consume DOM?

This fundamentally comes down to the way we are 'feeding' the microbial pool (in both models). Our assumption is that the microbes consume fresh inputs from the water- and acid- soluble, coarse organic

matter (pools C1/C2) and the aboveground DOM (pool C6) that exists is, in fact, what is left over and available to move to the soil. We decided to use this formulation to enable the C6 pool to be measurable as, for example, using the approach described in Soong *et al*., 2015. Belowground, microbes are assumed to be consuming soil DOM (pool C8) but those processes are implicit to the mineralization equations of those pools, and not related to the microbial assimilation pathways aboveground.

To help clarify this in the manuscript we have revised our descriptions and justification of why we have a microbial pool in MEMS – the primary purpose (at least in this initial model version) is to clearly differentiate between an "ex-vivo" more physical path to SOM formation and an in-vivo microbial processing one (*sensu* Cotrufo *et al*., 2015 and Liang *et al*., 2017). This formulation will be very helpful when trying to match real-world observations of the stoichiometry of different fractions with their corresponding pools in the model.

Cotrufo, M. F., *et al*. (2015). "Soil organic matter formation from biochemical and physical pathways of litter mass loss." *Nature Geosciences*.
Liang, C., *et al*. (2017). "The importance of anabolism in microbial control over soil carbon storage." *Nature Microbiology* **2**: 17105.

See quoted text shown above lines around 201 in the main manuscript and L163-174 in the supplementary:
Where $_jCx_{in}^{cy}$ *refers to DOM leaching from pool y to pool x on day j. The parameters used are detailed in Table 2 in the main manuscript, and/or defined in previous equation in this section. Note that pool C6 is not the DOM consumed by microbial biomass but rather the amount leftover after microbial activity. In this initial model version, the litter layer only refers to the aboveground component, but the same structure can equally apply to belowground C inputs such as root death. However, measurably, the DOM in the C6 pool is directly equivalent to the belowground soil DOM (C8). In MEMS v1.0, DOM enters the soil through the C6 pool only. When explicit inputs from belowground litter (e.g., roots) are simulated in future versions Eqs.* ***28-31*** *can apply for each soil layer adding the DOM that is in excess of microbial activity directly to pool C8 instead of the 'C6' shown in the equations above.*

In the LIDEL model there is a C5 microbial products pool also in the litter layer, why do you assume in MEMS that all microbial turnover is transferred to the mineral soil?

The LIDEL model doesn't represent soil, thus there was the need for a microbial product pool in it. The main reason why the C5 pool in MEMS v1 is a SOC pool is because there is little added value (or sense) and the downside of increased complexity if we were to include a specific microbial products pool in soil – heavy SOC pools are made mostly of microbial products. Furthermore, microbial turnover in SOC pools is implicit and thus the microbial products generated by these processes is captured only by the mineralization of each of these pools.

You choose decomposition to be independent of the size of biomass pool to avoid some problematic feedback. Then I suggest to simplify the model even more by replacing microbial biomass turnover by the sum of inputs to the biomass pool. Then you do not need to simulate this pool, save one state variable and several model parameters. If microbial biomass is required for data comparison, you can still compute it assuming near steady state with inputs (e.g. Wutzler 2013).

We discussed at length the possibilities of removing the microbial biomass pool and came to the conclusion that it is required to help us differentiate SOM formation pathways (as mentioned above) and in future versions the "point of entry" *sensu* Sokol *et al*. 2018. We acknowledge that your suggestion would likely work for this simple first version of the MEMS model, but in the next stages of model development the fresh organic matter inputs will come from above- and below-ground sources and we will need to be able to differentiate between different rhizosphere inputs, different root types and the aboveground litter. From this, it is our intention to be able to vary parameter values associated with the microbial pool of each point of entry (e.g., aboveground, topsoil, subsoil) so as to represent variability in microbial traits. We also require an explicit microbial pool for the next stages in model

development regarding N-immobilization. Since our submission of the manuscript, the Sokol *et al*., 2018 paper was published and discusses some of the details around our assumptions regarding the split between plant- and microbe-derived SOM, and the importance of getting this right.

Sokol, N. W., Sanderman, J., & Bradford, M. A. (2018). Pathways of mineral-associated soil organic matter formation: Integrating the role of plant carbon source, chemistry, and point of entry. *Global change biology*.

Detailed comments for model-data integration:

It should be clarified better also in the discussion, that the model performance was judged by comparing steady state MAOM pools to observations. I am still looking forward to a comparison where a model successfully simulated dynamics compared to observed changes decadal stock changes across many sites.

We agree – we're excited to test the model's ability to replicate 'short-term' changes in soil organic matter dynamics. We have now made it clear that model-data comparisons are against steady-state systems.

L376: averaging parameters is dangerous, because of nonlinearities. I suggest to use only one non-averaged parameter combination. You may pick the fold randomly.

We have made this change and chosen parameter values from a single fold (values were only very slightly different from the averages – see Table S2).

L417-425
To determine the optimized parameter values, a single fold was chosen at random from those that reported the lowest RMSE for each subset of training sites (i.e., each fold). Optimized values differ depending on which measured fraction is compared to model predictions (whether comparing pool C9 to measured MAOM-C, the sum of pools C5 and C10 to measured total POM-C, or the sum of pools C5, C8, C9 and C10 to measured bulk SOC). The new, optimized parameter values (Table S2) were derived from a randomly chosen fold that minimized RMSE when compared to the MAOM fraction.

L376: You can avoid the choice of one criterion among three data streams of MAOM-C, POM-C and bulk SOC by using a cost function based on the sum of squared residuals of all the data streams.

This is a good point. Thanks for the suggestion which we will apply for the next stage of calibration. For this initial parameter estimation, we performed the full optimization procedure on all data streams. While parameter values did vary, the results and general fit was similar regardless of which criterion we chose. Consequently, we do not feel that this change would make considerable difference to the results we are presenting and hope you will agree it would not be worth redoing the entire analysis for this change. An additional factor to consider is that our ongoing development of the MEMS model is already revising some of the parameters (many are being adjusted to accommodate nitrogen effects on carbon transfers) and therefore the values themselves may have little application beyond this initial version.

We do agree with your suggestion though and have added this to the discussion.

L422-428
The new, optimized parameter values (Table S2) were derived from a randomly chosen fold that minimized RMSE when compared to the MAOM fraction. This was chosen (instead of those optimized for POM or bulk SOC) since the MAOM fraction is typically the largest single soil C pool and using this approach led to the biggest overall decrease in RMSE when compared to all available data (Table S2). In future analyses, a more rigorous approach

may be to apply a cost function regarding all available measured pool data (e.g., including litter pool data when it is also measured) but for our initial model evaluation we random choice is deemed sufficient

Fig 5: The classification to land use not particularly helpful, because variables are very similar with a high range across these classes, including the mentioned significant different of MAOM:POM (L 485). Furthermore, plotting the distribution of observations and distribution of predictions separately does not help to judge model performance (L488).
I suggest instead inspecting and plotting the distribution of model-data residuals of several variables and relating these differences to classes and other environmental conditions. This would indicate which variables and processes are most urgent to extend MEMS v1, as done with the discussing Fig 7.

We understand your point and have in fact plotted these all residuals against the full range of environmental conditions. Unfortunately, these tend to make the results seem worse than they are because the dense number of points near to the 0-residual line cannot be shown well. However, to address your concern we have added a residual plot to the supplementary to illustrate individual residual points (new Figure S6). This figure does make an important point, but it is hard to determine clear recommendations of where to focus next developments purely from these figures.

Below we attach an overall summary of individual residuals against mean annual temperature of the sites and in the supplementary we show a similar figure but split by different environmental divisions (new Figure S6).

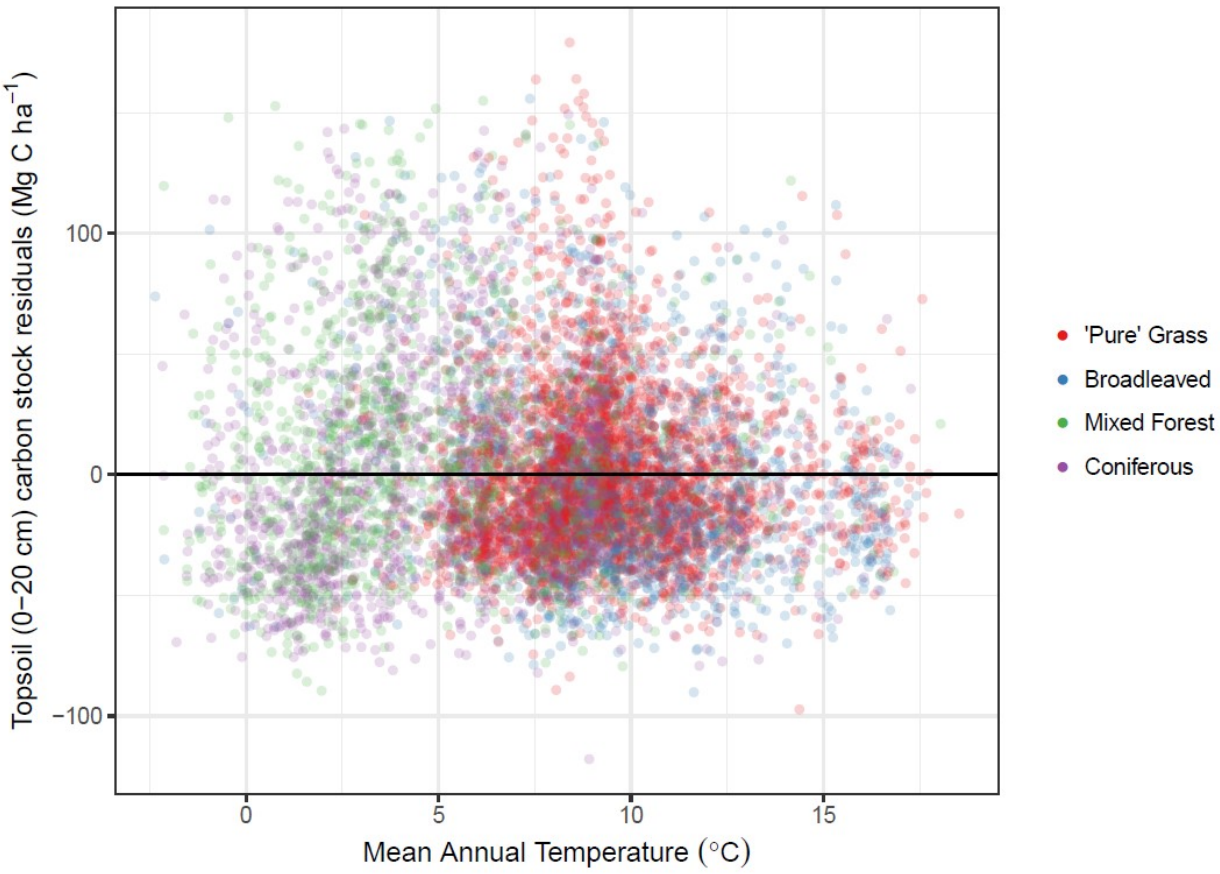

Other detailed comments main text:

Text in Figs 2 and 6 are hard to read. Can you provide a vector graphics of this figure? There are too many classes to distinguish by color, but I have no suggestion how to improve.

We did provide vector graphics versions with the manuscript but unfortunately as part of the peer review process they do not include them and instead choose to embed them in the file. We have tried to address this as described above. The full colour version of figure 2 is in the supplementary and we have replaced the main text figure with a one that is easier to interpret, as described above. We have also increased the font size and changed the resolution slightly of figure 6 to make it clearer. This is also obviously much clearer when viewed on the vectorized file. Also attached separately.

Fig 4: Suddenly, pH is popping up, but was never introduced as a driving variable. I suggest to shortly state that sorption rate is pH dependent, and refer to the eq. 35 in the Appendix.

We have now made this change.

See L266:
This parameter can be very difficult to generalise without requiring exhaustive information on soil physiochemical conditions (e.g., clay type, Fe/Al concentration, etc.), but the work of Mayes et al. (2012) presented an empirical relationship between K_lm and native soil pH, with pH acting as a proxy for mineralogical conditions. As a result, sorption rates to mineral surfaces are dependent on pH (see Equation 35 in supplementary). This relationship (derived from isotherms calculated for 138 soils of varying taxonomies) provides a good starting point for estimating K_lm and is also used by the MILLENNIAL model (Abramoff et al., 2017).

L 529: These are interesting effect of N in a C-only based model. While the microbially detailed models of Perveen 2014 and Wutzler 2017 attribute low litter N effects to N mining in older usually N-rich pool and accumulation of less processed material, MEMS attributes this to reduced microbial accessibility and reduced DOM production. Do you think that chemical and stoichiometric effects are two sides of the same coin, or are these competing hypotheses? I am looking forward to the version that explicitly simulates N fluxes.

Thanks, we are excited to be working on simulating N fluxes, which indeed are complex depending on the microbial N demand (stoichiometry), as well as on the energetic (chemistry) and accessibility (physics) of soil organic C pools. Rather than competing, in our opinion these are all simultaneously at play. We follow the LIDEL model (Campbell *et al*., 2016), according to which both N limitation and C chemistry (i.e., Lignocellulose index) drive microbial decomposition and DOM production, with the most limiting factor being the actual driver of the process. We find the recent model of N input effects on SOC dynamics proposed by Averill and Waring (2018) to be particularly effective at capturing this complexity and may follow their logic in our new model version which will include N.

Averill, C. and B. Waring (2018). "Nitrogen limitation of decomposition and decay: How can it occur?" *Global Change Biology* **24**(4): 1417-1427.
Campbell, E. E., *et al*. (2016). "Tracking the fate of litter carbon using the LItter DEcomposition and Leaching (LIDEL) model." *Soil Biology and Biochemistry* **100**: 160-174

Other detailed comments appendix:

To me its difficult to always keep a list of meaning of pool 1 to 10 in my head. Could you come up with more expressive pool names?

We are aware of this issue. The initial development of this first MEMS v1 model was intended to be an advancement from the LIDEL model and therefore we kept the same names to ease reference to that

model. However, we now know that this approach won't be effective as the model grows. For our MEMS v2.0 we are making this change.

L 70: I do no find more information on ub and uk in Table 2 in the main text. I suggest referring to eqs. 19-22.

Apologies for this omission. We have made this change.

L80
More information of the parameters uB, uk, B_x, la_x and k_x can be found in Campbell et al. (2016) and in the equations below, but briefly:
$_juB$ and $_juk$ are rate modifiers to represent the litter chemistry controls (LCI and available nitrogen) on microbial use efficiency, on day j

L 110-112: The long sentence did not became clear to me. Is L_j_C5_C4_gen really a combined flux of bioturbation, . . ., and DOC leaching? I thought the latter one is covered by eq. 33.

You are right that this was confusing. The C4 to C5 flux was inherited from the LIDEL model to represent microbial turnover and you are right in saying that DOC generation from this process is represented elsewhere. We have adjusted the text accordingly and hopefully it is now clearer.

L120
Where $_jC5_{gen}^{C4}$ refers to the fraction of carbon that is transferred from C4 to C5 (i.e., microbial products transported belowground when physical and hydrological processes mix between the input layer [aboveground litter only in MEMS v1.0] and soil layer) on day j.

eq 47: k8 does not match the text before that states k5.

We have made this change.

L256
While the maximum decay rates (k_x) for most pools are fixed constants, Campbell et al. (2016) suggested that k_3 is best estimated in relation to the maximum decay rate of the microbially-accessible litter (C2) pool (k_2).

Thanks for this work. I suspect MEMS to be included in further model comparisons as a complementary model.

Thank you for your insightful review. We hope the MEMS model can help to stimulate a discussion that advances SOM modelling in the coming years. It is our intention to participate in model comparisons with MEMS v2.0.

Responses to comments from Anonymous Referee #2 on "Unifying soil organic matter formation and persistence frameworks: the MEMS model" by Andy D. Robertson *et al.*

Reviewer comments in bold and our responses in normal text. Selected new text in the revised manuscript is pasted here in italics. Reference to the manuscript is given as line number (L).

Overall review

The authors present a new soil biogeochemistry model, MEMS v1.0, that explicitly represents biochemical complexity of litter pools, microbial biomass, mineral associated organic matter and particulate organic matter. The model has the capability of including variable CUE in litter decomposition and mechanisms leading to SOM stabilization and saturation of mineral associated carbon fraction. Four key model parameters are calibrated to reproduce soil fractionation observations of mineral associated and particulate organic matter fractions and the model is evaluated in reproducing topsoil SOC in more than 8000 sites across different land-uses in Europe with satisfactorily results.

Constructing models that are based on measurable carbon pools rather than on the old framework assigning turnover rates to a given number of unmeasurable carbon pools is a very important endeavor and the authors are definitely moving beyond conventional SOC modeling. It is especially important to have models that link litter decomposition processes and SOM formation processes, which is rarely the case, as stated by the authors (L 89-91). I am very much in favor of such a type of approach and supportive of the author's effort. The manuscript is very well written and clearly presented and the introduction frames very well the problem.

I would be happy to have a few clarifications on some technical aspects and about one important assumption related to the role of the microbial pool. These are written in a number of minor comments that hopefully can be addressed.

Many thanks for your constructive comments and praise. We have responded to each of your comments in detail below and hope to have satisfactorily addressed any concerns or queries you may have had. Regarding your points about the microbial pool please see our detailed response on those comments below. It is our hope that this publication and the resulting MEMS model can help to both stimulate a fruitful discussion and advance the practice of SOC modelling.

I would also invite the authors to tone down the role of MEMS v1.0 as "ecosystem model", since the current version is still far from being there. As a matter of fact, in several instances (e.g., Line 606) the authors state that the model is incomplete (e.g., lack of hydrological and nutrient cycle) and that these deficiencies will be addressed in future model developments. The model represents SOM dynamics at the "ecosystem scale". However, for various reasons but especially because the temporal dynamics are not evaluated in this article, I would invite to use cautious statements in the link with ecosystem models. Only the steady-state conditions are tested. A correct representation of temporal dynamics is key for coupling with other models. At this stage, this is a quite significant limitation for application in ecosystem models. Furthermore, feedbacks between soil and vegetation cannot be considered.

Thank you for your point. We are fully aware of the limitations of this first version of our model and readily acknowledge that it is not an ecosystem model yet. It was never our intention to 'oversell' the model's capability but to rather highlight the possibilities for integration with other ecosystem model components (e.g., plant growth, hydrology, etc.) given the more realistic model structure. You are certainly correct that being able to simulate non-steady-state dynamics will be the true test of our model and to date it is more of a working proof of concept model than one to directly compare with conventional SOM models.

Throughout the revised manuscript we have tried to play down links or comparisons with true ecosystem models. However, we do maintain that the model is designed to operate the ecosystem *scale*. We have also added a few points to highlight the limitations of our steady-state comparative approach.

L318-320
These driving variables are external inputs of the initial model version but may be obtained from coupled climate and plant growth submodels in future versions, when incorporated into a full ecosystem model.

L575-582
MEMS v1.0 was designed to consolidate recent advances in our understanding of SOM formation and persistence into a parsimonious mathematical model that uses a generalizable structure which, after further development, can be implemented in Ecosystem and Earth System model applications

L665-667
In its current capacity, MEMS v1.0 is far from being able to simulate full ecosystems and is limited in scope regarding the land use scenarios it can simulate accurately.

Other simplifications are that NPP is prescribed from MODIS, the model does not account for temporal dynamics of soil moisture or for nutrient cycles, the root:shoot ratio is prescribed for various biomes. However, these are overall clearly described. I would also appreciate some additional discussion about the issue in comparing pools, which are spun up at the equilibrium with observed pools (Line 366-367). The authors are aware of the issue and they briefly discussed it. However, most of the description of the results and the calibration effort convey somehow the intention to match C-pools as closely as possible. Given the expected difference between actual SOC and "steady- state" SOC, I would have allowed more freedom to the model and focus on comparing patterns as in Fig. 5 and 6 rather than absolute quantities.

The focus of comparing patterns rather than absolutes was indeed our initial end goal, however after we ran the model and saw relatively good agreement with absolutes as well we felt it important to report these results. We agree that there are many reasons why our simulated SOC stocks would not match those measured but our choice to only look at grasslands and forests was a way to examine those sites that may be in, or close to, equilibrium. Your point is a good one though and we have tried to adjust some of our language in the discussion to focus more on comparisons with general patterns than on exact numbers. Several qualifying statements have been included when we do compare with absolutes.

L452-454
In addition to comparing measured values with those predicted at steady-state (which may not be an accurate assumption for many sites), a more general comparison was performed to examine groups of sites under similar site conditions.

L565-569
While the model's performance comparing absolute C stocks appears good, this is done with the assumption that these topsoil C stocks at forest and grassland sites in our analysis are at steady-state. This is unlikely to be true and therefore it is encouraging when general trends are as expected (as is the case for many of the land uses and for many of the different environmental divisions; Figure 6).

L606-608
There are also limitations of our approach given that very few of the sites will likely be under true steady-state conditions, leading to further discrepancies between model predictions and measured values.

Despite these limitations, the manuscript is undoubtedly a novel contribution to the field and surely a step in the right direction.

Many thanks for your comments and time spent reviewing our manuscript. We certainly appreciate the opportunity to add the MEMS model to those currently driving progress in the field of SOM modelling.

Minor comments

Line 75. It is cited later on, however, Wieder et al 2015 would fit well also here.

We have now added this.

L80-82
Consequently, there have been several calls to represent this new understanding and re-examine how microbial activity is simulated in SOM models (Schmidt et al., 2011; Moorhead et al., 2014; Campbell and Paustian, 2015; Wieder et al., 2015).

Line 96. Maybe one sentence with additional explanations for K vs r strategies (e.g., copiotrophic and oligotrophic microbial functional groups) is necessary, not all the "modelers" may be aware of these concepts.

Thank you for the suggestion – we have now added this extra detail.

L103
A recent paradigm has emerged that emphasizes the role of microbial life strategies (e.g., K vs r, referring to copiotrophic and oligotrophic microbial functional groups) and carbon use efficiency (CUE) in the formation of SOM from plant inputs (Dorodnikov et al., 2009; Cotrufo et al., 2013; Lehmann and Kleber, 2015; Kallenbach et al., 2016).

Line 113-114. The issue related to the lack of inputs or information to derive model parameters and validate model responses, of course, is a very important one and may compromise practicality as written by the authors. However, modeling efforts in the direction of more mechanistic representations of the soil system can shed light on the importance of processes and interactions that were not accounted or quantified before, they may provide guesses for the magnitude of certain pools/fluxes and may motivate the collection of those data that are necessary to test mechanistic predictions. In other words, they can have a value in process explanation rather than a predictive value.

A good point, well raised. We have added this to the introduction help bolster the points we made. Thank you.

See L60-65:
Structuring a SOM model around these known and quantifiable biogeochemical pools and processes has the potential to drastically reduce uncertainty by enhancing opportunities for parameterization and validation of models with empirical data. Furthermore, mechanistic models can have value in process explanation as well their value in predictive capabilities; such models can pinpoint the processes that have the greatest influence on a system even when they are not traditionally determined empirically.

Line 174-178. In a certain way, also the CENTURY model, especially in more updated versions (e.g., Kirschbaum and Paul, 2002) accounts for nitrogen and lignin content of the litter, which are affecting the turnover rates of the various litter pools. Additionally, their subdivision in metabolic and structural litter pools is not far from the subdivision in the pools C1, C2, C3. This may be

acknowledged in the manuscript or if major differences, which I cannot recognize, do exist, they need to be remarked.

We feel that the MEMS interpretation of these divisions is different to those in CENTURY, but we do acknowledge the similarities. However, these alterations may not qualify as 'major differences' but rather different formulations of the same general ideas. For example, at this early stage the litter chemistry and N content of the inputs are fixed and therefore similar to the lignin:N effects in CENTURY, however when we include a discrete N submodel, N-availability will be dynamic and influence those processes differently through time.

With this first description of MEMS we do not mean to suggest that it is better or worse to any of the more conventional models (including CENTURY) but rather that it presents another way of addressing the same questions about SOM dynamics. In some respects, MEMS is very similar to other models, and in other respects it is quite different. A full model-vs-model comparison was obviously beyond the scope of this manuscript. Therefore, to avoid direct comparisons between the conventional SOM models and MEMS, we deliberately did not discuss specifics about how they differ. To hopefully address this comment, we have added a single sentence to help clarify our position.

See L186-188
This structure is similar to the LIDEL model (Campbell et al., 2016) and follows the hypotheses that both N availability and lignin content influence decomposition by affecting microbial activity (Aber et al., 1990; Manzoni et al., 2008; Sinsabaugh et al., 2013; Moorhead et al., 2013). Similar approaches have also been used in many of the updated traditional SOM models (e.g., lignin:N ratios in CENTURY; Kirschbaum and Paul, 2002).

Line 189-190. The assumption of considering a microbial pool (C4) for the litter component is probably the decision in terms of model construction, which leaves me more bewildered. This pool, presumably, is mostly located aboveground, even though is not stated explicitly, and does not have an explicit role in the turnover of soil organic matter. Now, if anything, I would have make the reverse choice. Because of accessibility constraints and relatively paucity of microbial biomass in the soil, the decomposition of SOM is likely controlled explicitly by microbial biomass, while the decomposition of litter, which is mostly located aboveground (especially for land covers different from grassland) and air exposed is unlikely limited by microbial biomass. Maybe, my understanding of the system is wrong, but it would be useful to have a clarification of the rationale of such an assumption and eventually of the potential consequences.

Your understanding of the systems is perfectly correct. However, our decision to explicitly represent microbes in the litter layer of MEMS v1.0 was based on their importance informing the relevant SOM formation pathways (i.e., direct *vs* microbially-processed), not their impacts on decomposition. Consequently, this is also why we deliberately did not limit the discussion of a microbial pool to aboveground litter only – our structure implies that there must be a microbial pool at each point of carbon input (e.g., the litter layer, rhizosphere, etc.) so that the model can account for the carbon inputs that are microbially processed, and the amount of DOM that results.

We have added some extra information in the main manuscript (excerpts below) but also wanted to include a little more detail here to help clarify our rationale of why we have a microbial pool. At potential different "points of entry", carbon inputs contribute to MAOM or POM formation in differential amounts depending on the microbial community (as per Sokol *et al*. 2018). This is represented by the MEMS model structure by having an explicit microbial pool when organic matter enters the system but not after it; belowground, microbial biomass and associated metabolic processes are implicit (i.e., we assume there is microbial activity and mineralization of the carbon within these soil pools but we do not represent these processes with discrete pools or fluxes).

Sokol, N. W., Sanderman, J., & Bradford, M. A. (2018). Pathways of mineral-associated soil organic matter formation: Integrating the role of plant carbon source, chemistry, and point of entry. *Global change biology*.

L201-205:
Many of the biogeochemical processes represented by MEMS v1.0 are assumed to be microbially mediated (and therefore result in exo-enzyme breakdown and CO2 production), but only two lead to C assimilation into a distinct microbial biomass pool – from the water-soluble and acid-soluble litter pools (C1 and C2, respectively). In the mineral soil (i.e., pools C5, C8, C9 and C10), microbial anabolism and catabolism are implicit and considered part of the turnover of each pool. This ensures parsimony and allows model parameters to represent the differences in microbial community for each pool, as opposed to the alternative of explicit microbial pools. The C transferred from the C1 and C2 litter pools into microbial biomass is defined by a dynamic CUE parameter controlled by the N content of the input material and the lignocellulose index (LCI; defined as the ratio between acid-insoluble to the sum of acid-soluble + acid-insoluble) of the litter layer (i.e., lower CUE results when a higher proportion of the litter is acid-insoluble). Including microbially-explicit processes in the litter layer helps to determine the proportion of C inputs that result in MAOM vs POM formation (see Liang et al., 2017) and allows for future model versions to account for distinctions between different points of entry for inputs (Sokol et al., 2018). The lack of C transferred from other pools (e.g., C3) into microbial biomass implies their decay from co-metabolism with the more labile C sources (i.e., Klotzbucher et al., 2011; Moorhead et al., 2013). Once assimilated within microbial biomass, the anabolism of microbial activity results in generation of microbial products (i.e., necromass) that form tightly bound aggregates of biofilms and small litter fragments around sand-sized soil particles (Huang et al., 2006; Buks and Kaupenjohann, 2016), and dissolved organic matter (DOM). These contribute to the heavy POM (C5) and litter DOM (C6) pools, respectively. While these processes are well supported by relevant literature, to retain parsimony MEMS v1.0 represents microbial metabolism processes implicitly as per their description in LIDEL.

Line 200. Please explain better what do you mean "represents microbial metabolism processes implicitly"

Apologies – the use of 'implicit' in this context was not correct. Hopefully the new sentence is clearer.

L210-217
Once assimilated within microbial biomass, the anabolism of microbial activity results in generation of microbial products (i.e., necromass) that form tightly bound aggregates of biofilms and small litter fragments around sand-sized soil particles (Huang et al., 2006; Buks and Kaupenjohann, 2016), and dissolved organic matter (DOM). These contribute to the heavy POM (C5) and litter DOM (C6) pools, respectively. While these specific processes are well supported by relevant literature, to retain parsimony and the generalizable structure required by an ecosystem scale model MEMS v1.0 represents microbial metabolism processes more generally (i.e., by linking them to a dynamic microbial CUE rather than specific community traits).

Line 268-269. It could also be, simply, that microbial growth is stimulated and there are more microbes that can also degrade faster the chemically recalcitrant substrates. If I understood correctly, this is not an effect that can be captured by the model without an explicitly microbial pool acting on POM (C5, C10) and MAOM (C8) decomposition.

As mentioned above, you are right for traditional SOM models. However, because our soil pools are physically-defined with a level of accessibility specific to that pool, our ultimate approach is to modify the parameters of processes for C-mineralization from each pool as the conditions (e.g., nutrient availability, input chemistry, point of entry) change. This would allow the different microbial community traits to be represented for each of the different pools. However, we acknowledge that this is more of a point for the next stages of model development and does not apply to MEMS v1.0.

Line 270-273. Generally speaking, microbial respiration will be related to microbial activity and CUE. Being not considered microbial activity in the soil, it is not very clear without looking in detail at the Supp. Material how respiration is computed and which fraction of the decomposition is assumed to be. While you refer to CO2 efflux, "respiration" is never mentioned in the Supplementary Material, which is quite surprising.

We have updated the terminology the refer to C-mineralization as the decomposition process which then results in CO2. We have added an extra sentence to the main text that states that microbial activity and the resulting respiration is computed through decomposition estimates after other processes are calculated, and we refer the reader to the supplementary for more detail. Some information in the supplementary has also been made clearer.

L281-285
Thus, the decay rate constants represent total mass loss potential, embodying DOM-C generation as well as CO_2 emissions, as per a recent decomposition conceptualization (Soong et al., 2015). The total amount of heterotrophic respiration is the sum of CO_2 produced from the biotic decay of all model pools after other fluxes (e.g., DOM generation) are calculated (more detail can be seen in the Supplementary).

Line 281. I would also add that pH controls are quite important. The authors are already well aware of this but neglecting soil moisture controls is a quite significant simplification.

We are aware and this is key to further development of the model. We have included the mention of pH here now.

L301-304
Simulating the influence of other important controls on decomposition, such as water, oxygen, pH and nutrients, are beyond the scope of this inaugural version of the MEMS model but are central to future development efforts.

Line 293. At this stage is not clear how NPP values are derived. Maybe, it is worth to state that this must be an external input to the model. This is actually what mostly separate a "soil organic matter model" from an "ecosystem model".

We have now added this extra information.

L312-320
Initializing MEMS v1.0 requires external inputs of basic site characteristics (climatic and edaphic conditions as well as land management information) and ideally measurements of daily C input. However, C inputs are rarely available at daily time scales. Consequently, for this inaugural version of the MEMS model we employ a simple function to interpolate daily C inputs from annual Net Primary Productivity (NPP), partitioning aboveground/belowground and to the simulated soil layer using land-use specific root:shoot ratios and a simple root distribution function (Poeplau, 2016). These driving variables are external inputs of the initial model version but may be obtained from coupled climate and plant growth submodels when incorporated into a full ecosystem model. Details of these approaches are given in the supplementary materials and all required driving variables are shown in Table 3.

Table 3. The text-box with "site-specific values required" applies to all the site condition variables (e.g., from NPP to soil temperature). This is not clear from the current Table where site-specific values seem to refer to "rock fraction of soil layer" only. I would suggest to use some curly bracket to envelope all these variables.

This has now been done to the best of our ability given the formatting requirements of the journal. We will ensure this is done and clear for the final typesetting.

Line 315-319. I am actually quite familiar with the global sensitivity analysis and I think I understood what the authors did. However, I am quite sure that the succinct explanation provided in these lines will remain unclear to most of the readers. I would suggest to either explaining it better (i.e., more extensively) or minimizing the explanation with a full discussion in the supplementary material.

We have now added further detail to our description in the main text. Hopefully this helps to make our methods clearer to all readers.

L325-358
The default parameter values (i.e., those governing C turnover and fluxes between pools) used by MEMS v1.0 are informed by data from relevant literature (Table 2). However, different studies may suggest different values based on discrete site conditions, meaning a priori estimates may not necessarily be generalizable across all sites that the model could simulate. A variance-based global sensitivity analysis was performed to determine each parameter's relative contribution to the change in each state variable (i.e., determining which parameters have the largest influence on the size of each model pool). The sensitivity analysis was repeated for different simulation lengths (1 – 1000 years) as different fluxes operate at different temporal scales, thereby meaning that the relative importance of each parameter changes through time. Initial pool sizes were set to 0 and the model was initialized to simulate a steady-state scenario based on average site conditions (derived from ~8000 forest and grassland sites in the Land-Use/Land Cover Area Frame Survey (LUCAS) dataset ([Toth et al., 2013] – see Table 3). Specifically, this meant starting a model run with no C in the system and gradually building up the litter and soil pools until they reached equilibrium based on driving variables (soil type, C inputs, climate) that remain fixed over time. To evaluate how much each model parameter (e.g., decay rates, DOM generation rates, etc.; see Table 2) effects the amount of C in each pool (i.e., C1-C11; Figure 1) parameter values were changed to be higher or lower from their baseline and pool sizes are tracked over simulation time. Note that all temperature modifier parameters (T_{ref}, T_{opt}, T_{Q10}, T_{lag} and T_{shp}; Table 2) were excluded in this sensitivity analysis as the resulting T_{mod} has the same effect on all decay rates. Maximum and minimum values of all other parameters (n = 24) were defined as 50 % above and below the literature-derived (baseline) value (Table 2). Using Latin Hypercube techniques to sample within the full parameter space, a global sensitivity varying all parameters was used to determine total variance for changes to each model pool (i.e., how much each pool changes in size when all parameters vary up to 50 %). Then, in turn, each individual parameter was fixed at its baseline value while all others varied. This defines each parameter's contribution to a pool's variance, averaged over variations in all other parameters (Sobol, 2001; Saltelli et al., 2008) (i.e., how much each pool changes in size when all parameters, except one, vary up to 50%). When normalized over the global sensitivity variance, a contribution index provides the proportion of variance explained by each parameter. The analysis was run 10,000 times to define the total parameter space and the whole procedure was repeated annually for simulation lengths between 1 to 1000 years. Put simply, 10,000 different combinations of parameter values between the minimums and maximums were used to repeatedly run the model for 1000 years given average site conditions. The results showing changes in pool size correspond to the changes in parameter values (e.g., when maximum decay rate of MAOM is increased, pool C9 may decrease in size but others may increase). The impact that a single parameter has on pool size, compared to that of all parameters, is described by the contribution index, where the total effect of all the parameters is equal to the maximum change in pool size. Note that the results of a global sensitivity analysis of this kind are non-directional and do not indicate whether a parameter increases or decreases a pool size, but rather that it simply changes from the baseline.

Line 340. I know that this is probably the only option the authors had, but I hope they are well aware of the limitations of MODIS NPP product; maybe a sentence forewarning the reader would be necessary.

We are indeed aware of the limitations of using the MODIS NPP estimates. We have also checked a 10-year average of NPP data for each site and noted the variability (and considered redoing the analysis). However, the variability for one site's 10-year average is considerably lower than the variability across Europe and therefore we concluded there was little value in redoing everything, given our limited expectations and reliance on the simulated absolute values.

L380-384
Complimented with geo-referenced estimates of annual NPP from MODIS satellite data (ORNL DAAC, 2009), and daily temperature data from the Climate Prediction Center's Global Temperature (CPC-GT) database (NOAA, 2018), this provided all driving variables required to run MEMS v1.0. The use of modelled/interpolated NPP and climate data is not recommended over measurement data directly collected from the site(s) being simulated, but for the analysis herein these measured data were unavailable.

Line 345. The reference Cotrufo et al 2018 explaining the derivation of the POM and MAOM pools is not published. I guess for the sake of this article is fine, but of course, it would be a great contribution to the community if the values of POM and MAOM for the 154 sites would be provided as a part of the LUCAS database or somewhere as part of the article.

We agree and will make these available as part of this paper submission. The data will available at: http://esdac.jrc.ec.europa.eu/

Line 368-369. This is probably more a philosophical than a practical point. However, I wonder if a rigorous numerical optimization for such type of models, where the model structure is very uncertain and difference between observed and simulated SOC could be related more to the initialization problem rather than to model structure or parameters is really needed. Given the fact that 4 parameters only were optimized and several replicates were made, this is probably an added value and unlikely a problem here, but still I wonder if is not giving too much weight to the data. How do the results look alike without optimization? This is briefly stated in Line 469-470 but it would actually
be interesting to look at it in more detail.

The pre- and post-optimized results did not differ significantly for some environmental divisions (e.g., hot, wet, sandy, grasslands) but did for others. We tend to agree with you that our optimization was a little more than what was needed given the early stage of model development, however we wanted to demonstrate how the parameter estimation approach could apply using real measured data. We performed several analyses to assess model performance before and after optimization, but we feel the manuscript already includes a lot of detail and this extra information would be of little value for the majority of readers.

Line 379. Maybe an explicit statement that optimized parameter values are reported in Table S2 would be useful here.

We did refer to this table here already but have added an extra reference to hopefully make it clearer.

L422-426
The new, optimized parameter values (Table S2) were derived from a randomly chosen fold that minimized RMSE when compared to the MAOM fraction. This was chosen (instead of those optimized for POM or bulk SOC) since the MAOM fraction is typically the largest single soil C pool and using this approach led to the biggest overall decrease in RMSE when compared to all available data (Table S2).

Line 386-387. How seasonal variability in C-inputs and temperature is accounted for? This is not very clear from the manuscript.

The annual temporal dynamics of C-inputs are derived from a simple distribution function for this first version. We assume a normal distribution around mid-summer so that 75% of the C inputs are added between April and August (Northern Hemisphere). This is a very simplistic way of doing things and is the same for all land use types and locations in our analysis. However, we felt this was more realistic than the same amount every single day. Of course, because we are simulating a steady-state system the resulting difference in effect is minimal but in future versions these C inputs will be coupled to a plant growth model which will be much more accurate.

Regarding seasonal temporal dynamics of temperature, we simply use the daily values for each site and therefore we hope the values used are accurate and account for seasonal variability. This is already stated in the main text.

We have added a little information about this to the main text and point the reader to the supplementary for more detail.

L430-432
Driving variables of edaphic conditions and land-use type were extracted for each site from LUCAS and combined with daily estimates of C inputs and temperature (derived from simple interpolations assuming a normal distribution of MODIS annual NPP data [see Supplementary for details] and CPC-GT daily maximum and minimum air temperature data, respectively). Where these data were unavailable, the site was removed from further evaluation.

Line 407. The value for NPP and sand content differ from the mean value provided in Table 3.

Yes, well noticed. However, the difference comes from the fact that in our methods (line 407) we refer to the median values whereas table 3 states the means. We felt the medians were a better way of describing the overall dataset we were using but the means in table 3 were simply a way of showing the average value – the actual values used in our analysis obviously varied with each site.

Figure 2. What is the initial condition for the simulation of 1000 years depicted in Figure 2? Do you start from nearly steady state carbon pools or from carbon pools equal to "zero"?

We start with the carbon pools equal to zero. We did repeat the process with several different starting condition scenarios, but the overall effects were the same. We chose this one simply because it was the easiest to interpret (although we acknowledge that it has so many colours it is still hard to interpret fully). We have added this information to both the new figure legend and in the methods section.

L332-336
Initial pool sizes were set to 0 and the model was initialized to simulate a steady-state scenario based on average site conditions (derived from ~8000 forest and grassland sites in the Land-Use/Land Cover Area Frame Survey (LUCAS) dataset ([Toth et al., 2013] – see Table 3). Specifically, this meant starting a model run with no C in the system and gradually building up the litter and soil pools until they reached equilibrium based on driving variables (soil type, C inputs, climate) that remain fixed over time.

Line 455. Why colder temperatures favor POM? Is this related to the sensitivity of decomposition?

Partially. The main reason why this relationship occurs in MEMS v1.0 is because the MAOM and POM pools reach different equilibrium amounts under different temperatures – under steady-state, MAOM will reach equilibrium at roughly the same amount in all temperatures (i.e., near to the saturation limit), however the POM pools do not saturate and so when temperature is low, decomposition is low, and they will accumulate more before reaching equilibrium. Ultimately you are correct in assuming that temperature is assumed to have a bigger effect on the decomposition of POM than on the decomposition of MAOM (*sensu* Benbi *et al*., 2014). Our early attempts to differentiate between these sensitivities showed exciting results but were not based on rigorously tested measurements. A key focus of the next stages in model development is in the different sensitivities for the different pools so we hope to include these explicitly in MEMS v2.0.

Benbi D K, Boparai A K, Brar K. 2014. Decomposition of particulate organic matter is more sensitive to temperature than the mineral associated organic matter. *Soil Biol Biochem*.**70**: 183–192.

Line 473-475. Table 2. Maybe I am missing something obvious but the units of decay parameters as "k1" to "k10" should be [gC gC-1 day-1], otherwise when multiplied by the pool (Eq. 1-11 in the supplementary material) you will get [gC^2 day-1] rather than [gC day-1].

Thanks for pointing out this error. We meant to simply write day^{-1} and this results in the same effect. We have now changed throughout.

Line 491. This is definitely expected given that variability in litter input, e.g., litter composition and stoichiometry root: shoot ratios are underestimated and soil moisture is not accounted for.

Agreed. We have now added this extra information.

L602-610
While average agreement between measured and modelled soil C stocks was very good for MEMS v1.0, the model failed to capture the wide range in total POM-C stocks that were observed at the fractionated LUCAS sites (Figure 5). This may be because this first version of the model does not include several of the key controls on POM dynamics, such as water/oxygen limitations (Keiluweit et al., 2016), aggregation (Gentile et al., 2011), activity of soil fauna (Frouz, 2018) and nutrient availability (Bu et al., 2015; Averill and Waring, 2018). There are also limitations of our approach given that very few of the sites will likely be under true steady-state conditions, leading to further discrepancies between model predictions and measured values. Furthermore, the variability in driving variables of litter chemistry, N content and root:shoot ratios are underestimated when using our approach of grouping many different land uses into broad classes.

Line 496-497. For almost all of the analyzed sub-groups in terms of site-conditions of Figure 6, bulk SOC observations are mostly between 50-75 MgC/ha. I think this relatively narrow range complicates the identification of the control exerted by temperature, precipitation, soil texture or biomes and therefore also the model testing. A more reasonable test will require more distinguished values of SOC across different conditions, probably using other biomes and climates.

We agree and accordingly we are currently in the process of fractionating soils from the NEON network of sites that includes a wide range of ecotypes and climates – see https://www.neonscience.org/field-sites/field-sites-map. Once available, it is our hope that these data will help to improve the ability of the MEMS model to simulate a much more diverse set of soils. The relatively narrow range in this analysis of the LUCAS sites results primarily from the very large number of sites. Our initial analysis here was to try and see if general trends looked good and now we are moving on to more site-specific comparisons where we have much higher quality input data.

Line 521. I don't want to sound too pessimistic and overall I really like the approach of the authors but bridging the gap toward Ecosystem and Earth System Models still requires a considerable amount of work to test the reliability of temporal dynamics and plant-soil feedbacks. This should be stated in the manuscript.

We agree. We acknowledge the limitations of this early model version and have down-played the point slightly. However, we do feel that the change in approach and model structure can pave the way for an easier link to existing plant growth models and ecosystem models.

L564-566
MEMS v1.0 was designed to consolidate recent advances in our understanding of SOM formation and persistence into a parsimonious mathematical model that uses a generalizable structure which, after further development, can be implemented in Ecosystem and Earth System model applications.

Line 552. Also the dynamics of microbial pool in the soil is not explicitly simulated; however, the underestimation of variability is most likely due to underestimation of variability in the inputs and the steady-state assumption in the model, as you wrote in the next few lines.

We have added to this as shown above. Also, we hope the extra clarification of how microbial activity is simulated implicitly in the soil pools will help to clarify this point.

Line 558-559. I am not sure why soil moisture controls should be so important at high-latitude, these sites are rarely water limited, I would expect lack of soil-moisture controls to be more important in South-Europe.

You are right that these sites are not water limited but rather they are water saturated. In these situations, it is possible that anaerobic conditions persist and limit C-mineralisation. You are right that water limitations on the other end of the spectrum (too dry) will be prevalent in Southern Europe, and this is another source of high residuals when we do not include soil moisture controls.

Line 621-622. This is a great point, and I am looking forward for further work of the authors along this line.

Thank you. We are also keen to work more towards these goals.

Figure 1. Just as a suggestion, up to the authors, it would be nice to have some of the parameters of Table 2 represented also in this plot to link the main fluxes to some of the key parameters regulating the flux.

While we tend to agree that it could be nice to have a single figure with all the information on it, we chose to keep figure 1 as simple as possible so it can serve as a simple way of conveying the overall structure, rather than all the details. We appreciate the suggestion though and will look into including more details on future figures.

MARKED-UP MANUSCRIPT VERSION BELOW THIS POINT

Unifying soil organic matter formation and persistence frameworks: the MEMS model

Andy D. Robertson*[1,2], Keith Paustian[1,2], Stephen Ogle[2,3], Matthew D. Wallenstein[1,2], Emanuele Lugato[4], M. Francesca Cotrufo[1,2]

[1] Department of Soil and Crop Sciences Colorado State University, Fort Collins, CO 80523, USA
[2] Natural Resources Ecology Laboratory, Colorado State University, Fort Collins, CO 80523, USA
[3] Department of Ecosystem Science and Sustainability, Colorado State University, Fort Collins, CO 80523, USA
[4] European Commission, Joint Research Centre (JRC), ~~Directorate for Sustainable Resources, Via E. Fermi 2749, I-21027~~, Ispra (VA), Italy

Correspondence to: Andy D. Robertson (Andy.Robertson@colostate.edu)

Abstract. Soil organic matter (SOM) dynamics in ecosystem-scale biogeochemical models have traditionally been simulated as immeasurable fluxes between conceptually-defined pools. This greatly limits how empirical data can be used to improve model performance and reduce the uncertainty associated with their predictions of carbon (C) cycling. Recent advances in our understanding of the biogeochemical processes that govern SOM formation and persistence demand a new mathematical model with a structure built around key mechanisms and biogeochemically-relevant pools. Here, we present one approach that aims to address this need. Our new model (MEMS v1.0) is developed upon the Microbial Efficiency-Matrix Stabilization framework which emphasises the importance of linking the chemistry of organic matter inputs with efficiency of microbial processing, and ultimately with the soil mineral matrix, when studying SOM formation and stabilization. Building on this framework, MEMS v1.0 is also capable of simulating the concept of C-saturation and represents decomposition processes and mechanisms of physico-chemical stabilization to define SOM formation into four primary fractions. After describing the model in detail, we optimise four key parameters identified through a variance-based sensitivity analysis. Optimisation employed soil fractionation data from 154 sites with diverse environmental conditions, directly equating mineral-associated organic matter and particulate organic matter fractions with corresponding model pools. Finally, model performance was evaluated using total topsoil (0-20 cm) C data from 8192 forest and grassland sites across Europe. Despite the relative simplicity of the model, it was able to accurately capture general trends in soil C stocks across extensive gradients of temperature, precipitation, annual C inputs and soil texture. The novel approach that MEMS v1.0 takes to simulate SOM dynamics has the potential to improve our forecasts of how soils respond to management and environmental perturbation. Ensuring these forecasts are accurate is key to effectively informing policy that can address the sustainability of ecosystem services and help mitigate climate change.

1 Introduction

The biogeochemical processes that govern soil organic matter (SOM) formation and persistence impact more than half of the terrestrial carbon (C) cycle, and thus play a key role in climate–C feedbacks (Jones and Falloon, 2009; Arora *et al.*, 2013). In order to predict changes to the C cycle, it is imperative that mathematical models describe these processes accurately. However, most ecosystem-scale biogeochemical models represent SOM dynamics with first-order transfers between conceptual pools defined by turnover time, limiting their capacity to incorporate recent advances in scientific understanding of SOM dynamics (Campbell and Paustian, 2015). Due to the use of

conceptual pools, empirical data from SOM fractionation cannot be used directly to constrain parameter values that govern fluxes between pools because diverse SOM compounds can have similar turnover times but are differentially influenced by environmental variables (Schmidt *et al*., 2011; Lehmann and Kleber, 2015). As a result, empirical data is commonly abstracted and transformed before being used to parameterize or evaluate the processes of SOM formation and persistence that the model is intended to simulate (Elliott *et al*., 1996; Zimmermann *et al*., 2007). This has resulted in many conventional SOM models (e.g., RothC, [Jenkinson and Rayner, 1977], DNDC [Li *et al*., 1992], EPIC [Williams *et al*., 1984] and CENTURY [Parton *et al*., 1987]) being structurally similar (i.e., partitioning total SOM into discrete pools based on turnover times determined from radiocarbon experiments; see Stout and O'Brien [1973] and Jenkinson [1977]) but each taking different approaches to simplify the complex mechanisms that govern SOM dynamics. Consequently, simulations of SOM can vary greatly between models, often predicting contrasting responses to the same driving inputs and environmental change (e.g., Smith *et al*., 1997).

Structuring SOM models around functionally-defined and measurable pools that result from known biogeochemical processes is one way to help minimise these discrepancies. Two recent insights into SOM dynamics present a path towards addressing this issue. There is now strong evidence that: 1) low molecular weight, chemically labile molecules, primarily of microbial origin (Liang *et al*., 2017), persist longer than chemically recalcitrant C structures when protected by organo-mineral complexation (Mikutta *et al*., 2006; Kögel-Knabner *et al*., 2008; Kleber *et al*., 2011); and 2) each soil type has a finite limit to which it can accrue C in mineral-associated fractions (i.e., the C-saturation hypothesis) (Six *et al*., 2002; Stewart *et al*., 2007; Gulde *et al*., 2008; Ahrens *et al*., 2015). Structuring a SOM model around these known and quantifiable biogeochemical pools and processes has the potential to drastically reduce uncertainty by enhancing opportunities for parameterization and validation of models with empirical data. Furthermore, mechanistic models can have value in process explanation as well their value in predictive capabilities; such models can pinpoint the processes that have the greatest influence on a system even when they are not traditionally determined empirically.

Conventional SOM models readily acknowledge the importance of microbes in plant litter decomposition and SOM dynamics but model improvement was initially constrained by the concept that stable SOM included 'humified' compounds (Paul and van Veen, 1978). This quantified stable SOM using an operational proxy (high pH alkaline extraction) rather than relating stabilization to the mechanisms that are now widely recognised, such as organo-mineral interactions and aggregate formation (Lehmann and Kleber, 2015). As our contemporary understanding of stable SOM moves away from humification theory, so too must the way we represent SOM stabilization pathways in biogeochemical models. Similarly, many SOM models partition plant residues into labile and recalcitrant pools with turnover times that reflect the assumption of 'selective preservation' (i.e., chemically recalcitrant litter-C is only used by microorganisms when labile compounds are scarce). While many existing models do include a flux from labile residues into stable SOM, this is typically a much smaller absolute amount than the flux from recalcitrant residues. Evidence indicates that biochemically recalcitrant structural litter C compounds may not be as important in the formation of long-term persistent SOM as originally thought (Marschner *et al*., 2008; Dungait *et al*., 2012; Kallenbach *et al*., 2016). Instead, they form light particulate organic matter (POM) (Haddix *et al*., 2015), a relatively vulnerable fraction of SOM with a turnover time of years to

decades (von Lützow *et al*., 2006; 2007). Consequently, there have been several calls to represent this new understanding and re-examine how microbial activity is simulated in SOM models (Schmidt *et al*., 2011; Moorhead *et al*., 2014; Campbell and Paustian, 2015; Wieder *et al*., 2015).

Current conceptual frameworks more clearly link the role of microbes to SOM dynamics (e.g., Cotrufo *et al*., 2013 and Liang *et al*., 2017), and generally isolate two discrete litter decomposition pathways for SOM formation (Cotrufo *et al*., 2015): a 'physical' path through perturbation and cryomixing to move fragmented litter particles into the mineral soil forming coarse POM, *vs* a 'dissolved' path where soluble and suspended C compounds are transported vertically through water flow and, when mineral surfaces are available, form mineral associated organic matter (MAOM). Microbial products and very small litter particles can be transported by both pathways, forming a heavy POM fraction with 'biofilms' and aggregated litter fragments around larger mineral particles (i.e., sand; Heckman *et al*., 2013; Ludwig *et al*., 2015; Buks and Kaupenjohann, 2016). Attempts to formulate these empirical observations of litter decomposition into mathematical frameworks recently culminated with development of the LIDEL model (Campbell *et al*., 2016), which in turn built upon the relationships of litter decomposition described by Moorhead *et al*. (2013) and Sinsabaugh *et al*. (2013). While the LIDEL model was evaluated against a detailed lab experiment of litter decomposition (Soong *et al*., 2015), it does not simulate SOM pools and dynamics. In nature, litter decomposition processes and SOM formation processes are necessarily coupled but are often studied and modelled separately. However, models that link litter decomposition to SOM formation are required to represent SOM dynamics in ecosystem models.

Beside the processes of leaching and fragmentation that control the two pathways mentioned above, litter decomposition processes that form SOM are governed by the balance between microbial anabolism and catabolism (Swift *et al*., 1979; Liang *et al*., 2017). A recent paradigm has emerged that emphasizes the role of microbial life strategies (e.g., K *vs* r, referring to copiotrophic and oligotrophic microbial functional groups) and carbon use efficiency (CUE) in the formation of SOM from plant inputs (Dorodnikov *et al*., 2009; Cotrufo *et al*., 2013; Lehmann and Kleber, 2015; Kallenbach *et al*., 2016). As a result, scientists have explored several approaches to represent microbes in SOM models. Research has indicated that explicitly representing microbes in a SOM model can provide very different predictions of SOM dynamics and include important feedbacks such as acclimation, priming and pulse responses to wet-dry cycles (Bradford *et al*., 2010; Kuzyakov *et al*., 2010; Lawrence *et al*., 2009; Schmidt *et al*., 2011). This research has shown that, compared to conventional models, microbially-explicit SOM models have drastically different simulated responses to environmental change (Allison *et al*., 2010; Wieder *et al*., 2015; Manzoni *et al*., 2016). However, these responses are generally validated against data at microsite spatial scales and are not necessarily generalizable over larger spatial scales (Luo *et al*., 2016).

Microbes have been explicitly represented in SOM models in many ways and for many years, from relatively simple approaches using a single microbial biomass pool or fungal:bacterial ratios (e.g., McGill *et al*., 1981, Wieder *et al*., 2013 and Waring *et al*., 2013), to more complex associations with microbial guilds or community dynamics based on dominant traits derived through genetic profiling (Miki *et al*., 2010; Allison *et al*., 2012; Wallenstein and Hall, 2012). The MIcrobial-MIneral Carbon Stabilization (MIMICS) model (Wieder *et al*., 2014) consolidated existing research at the time and uses the size of a microbial biomass pool together with Michaelis–

Menten kinetics to feedback on C decay rates of SOM pools. While the MIMICS model and others (for an example see Manzoni *et al*., 2016), provide a potentially viable framework for explicitly representing microbes in a SOM model, it remains unclear whether this is practical given the lack of input data required to drive and validate these relationships (Treseder *et al*., 2012; Sierra *et al*., 2015). Furthermore, parsimony and analytical tractability are both key concerns for ecosystem models designed to operate over large spatial and temporal scales. While microbially–explicit models may be essential for addressing research questions at small spatial scales, they may introduce unnecessary, additional uncertainty to global simulations (Stockmann *et al*., 2013).

While microbial efficiency largely controls SOM formation rates, and microbial products are major components of the MAOM and the coarse, heavy POM fractions of SOM (Christensen 1992; Heckman *et al*., 2013) the long-term persistence of SOM is determined by mineral associations that are subject to saturation. Saturation limits for SOM were proposed more than a decade ago (Six *et al*., 2002) and have been supported by several empirical studies (e.g., Gulde *et al*., 2008; Stewart *et al*., 2008; Feng *et al*., 2012; Beare *et al*., 2014). Briefly, the concept of C-saturation suggests that each soil has an upper limit to the capacity to store C in mineral-associated (i.e., silt + clay, < 53µm) fractions, due to biochemical and physical stabilization mechanisms (e.g., cation bridging, surface complexation and aggregation) that are limited by a finite area of reactive mineral surfaces. While saturation kinetics are easy to define conceptually (Stewart *et al*., 2007), C-saturation as a concept has been adopted by only a few SOM models (Struc-C, Malamoud *et al*, 2009; COMISSION, Ahrens *et al*., 2015; MILLENNIAL, Abramoff *et al*., 2017). This is partly because its use in a SOM model requires a robust estimate of the specific site's saturation capacity. SOM saturation has been modelled using i) empirical regressions between silt + clay content and C concentration of that fraction (Six *et al*. 2002, as applied in COMISSION), and ii) empirical relationships between clay content and the derived 'Q_{max}' parameter of Langmuir isotherm functions (Mayes *et al*., 2012, as applied in MILLENNIAL). As noted by Ahrens *et al*. (2015), the use of C-saturation kinetics in an ecosystem model would require a map of mineral-associated C saturation capacity, and since soil C stocks in silt + clay fractions can make up the majority of total soil C stocks, a lot of weight would be put on that single driving variable for each site. However, it is worth noting that when applying C-saturation concepts, only the mineral-associated organic matter (MAOM) fraction saturates. Other SOM fractions (e.g., particulate organic matter, POM) theoretically have no saturation limit (Stewart *et al*., 2008; Castellano *et al*., 2015~~; Cotrufo *et al*., 2018~~).

Attempts to consolidate the concepts of microbial control on litter decomposition and mineral control on SOM stabilization resulted in the MEMS framework (Cotrufo *et al*. 2013). To date, we are aware of only one attempt to represent MEMS within a mathematical model, the MILLENNIAL model (Abramoff *et al*., 2017). However, this model does not simulate litter decomposition explicitly and as a result does not include the impact of litter input chemistry, which is a fundamental component of the MEMS framework and needed to improve ecosystem modelling, as discussed previously.

In this study we describe and demonstrate the application of a new mathematical model (MEMS v1.0) that applies three major concepts of SOM dynamics: 1) litter input chemistry-dependent microbial CUE informing SOM formation (Cotrufo *et al*., 2013), 2) separate dissolved *vs* physical pathways to SOM formation (Cotrufo *et al*., 2015); and 3) soil C-saturation related to litter input chemistry (Castellano *et al*., 2015). The scope of this inaugural

model description is limited to representing these three concepts and is not intended to include every mechanism relevant to SOM cycling. Our objective is to demonstrate the benefits of structuring a SOM model around key biogeochemical processes, rather than turnover times. Using measured SOM physical fractions from 154 forest and grassland sites across Europe ~~(Cotrufo *et al.*, 2018)~~, key parameters were optimised to improve model performance when simulating POM-C (consisting of both light and heavy POM) and MAOM-C, under equilibrium conditions. The resulting model was then used to test whether the behaviour of simulated SOM dynamics concur with the expected theoretical relationships. Finally, the model performance in predicting soil C stocks at equilibrium was evaluated by simulating 8192 forest and grassland sites across Europe, representing a diverse set of driving variables (i.e., climate, soil type and vegetation type).

2 Materials and Methods

2.1 Model description

The MEMS model (herein MEMS v1.0) is designed to be as parsimonious as possible while simulating the spatial and temporal scales relevant to management and policy decision making. The model is structured (Figure 1) to simulate plant litter decomposition explicitly with decomposition products defining C inputs to discrete soil pools that can be isolated with common SOM fractionation techniques (Table 1). Each state variable in MEMS v1.0 can be quantified directly using common measurement protocols and therefore calibration/evaluation data can be generated with a single fractionation scheme (Table S1). Detailed information about the model structure, the mathematical representation (i.e., differential equations) and how each mechanism is described mathematically can be found in the supplementary material. All model parameters can be found in Table 2.

MEMS v1.0 is a~~n ecosystem scale~~ SOM model that operates at the ecosystem-scale on a daily timestep. Carbon inputs to the model are resolved for each source (in the case of multiple input streams, e.g., manure, crop residue, compost) discretely, partitioning daily C inputs between solid-phase (C1, C2, C3) and dissolved (C6) litter pools as a function of litter chemistry (nitrogen [N] content and the acid-insoluble [i.e., 'lignin'] fraction) that influences microbial decomposition processes. This structure is similar to the LIDEL model (Campbell *et al.*, 2016) and follows the hypotheses that both N availability and lignin content influence decomposition by affecting microbial activity (Aber *et al.*, 1990; Manzoni *et al.*, 2008; Sinsabaugh *et al.*, 2013; Moorhead *et al.*, 2013). Similar approaches have also been used in many of the updated traditional SOM models (e.g., lignin:N ratios in CENTURY; Kirschbaum and Paul, 2002). These input partitioning coefficients can be determined experimentally for each C input source (Table 1 & S1). Upon reaching the soil, C compounds are then subject to biotic and abiotic processes that transform and transport organic matter through an organic horizon and subsequent mineral soil layers. As described here, MEMS v1.0 currently only simulates a surface organic horizon and a single mineral soil layer, and does not yet differentiate between above- and below-ground litter input chemistry to avoid requiring additional input parameters on root litter chemistry. However, the model architecture is sufficiently generalizable to apply to multiple soil layers and/or multiple discrete sources of C input. Where possible we use the parameter names and abbreviations from the LIDEL model (Campbell *et al.*, 2016).

2.1.1 Microbe mediated transformations and dissolved organic matter (DOM) production

Many of the biogeochemical processes represented by MEMS v1.0 are assumed to be microbially--mediated (and therefore result in exo-enzyme breakdown and CO_2 production), but only two lead to C assimilation into a distinct microbial biomass pool – from the water-soluble and acid-soluble litter pools (C1 and C2, respectively). In the mineral soil (i.e., pools C5, C8, C9 and C10), microbial anabolism and catabolism are implicit and considered part of the turnover of each pool. This ensures parsimony and allows model parameters to represent the differences in microbial community for each pool, as opposed to the alternative of explicit microbial pools. The C transferred from the C1 and C2 litter pools into microbial biomass is defined by a dynamic CUE parameter controlled by the N content of the input material and the lignocellulose index (LCI; defined as the ratio between acid-insoluble to the sum of acid-soluble + acid-insoluble) of the litter layer (i.e., lower CUE results when a higher proportion of the litter is acid-insoluble). Including microbially-explicit processes in the litter layer helps to determine the proportion of C inputs that result in MAOM *vs* POM formation (see Liang *et al*., 2017) and allows for future model versions to account for distinctions between different points of entry for inputs (Sokol *et al*., 2018). The lack of C transferred from other pools (e.g., C3) into microbial biomass implies their decay from co-metabolism with the more labile C sources (i.e., Klotzbucher *et al*., 2011; Moorhead *et al*., 2013). Once assimilated within microbial biomass, the anabolism of microbial activity results in generation of microbial products (i.e., necromass) that form tightly bound aggregates of biofilms and small litter fragments around sand-sized soil particles (Huang *et al*., 2006; Buks and Kaupenjohann, 2016), and dissolved organic matter (DOM). These contribute to the heavy POM (C5) and litter DOM (C6) pools, respectively. While these specific processes are well supported by relevant literature, to retain parsimony and the generalizable structure required by an ecosystem scale model MEMS v1.0 represents microbial metabolism processes ~~implicitly~~more generally (i.e., by linking them to a dynamic microbial CUE rather than specific community traits). ~~as per their description in LIDEL.~~

Even though not all pools explicitly produce microbial biomass, all pools do produce DOM. Recent studies have shown that DOM and small suspended particulates result from the decomposition and fragmentation of all forms of inputs including those characterized as 'inert', such as pyrolized material (Soong *et al*., 2015). Consequently, the model assumes that all microbially-mediated decomposition produces some C in DOM with rates specific to the pool from which the C originates. Since DOM generation is strongly influenced by the elemental composition of the ~~litter~~ input material (Soong *et al*., 2015), it is intrinsically linked to microbial CUE, employing the same formulation as LIDEL, which accounts for input N content and LCI of the litter layer (Campbell *et al*., 2016). At present, root exudation is not explicitly represented but the presence of a soil DOM pool (C8) will allow for incorporation of root exudation processes in later versions. More detail regarding the microbially transformed organic matter inputs *vs* those directly incorporated into the soil can be found in the supplementary materials.

2.1.2 Perturbation and physical transport

While microbial activity directly influences DOM production and therefore its transport with water flow (pool C8), the physical pathway to SOM formation (i.e., forming pools C5 and C10; POM) results from perturbation and fragmentation processes (Cotrufo *et al*., 2015). The exact mechanisms of perturbation are hard to generalize over the globally diverse conditions that an ecosystem scale model such as MEMS v1.0 is designed to operate. Consequently, the litter fragmentation and perturbation rate (LIT_{frg}) in MEMS v1.0 is represented as a first-order

process where the default value of LIT_{frg} was informed by empirical estimates (e.g., Scheu and Wolters, 1991; Paton *et al*., 1995; Yoo *et al*., 2011); but uncertainty can be reduced by relating this rate to specific site conditions that reflect, in particular, soil macro- and mesofauna activity. The division of litter fragmentation between the C5 and C10 pool is derived from fractionation results that separate the light and heavy POM. The split between these two fractions appears to vary with land use (Poeplau and Don, 2013), although the exact relationship is unclear. Consequently, MEMS v1.0 applies an average over all land uses. Particulate organic matter is divided between a heavy and a light pool because recent evidence suggests the two fractions are differentially influenced by temperature and management linked to aggregation and land-use change (deGryze *et al*., 2004; Tan *et al*., 2007; Poeplau *et al*., 2017). Furthermore, the heavy, coarse POM pool can play an important role in soil nutrient cycling (Wander, 2004) and it has a different turnover time to either the MAOM or light POM fraction (Crow *et al*., 2007; Poeplau *et al*., 2018).

2.1.3 Liquid phase transport

Vertical transport of DOM can be simulated as a function of water flow in a process-based soil hydrology model. However, in this first, standalone version, MEMS v1.0 assumes that DOM is transported rapidly downward through percolation and advection according to a constant water flux. As with the LIT_{frg} parameter, the rate of vertical C transport (controlled by parameter DOC_{frg}) would ideally be site-specific, but is currently fixed at a general, default value informed by relevant literature (Trumbore *et al*., 1992; Kindler *et al*., 2011). More information can be found in the supplementary material and in Table 2.

2.1.4 Sorption and desorption with mineral surfaces

The organo-mineral complexes that define a large portion of MAOM-C in MEMS v1.0 operate under the principles of Langmuir isotherms, which have also been used in the COMISSION and MILLENNIAL models (Ahrens *et al*. (2015) and Abramoff *et al*. (2017), respectively). These isotherms represent a net C transfer between soil DOM (pool C8) and MAOM (pool C9) that encapsulates all sorption mechanisms (e.g., cation bridging, surface complexation, etc.). While MEMS v1.0 uses the same general Langmuir saturation function as the MILLENNIAL model, it estimates maximum sorption capacity (parameter Q_{max}) differently. Here, we use sand content to derive the maximum C concentration of the silt + clay fraction according to a regression calculated by pooling all soils data reported by Six *et al*. (2002). This is then converted to C density using the site-specific soil bulk density provided as a driving variable to the model.

In addition to the Q_{max} parameter, the isotherm saturation function also relies on an estimate of a specific soil's 'binding affinity' (parameter K_{lm}). Typically, this is a product of a soil's specific mineralogy, influencing the type of organo-mineral bonds that are formed and the strength of those bonds (Kothawala *et al*., 2009). Furthermore, the type of C compounds being sorbed are also key to defining an isotherm's binding affinity (Kothawala *et al*., 2008; Kothawala *et al*., 2012). This parameter can be very difficult to generalise without requiring exhaustive information on soil physiochemical conditions (e.g., clay type, Fe/Al concentration, etc.), but the work of Mayes *et al*. (2012) presented an empirical relationship between K_{lm} and native soil pH, with pH acting as a proxy for mineralogical conditions. As a result, sorption rates to mineral surfaces are dependent on pH (see Equation 35 in supplementary). This relationship (derived from isotherms calculated for 138 soils of varying taxonomies)

provides a good starting point for estimating K_{lm} and is also used by the MILLENNIAL model (Abramoff *et al*., 2017). It is worth noting that desorption is implicit in the Langmuir saturation function used by MEMS v1.0 (unlike the explicit representation in COMISSION, Ahrens *et al*., 2015), meaning that when the MAOM pool reaches saturation the net transfer from soil DOM to MAOM may be negative and C is transferred from MAOM to DOM. The simulated sorption–desorption processes in MEMS v1.0 are directly derived from empirical data and are similar to other SOM models (Wang *et al*., 2013; Ahrens *et al*., 2015; Dwivedi *et al*., 2017).

2.1.5 Heterotrophic respiration and controls on microbial activity

Aside from the litter layer DOM (pool C6), each of the state variables in MEMS v1.0 decay with unique specific maximum rates, with the resultant C flux being partitioned into CO_2 (aggregated into the C7 sink term) and an accompanying decomposition product flux into other pools, mainly DOM. Thus, the decay rate constants represent total mass loss potential, embodying DOM-C generation as well as CO_2 emissions, as per a recent decomposition conceptualization (Soong *et al*., 2015). The total amount of heterotrophic respiration is the sum of CO_2 produced from the biotic decay of all model pools after other fluxes (e.g., DOM generation) are calculated (more detail can be seen in the supplementary). While the maximum specific decay rates for most pools are fixed parameters informed by empirical data (**Error! Reference source not found.**), several studies suggest linking decay rates of recalcitrant compounds to those of more microbially-accessible compounds (Moorhead *et al*., 2013; Campbell *et al*., 2016). This follows similar hypotheses to the priming effect, that chemically recalcitrant compounds (e.g., lignin, cutin and suberin) are processed co-metabolically when microbes act preferentially on more energetically favourable compounds nearby (Carrington *et al*., 2012; Větrovský *et al*., 2014). Consequently, MEMS v1.0 applies this through use of the same functions as those used by the LIDEL model (Campbell *et al*., 2016), estimating the maximum specific decay rate of pool C3 with a relationship to parameter k_2 (i.e., the maximum specific decay rate of the acid-soluble litter fraction, pool C2). At present, CO_2 emitted from soil mineralization of DOM is associated with the values presented in Kalbitz *et al*. (2005).

2.1.6 Decay rate modifiers

Temperature is used as the main environmental control on maximum specific decay rates of each pool. The rate modifying function used by MEMS v1.0 is adapted from that of the StandCarb model (Harmon and Domingo, 2001). This function is consistent with empirical data and enzyme kinetics, implying that microbial decomposition rates peak at an optimum temperature with reduced rates above and below. Coefficients that define the function also include the Q_{10} and reference temperature for that specific pool. Therefore, the function can utilise empirical data if available for a site. This is a relatively simple function that only accounts for temperature. Simulating the influence of other important controls on decomposition, such as water, oxygen, pH and nutrients, are beyond the scope of this inaugural version of the MEMS model but ~~will be incorporated in~~are central to future development efforts.

2.1.7 Model implementation and driving variables

MEMS v1.0 is a series of ordinary differential equations solved for discrete time steps by numerical integration using finite differencing techniques from the Runge-Kutta family of solvers. Implementation is performed through the deSolve package (Soetart *et al*., 2010) written for R (all equations and associated detail can be found in

Supplementary Information). Parameters used to solve MEMS v1.0 are described along with their default values and associated references in Table 2.

Initializing MEMS v1.0 requires external inputs of basic site characteristics (climatic and edaphic conditions as well as land management information) and ideally ~~uses~~ measurements of daily C input. However, C inputs are rarely available at daily time scales. Consequently, for this inaugural version of the MEMS model we employ a simple function to interpolate daily C inputs from annual Net Primary Productivity (NPP), partitioning aboveground/belowground and to the simulated soil layer using land-use specific root:shoot ratios and a simple root distribution function (Poeplau, 2016). These driving variables are external inputs of the initial model version but may be obtained from coupled climate and plant growth submodels in future versions, when incorporated into a full ecosystem model. Details of these approaches are given in the supplementary materials and all required driving variables are shown in Table 3. Since the major C pools can each be quantified using common analytical methods (Table S1), the best way of initializing the size of these pools in MEMS v1.0 is to use measured data. However, when measured data are not available, a typical site simulation employs a spinup that runs the model to steady-state conditions based on average climatic and edaphic conditions, as well as average C inputs.

2.2 Global sensitivity analysis

The default parameter values (i.e., those governing C turnover and fluxes between pools) used by MEMS v1.0 are informed by data from relevant literature (**Error! Reference source not found.**Table 2). However, different studies may suggest different values based on discrete site conditions, meaning *a priori* estimates may not necessarily be generalizable across all sites that the model could simulate. A variance-based global sensitivity analysis was performed to determine each parameter's relative contribution to the change in each state variable (i.e., determining which parameters have the largest influence on the size of each model pool). The sensitivity analysis was repeated for different simulation lengths (1 – 1000 years) as different fluxes operate at different temporal scales, thereby meaning that the relative importance of each parameter changes through time. Initial pool sizes were set to 0 and the model was initialized to simulate a steady-state scenario based on average site conditions (derived from ~8000 forest and grassland sites in the Land-Use/Land Cover Area Frame Survey (LUCAS) dataset ([Toth *et al*., 2013] – see Table 3). Specifically, this meant starting a model run with no C in the system and gradually building up the litter and soil pools until they reached equilibrium based on driving variables (soil type, C inputs, climate) that remain fixed over time. To evaluate how much each model parameter (e.g., decay rates, DOM generation rates, etc.; see Table 2) effects the amount of C in each pool (i.e., C1-C11; Figure 1) parameter values were changed to be higher or lower from their baseline and pool sizes are tracked over simulation time. Note that all temperature modifier parameters (T_{ref}, T_{opt}, T_{Q10}, T_{lag} and T_{shp}; Table 2) were excluded in this sensitivity analysis as the resulting T_{mod} has the same effect on all decay rates. Maximum and minimum values of all other parameters (n = 24**Error! Reference source not found.**) were defined as 50 % above and below the literature-derived (baseline) value (Table 2). Using Latin Hypercube techniques to sample within the full parameter space, a global sensitivity varying all parameters was used to determine total variance for changes to each model pool (i.e., how much each pool changes in size when all parameters vary up to 50 %). Then, in turn, each individual parameter was fixed at its baseline value while all others varied. This defines ~~the~~ each parameter's contribution to a pool's variance ~~from each parameter~~, averaged over variations in all other

parameters (Sobol, 2001; Saltelli *et al*., 2008) (i.e., how much each pool changes in size when all parameters, except one, vary up to 50%). When normalized over the global sensitivity variance, a contribution index provides the proportion of variance explained by each parameter. The analysis was run 10,000 times to define the total parameter space and the whole procedure was repeated annually for simulation lengths between 1 to 1000 years. Put simply, 10,000 different combinations of parameter values between the minimums and maximums were used to repeatedly run the model for 1000 years given average site conditions. The results showing changes in pool size correspond to the changes in parameter values (e.g., when maximum decay rate of MAOM is increased, pool C9 may decrease in size but other pools may increase). The impact that a single parameter has on pool size, compared to that of all parameters, is described by the contribution index, where the total effect of all the parameters is equal to the maximum change in pool size. Note that the results of a global sensitivity analysis of this kind are non-directional and do not indicate whether a parameter increases or decreases a pool size, but rather that it simply changes from the baseline.

2.3 Model response to changes in driving variables

To determine the model's steady-state response to changes in each individual driving variable, a local one-at-a-time (OAT) sensitivity analysis was performed by sequentially simulating different equilibrium conditions for 1000 years. The baseline estimates for edaphic inputs, temperature and C input quantity were informed by the LUCAS dataset ([Toth *et al*., 2013] – see Table 3 and below for more details), with mean values defining the mid-points and ranges defined as the minima and maxima. Litter chemistry driving variables were adapted from the ranges described by Campbell *et al*. (2016). Note that while typically described as a sensitivity analysis, an OAT approach is not as robust as variance-based techniques because it cannot determine interactions between input variables. However, OAT results are easier to interpret as there are no confounding impacts and relationships observed are solely a result of changing one variable. Additionally, we assess the model's qualitative relationships between driving variables by comparison to a study by Castellano *et al*. (2015); combinations of high/low sand content and high/low soil pH were used to examine whether model projections agree with the hypothesized relationships between input litter chemistry and MAOM-C stocks at steady–state. In these scenarios, ~~Alfalfa~~ alfalfa (*Medicago sativa*) and ~~Ponderosa~~ ponderosa ~~Pine~~ pine (*Pinus ponderosa*) were used as examples of a high- and low-quality litter input, respectively, with litter chemistry driving variables adopted from Campbell *et al*. (2016).

2.4 Parameter optimization

2.4.1 LUCAS dataset and soil fractionation data

Parameter optimization for MEMS v1.0 used data from the LUCAS dataset (Toth *et al*., 2013). This dataset contains basic soil properties including C data for almost 20,000 sites across Europe, sampled in 2009, representing a wide spatial range over 25 countries with diverse gradients of soil types, climates and land uses (Figure S1). Complimented with geo-referenced estimates of annual NPP from MODIS satellite data (ORNL DAAC, 2009), and daily temperature data from the Climate Prediction Center's Global Temperature (CPC-GT) database (NOAA, 2018), this provided all driving variables required to run MEMS v1.0. The use of modelled/interpolated NPP and climate data is not recommended over measurement data directly collected from the site(s) being simulated, but for the analysis herein these measured data were unavailable.

A representative subsample (Figure S2) of forest and grassland sites from LUCAS were selected for fractionation to generate data for POM and MAOM pools (see dataset online available at the European Soil Data Centre ~~Cotrufo *et al.*, 2018~~). Specifically, topsoil (0-20 cm) samples from 78 grassland sites and 76 forested sites were fractionated by size (53 µm) after full soil dispersion in dilute (0.5 %) sodium hexametaphosphate with glass beads on a shaker ~~(see Cotrufo *et al.*, 2018 for more details)~~. The fraction passing through (< 53 µm) was collected as the MAOM, while the fraction remaining on the sieve was collected as the POM. It is worth noting that this fractionation did not separate the POM into a light and a heavy POM, as represented in MEMS v1.0 (i.e., C5 and C10), thus these model fractions were combined for data-model comparisons (see below). After drying to constant weight in a 60 °C oven, each fraction was analysed for C and N concentration in an elemental analyser (LECO TruSpec CN). Samples from sites with a soil inorganic C content greater than 0.2 % (as reported in the LUCAS database) were acidified before elemental analyses to remove carbonates, so that the %C of each fraction represented the organic C only. Carbon concentrations of each fraction and the total soil organic carbon (SOC) were converted to stocks for the top 20 cm soil layer using bulk density estimates reported with the LUCAS database. A georeferenced summary of these 154 sites can be seen in Figure S2 and summary information of the fractionation data and comparisons between land use classes is shown in Figures S3 and S4.

2.4.2 Optimization procedure

Informed by the global sensitivity analysis, four parameters accounted for ~60 % of the variation in steady-state bulk (and MAOM/total POM) soil C stocks. These were *Nmid*, *k5*, *k9* and *k10* (see Table 2 **Error! Reference source not found.**for details) and were used for optimization to improve model performance. Maximum and minimum values representing realistic ranges of each parameter were informed by relevant literature and rounded to appropriate boundaries (Table 2; Table S2): *Nmid* (0.875, 2.625), *k5* (6.0^{-5}, 1.0^{-3}), *k9* (1.0^{-5}, 4.0^{-5}), *k10* (1.0^{-4}, 1.0^{-3}). These values set the limits for Latin Hypercube sampling to define 1024 unique parameter sets that, together, span the full range of each parameter. The fractionated LUCAS site data was used to train and test the model, applying a repeated *k*-fold cross-validation approach (Kuhn and Johnson, 2013) to identify best parameter values for the full variation of conditions at all 154 sites. Comparisons were made between measured soil C stocks and those resulting from steady-state simulations for each site. Of these sites, 120 (78 %) were used for training and the remaining 34 (22 %) were used for testing. Root mean squared error (RMSE) was applied as the objective function. Using the training results, the set of parameters that reported the lowest RMSE for each fraction was used to ensure this 'best' parameter set also performed well (i.e., RMSE was within 10 % of that reported for the training sites) against the 34 sites of measured data withheld for testing. This process was repeated 10 times using different subsets of the 154 sites for training and testing (i.e., 10 'folds' in the cross-validation approach).

To determine the optimized parameter values, a single fold was chosen at random from those ~~the parameter set~~ that reported the lowest RMSE for each subset of training sites (i.e., each fold) ~~was selected and values from all 10 folds were averaged~~. Optimized values differ depending on which measured fraction is compared to model predictions (whether comparing pool C9 to measured MAOM-C, the sum of pools C5 and C10 to measured total POM-C, or the sum of pools C5, C8, C9 and C10 to measured bulk SOC). The new, optimized parameter values (Table S2) were derived from ~~the~~ a randomly chosen fold~~averaging of those~~ that minimized RMSE when

compared to the MAOM fraction. This was chosen (instead of those optimized for POM or bulk SOC) since the MAOM fraction is typically the largest single soil C pool and using this approach led to the biggest overall decrease in RMSE when compared to all available data (Table S2). In future analyses, a more rigorous approach may be to apply a cost function regarding all available measured pool data (e.g., including litter pool data when it is also measured) but for our initial model evaluation we deemed this random choice sufficient.

2.5 Model evaluation for forests and grasslands in Europe

Having optimized key parameter values, the new global parameter set for MEMS v1.0 was used to simulate the remaining forest and grassland sites of the LUCAS dataset for independent evaluation. Driving variables of edaphic conditions and land-use type were extracted for each site from LUCAS and combined with daily estimates of C inputs and temperature (derived from simple interpolations assuming a normal distribution of MODIS annual NPP data [see Supplementary for details] and CPC-GT daily maximum and minimum air temperature data, respectively). Where these data were unavailable, the site was removed from further evaluation. Three forest land-use classes (as described in LUCAS) were included, along with the pure grassland land-use class. This resulted in a final dataset of 8192 sites (3487 grasslands, 1713 coniferous forests, 1590 broadleaved forests and 1402 'mixed' forests). Mixed forests are defined to contain coniferous and broadleaved species that each contribute > 25% to total tree canopy. Summary information for these sites can be found in Figure S1. To differentiate between input litter chemistry, root:shoot ratios and root distribution of the four land-uses, generic driving variables for each were derived from relevant literature. Details of these inputs are shown in Table 3.

Each of the 8192 sites was initialized with zero pool sizes and simulated for 1000 years to achieve steady-state conditions. This assumed the same intra-annual distribution of daily temperature and C input for each year. Organic carbon content reported in LUCAS was converted to SOC stock using the estimated bulk density reported with the database and reduced according to the measured rock/gravel content (Equation 1), i.e.,

$$SOC = C_{conc} * {}^{L}\rho * (1 - {}^{L}rock) \quad (1)$$

Where SOC is soil organic carbon stock in Mg C ha^{-1}, C_{conc} is the measured C content in percent, ${}^{L}\rho$ is the bulk density of soil layer L in g cm^{-3} and ${}^{L}rock$ is the rock content of soil layer L expressed as a fraction. This total SOC stock, was compared to MEMS v1.0 model output. In addition to comparing measured values with those predicted at steady-state (which may not be an accurate assumption for many sites), a more general comparison was performed to examine groups of sites under similar site conditions. Model performance was evaluated for several classes of environmental conditions, with sites divided into above and below median values of mean annual temperature (MAT, 8.3 ºC), mean annual precipitation (MAP, 687 mm), annual NPP (647 gC m^{-2} yr^{-1}) and sand content (50 %), for each land-use type. Several standard metrics for error and bias were used to evaluate model performance following the flowchart presented in Smith *et al*. (1997), including Mean Absolute Error (MAE), Mean Bias Error (MBE), Root Mean Square Error (RMSE), modelling efficiency (EF), and Coefficient of Determination (CofD). Additionally, we used 16 environmental classes to derive an estimate of measurement uncertainty based around sites of similar conditions (e.g., hot, wet, low input, sandy soil) for each land use. To include both measurement and simulation error in the same evaluation metric, we applied a modified *F*-test

statistic that uses lack-of-fit sum of squares to account for both experimental and prediction uncertainty (see Sima *et al*., 2018 for more information). The variance required to calculate these was derived by using the full number of environmental classes as described above (n = 16). Due to the lower number of fractionated sites in each group, only temperature and sand content were used as environmental classes (i.e., n = 4) to evaluate performance at these 154 sites. One-way ANOVAs were performed to show where average model results were significantly different from average measured C stocks. An α level of 0.05 was used to determine the significance of the ANOVA and *F*-tests. Finally, we also use the standard errors for bulk topsoil C stocks of each environmental class to determine the significance of RMSE assuming a two-tailed Student's t distribution and 95% confidence interval, as described by Smith *et al*. (1997). All data processing and statistical analysis was performed in R (v3.4; R Core Modelling Team, 2018).

3 Results

3.1 Sensitivity and behaviour of MEMS v1.0

3.1.1 Parameter sensitivity at different timescales

Bulk SOC stocks were sensitive to different sets of parameters depending on the duration of the simulation (Figure 2; Figure S5). Parameters that define litter fragmentation and perturbation rates (*LITfrg*) or microbial CUE (mainly *LCmax*, *Nmax* and *Nmid*) are responsible for rapid (< 2 years) changes in C stocks, particularly those in the litter layer and light POM. As simulation time increases, the influence of these parameters declines relative to the litter and POM decay rate parameters, particularly *k5* and *k10*. Fifty years after simulations are initialized, more than 75% of the sensitivity in total soil C stock was due to the maximum specific decay rate of light POM (i.e., parameter *k10*). After this point, its relative contribution to total C stock sensitivity diminishes as the parameters that define MAOM-C sorption become more important (i.e., coefficients that determine the regression to calculate MAOM-C saturation capacity [*scIcept* and *scSlope*]). Overall, our sensitivity analysis showed that the expected dynamics with different processes (e.g., litter fragmentation, microbial processing and sorption) are operating at the appropriate timescales to structure SOM dynamics, and their associated parameters are more, or less, important depending on the initial pool sizes and model run/experiment duration. Figure 2 can be interpreted as a depiction of how each pool of MEMS v1.0 accumulates over time.

3.1.2 Soil carbon response to changing environmental conditions

Alone, each driving variable (edaphic conditions, temperature, and input litter quantity/quality) in MEMS v1.0 has a discrete and non-linear relationship to the proportion of soil C stored in the MAOM and POM pools under steady-state conditions (Figure 3). This analysis alters only one driving variable at time while holding others constant at an average value. Bulk C stocks are predicted to be mostly MAOM in all cases except when C inputs (*annNPP*) are very high (i.e., > 1.5 kg C m^{-2} yr^{-1}; Figure 3). This results from the fact that the MAOM pool will saturate at high input rates whereas the POM pools do not (Castellano *et al*., 2015~~; Cotrufo *et al*., 2018~~). Sand content and soil pH influence a site's MAOM saturation capacity, and therefore a low capacity (i.e., high sand content) with mineralogy associated with weaker organo-mineral bonding (i.e., high soil pH) has proportionally more total POM. Litter input chemistry variables also have different, and sizable, impacts on whether SOM forms

and persists primarily in MAOM or in POM (as denoted by the MAOM:POM ratio). Note that POM in the MAOM:POM ratio refers to total POM (i.e., pools C5 and C10 combined). The fraction of litter input that is hot-water extractable (*fSOL*) is a key determinant of MAOM formation rates and when *fSOL* is high, MAOM-C stocks at steady-state are predicted to be more than ~~4~~ four times higher than POM-C stocks (Figure 3). Conversely, when input material has a high acid-insoluble (*fLIG*) content and a low N content (*LitN*) the size of the organic horizon increases and, over time, POM-C stocks approach a 1:1 ratio with MAOM-C stocks. Figure 3 shows the impact of changing one driving variable while all others remain constant. When many of these inputs vary at the same time, the relationships to MAOM:POM can be very different (for example, the model predicts twice as much POM-C as MAOM-C when simulating a sandy soil with coniferous vegetation and high *annNPP*).

MAOM-C saturation in the model is largely dependent on an interaction between the quantity of C inputs, the soil texture (i.e., sand content) and mineralogy (i.e., for which soil pH is used as a proxy).

514 FigureFigure 4 shows that our mathematical formulation of sorption to mineral surfaces generated a very similar
515 relationship to that proposed by Castellano *et al*. (2015). When C inputs are low, litter input chemistry has the
516 greatest influence on the MAOM-C stock under steady-state conditions. This is particularly true in soils with the
517 strongest mineral bonding (i.e., low pH) and high sorption capacity (i.e., low sand %; Figure 4 top right panel).
518

519 **3.2 Improved simulation due to parameter optimization**

520 Initial parameter values derived from relevant literature provided good estimates judging from model performance
521 with measured fractionation data (Table S2). Prior to optimisation, the difference between measured and modelled
522 bulk soil C stocks of fractionated LUCAS sites was insignificant for all four land-uses (one-way ANOVA, $p >$
523 0.05). However, accounting for experimental and simulation uncertainty (variance calculated by four groups:
524 divisions of high/low mean annual temperature and sand content) MEMS v1.0 only accurately described bulk
525 SOC stocks for the grassland land-use class (F-statistic < 0.05). After optimisation, overall model fit with all soil
526 C fractions (MAOM, total POM and bulk) was improved by increasing the maximum decay rate of MAOM
527 (parameter *k9*) and decreasing the maximum decay rate of light POM (parameter *k10*), the maximum decay rate
528 of coarse, heavy POM (parameter *k5*), and the inflection point for the logistic curve that defines the N effect on
529 microbial CUE (parameter *Nmid*). This resulted in a lower RMSE against all measured data compared to baseline
530 values (Table S2). Despite the improved model fit, the error in simulated values for broadleaved forest sites was
531 still more than the error inherent to the measured data (at a 95% threshold and as defined by the modified F-test
532 from Sima *et al*., 2018). This was primarily caused by two sites where measured total POM-C stocks were reported
533 to be > 95 Mg C ha^{-1} in the top 20 cm (Figure 5). When these sites were removed from statistical comparisons
534 there were no significant differences between modelled and measured bulk SOC stocks for any land use class.
535

536 Measured fractionation data from the four major land-use classes showed a wide range of soil C stocks and a
537 significantly different MAOM:POM ratio between grassland and forests (Figure 5; Figure S4). This was
538 predominantly due to grassland topsoil (0-20 cm) having more MAOM and less total POM, compared to
539 coniferous soils (Figure S3). On average, simulations of the fractionated sites agreed well with measured data,
540 demonstrating no significant differences ($p > 0.05$) between measured and modelled C stocks of total POM or
541 bulk soil for all land uses, and for MAOM at broadleaved, mixed and coniferous forest sites (Figure 5). The only
542 statistically significant difference was between measured and modelled MAOM-C stocks for grassland sites ($p <$
543 0.01). However, measurements have a considerably larger range between minimum and maximum values than
544 did model simulations, particularly for total POM, which largely explained the high overall RMSE when
545 comparing all 154 sites (Table S2).
546

547 **3.3 Model evaluation for forests and grasslands in Europe**

548 Despite only including a few of the many factors that influence SOM dynamics, MEMS v1.0 was able to capture
549 the expected relationships between site conditions and total mineral soil C stocks based on an evaluation of the
550 optimized model with independent data (Figure 6). Mean absolute error over all sites (n = 8192) was low (MBE
551 = 1.1 MgC ha^{-1}) and CofD was above 1, indicating that the simulated C stocks capture the trend of the measured

552 data better than the mean of the measurements (Table 4). The main lack of fit was observed as the model
553 consistently underestimated bulk soil C stocks in forest systems with low mean annual temperature (MAT < 8.3
554 ºC) and sandy soil textures (sand content > 50 %) (Figure S6). When divided by land-use classes, grassland sites
555 had the lowest residuals and mixed forest sites had the highest (Figure 6; Figure S6). Using low and high divisions
556 of MAT, MAP, sand content and C input quantity, to account for variance between each of these groups (n=16),
557 RMSE indicated that the model predictions of C stocks fell within the 95 % confidence interval of the
558 measurements for coniferous and mixed forest sites. Using the same groups but also accounting for simulated
559 variance indicated that the accuracy of MEMS v1.0 predictions were statistically significant for all land uses
560 besides broadleaf forest sites (F-statistic > 0.05;
561
562

563 TableTable 4). A geographic analysis of model performance indicated that the model performed best across France
564 and Northeastern Europe but poorly across the UK, Ireland and Southern Sweden (Figure 7). Furthermore, topsoil
565 C stocks of broadleaved sites in Southeastern Europe, particularly Romania, were consistently overestimated by
566 the model, especially when sites had low MAP (Figure 6; Figure 7).
567
568 In general, discrepancies between measured and modelled values were largest for the broadleaved forest land use
569 class (Figure S6). Results from analysis of the fractionated sites suggest that the model cannot achieve the very
570 high POM-C stocks measured at some sites. Optimized parameter values aim to produce a good overall model fit
571 but are unlikely to be able to capture the full range of measured values (for example, the lowest bulk topsoil C
572 stock for a broadleaved site was 7 Mg C ha^{-1} whereas the highest was 218 Mg C ha^{-1}). A summary of model
573 performance against these 8192 evaluation sites is shown in Table 4. While the model's performance comparing
574 absolute C stocks appears good, this is done with the assumption that these topsoil C stocks at forest and grassland
575 sites in our analysis are at steady-state. This is unlikely to be true and therefore it is encouraging when general
576 trends are as expected (as is the case for many of the land uses and for many of the different environmental
577 divisions; Figure 6).

4 Discussion

MEMS v1.0 was designed to consolidate recent advances in our understanding of SOM formation and persistence into a parsimonious~~, ecosystem scale,~~ mathematical model that uses a generalizable structure which, after further development, can be ~~developed further and~~ implemented in Ecosystem and Earth System model applications. In this study we aimed to provide proof-of-concept that a model structure built around known biogeochemical mechanisms (Figure 1) and measurable pools could be advantageous for application over varied site conditions. Another advantage of using this novel structure is that each aspect is empirically quantifiable, allowing for straightforward model evaluation of both total and fractionated SOM, addressing a common concern among conventional SOM models (Campbell and Paustian, 2015).

4.1 Sensitivity and behaviour of MEMS v1.0

The relationships between model driving variables and soil C stocks at steady-state highlight the importance of litter chemistry on relative proportions of MAOM and total POM in MEMS v1.0 (Figure 3). This is generally because both POM pools accumulate C when input litter has a high acid-insoluble fraction and a low N content, resulting from reduced microbial accessibility and reduced DOM production (Scheibe and Gleixner, 2014). This trend is also common in empirical studies and often associated with land-use change from herbaceous to woody vegetation (Filley *et al*., 2008). Many of the parameters that influence the processes of POM formation and persistence (e.g., *LITfrg*, *Nmid*, *LCImax*, etc.) have relatively high importance (i.e., sensitivity) to changes in total SOM within relatively short time frames (i.e., < 10 years; Figure 2). This captures an important real-world trend that POM is typically more vulnerable to decomposition with disturbance compared to MAOM (Cambardella and Elliott, 1992). Consequently, the model is able to simulate this impact with processes and associated parameters operating at the appropriate time-scale.

One main objective of structuring MEMS v1.0 around empirically-defined biogeochemical processes is so that it can accurately represent the timescales on which different processes operate, rather than being solely dependent on turnover times of conceptual pools. This is particularly relevant given our new understanding that the MAOM fraction has short-term dynamics (Jilling *et al*., 2018). Consequently, it is reassuring to see that this knowledge, which is incorporated into the MEMS v1.0 design, can be seen in Figure 2 (and Figure S5), where the parameters that operate on short time-scales also have an immediate impact on the MAOM pool given the complexity of controls in the model structure. The model's agreement with the hypothesized relationship from Castellano *et al*. (2015) is also reassuring, and represents an important proof of concept that associates litter chemistry and C saturation capacity with MAOM-C stocks at steady-state (Figure 4).

4.2 Model evaluation of MEMS v1.0

While average agreement between measured and modelled soil C stocks was very good for MEMS v1.0, the model failed to capture the wide range in total POM-C stocks that were observed at the fractionated LUCAS sites (Figure 5). This may be because this first version of the model does not include several of the key controls on POM dynamics, such as water/oxygen limitations (Keiluweit *et al*., 2016), aggregation (Gentile *et al*., 2011), activity of soil fauna (Frouz, 2018) and nutrient availability (Bu *et al*., 2015; Averill and Waring, 2018). ~~Furthermore~~There are also limitations of our approach given that~~,~~ very few of the sites will likely be under true steady-state

conditions, leading to further discrepancies between model predictions and measured values. Furthermore, the variability in driving variables of litter chemistry, N content and root:shoot ratios are underestimated when using our approach of grouping many different land uses into broad classes.

When examining the comparison between measured and modelled bulk soil C stocks for the 8192 forest and grassland sites, residuals were particularly large for high latitude forestry sites in southern Sweden and the UK (Figure 7). We hypothesize that this is primarily due to the fact that MEMS v1.0 does not simulate soil moisture controls on decomposition, and temperature effects are applied through a simple function. In reality, these sorts of forest soils are known to have very high total POM-C stocks, resulting from decades of consistent inputs and cold, wet climates resulting in low decomposition rates (Berg, 2000). Differences between measured and modelled soil C stocks are also likely due to uncertainties with driving variables and specifically the MODIS estimates of NPP. The 2009 NPP data from MODIS were used to estimate the C inputs to soils in our simulations, and these data may not be representative of the average historical C inputs for those sites, which would impact the observed amounts of soil C.

4.3 Improving the parameters of MEMS v1.0

The current iteration of the MEMS model is not intended to be able to simulate all scenarios and environmental conditions, but this study indicates it can be reasonably accurate in simulating forest and grassland sites in Europe under steady-state conditions (Figure 6; Table 4). That said, several of the parameters in MEMS v1.0 are either poorly constrained or loosely defined in the current model. The *LITfrg* parameter, for example, defines a fixed litter fragmentation and perturbation rate that transfers C from the structural litter pools (C2 and C3) belowground (to C5 and C10). The global sensitivity analysis of MEMS v1.0 indicates that *LITfrg* is particularly important for several model pools and total SOC early in a simulation (Figure 2; Figure S5). There are several areas of research that may help make this process more mechanistic in MEMS and allow for feedbacks with site conditions (e.g., Scheu and Wolters, 1991; Yoo *et al*., 2011). One option to generalise the vertical transport of structural litter into the soil may be to apply a diffusion approach that can be valid at the ecosystem scale, as described in the SOMPROF model (Braakhekke *et al*., 2011). More empirical data to link site conditions to perturbation processes (e.g., cryoturbation, bioturbation, churning clays) would help with this area of MEMS model development.

As with vertical distribution of physical SOM, the transport of DOM vertically between layers lacks a mechanistic foundation in MEMS v1.0. A noteworthy approach that attempts to simulate this transport while also representing bioturbation through diffusion and sorption-desorption processes is presented in the COMISSION model (Ahrens *et al*., 2015). While these models apply more mechanistic functions to represent these key processes, one can debate whether the increased complexity and computational demands are necessary. This, of course depends on the model objectives and in MEMS v1.0 we have prioritised parsimony and deliberately minimised the number of algorithms and parameters. While the model cannot yet address hypotheses about litter fragmentation or DOM leaching, the generic structure of MEMS v1.0 can incorporate these processes in a more explicit manner in future versions.

Additional parameters of MEMS v1.0 that are poorly constrained include those associated with the LIDEL model. These parameters (specifically those related to DOM generation and microbial assimilation, see Table 2) were estimated using Bayesian analysis that employed empirical data (Soong *et al*., 2015), but resulted in large posterior distributions with high uncertainty as noted by Campbell *et al*. (2016). Consequently, more data is required from different litter types to help constrain these parameter values. In particular, the amount of DOM leached from decaying microbial biomass (parameter la_2) is particularly important for MAOM formation when the pool is relatively small (< 25 years in Figure 2). MEMS v1.0 currently uses the estimated value from Campbell *et al*. (2016) for this parameter (0.19 g DOM g decayed microbial biomass^{-1}) but it is worth noting the reported posterior interval width was more than double this value (0.398 g DOM g decayed microbial biomass^{-1}). Similarly, the rate of microbial product generation from microbial biomass (parameter *B3*) was seen to be even more variable (Campbell *et al*., 2016). Empirically, the rate that microbial products are generated from microbial turnover is highly variable depending on the microbial community and the site conditions (Xu *et al*., 2014). While improving these parameters was outside the scope of this study, the path towards improved model performance can be addressed with new empirical data that better inform the model parameters.

4.4 Opportunities for further development in MEMS v1.0

In its current capacity, MEMS v1.0 is far from being able to simulate full ecosystems and is limited in scope regarding the land use scenarios it can simulate accurately. Specifically, the initial model does not simulate the hydrological or nitrogen cycles, and currently operates on a single soil layer. However, MEMS v1.0 has been built to have a modular architecture, with careful consideration given to how additional processes can be addressed through future model development.

The relationship between C and N in soils is fundamental to SOM dynamics (McGill and Cole, 1981), and therefore simulating the N cycle is at the forefront of plans to develop in the MEMS model. Since the MEMS model structure is based on soil fractions that can be physically isolated, each current soil C pool in MEMS v1.0 (i.e. pools C5, C8, C9 and C10) can also have a direct equivalent for N, and be consistent with the fractionation scheme for the C dynamics (Table S1). However, additional pools of nitrate and ammonium (and associated mechanisms to describe N- fixation, nitrification and denitrification) are needed to accurately describe plant-soil nutrient feedbacks. This highlights a major objective of future MEMS model development, i.e., to ensure the model can be easily coupled with existing modules that describe other aspects of the ecosystem (e.g., plant growth routines).

Another key feature of MEMS v1.0 is its ability to test specific hypotheses directly against empirical data, such as effects of soil priming on soil C stocks, effects of microbial feedbacks on OM sorption to mineral surfaces, or the effects of soil fauna on SOM formation. Because each of the existing model pools can be isolated physically and quantified, the rates of flux between these pools can also be quantified with isotopic tracer studies. Not only does this mean parameterization and evaluation data can be generated easily, but also that experiments can be designed with this mathematical framework in mind, specifically generating the data required to develop, evaluate and improve the model. While the current scope of MEMS v1.0 does not address all climate-C feedbacks, it does provide the basis for a more mechanistic model that can simulate SOM dynamics at the ecosystem scale.

5 Conclusions

As a carbon model designed around the processes that govern SOM formation, MEMS v1.0 provides an analytically tractable framework that can be used to test specific hypotheses by pairing empirical experiments with model simulations. While the inaugural version of this new model has limitations for direct evaluation with real-world measurements, on average, its performance with simulating steady–state conditions equates well with topsoil C stocks measured for ~8000 forest and grassland sites across Europe. Using a structure that aligns with our contemporary understanding of soil C dynamics, we also show that MEMS v1.0 is capable of accurately proportioning SOM between particulate and mineral-associated fractions by accounting for litter chemistry of the input material. By using litter chemistry to inform SOM formation pathways and edaphic conditions to inform the C-saturation capacity of a soil, MEMS v1.0 also shows consistent trends with experimental findings.

Next steps for MEMS model development will require detailed routines of N and hydrological cycling, as well as additional external drivers of SOM dynamics (e.g., land management practices). To reliably incorporate these aspects in the MEMS model will require effective collaboration between modellers and experimentalists to design studies that can both i) elucidate the underlying mechanisms that MEMS is built upon and ii) generate the parameterization and validation data required to reduce model uncertainty. Successful execution of this strategy will ~~advance development of~~help to develop an ecosystem scale model that can improve assessments of management and policy action on sustainability of soils and associated ecosystem services.

Code and data availability

The LUCAS dataset can be found at https://esdac.jrc.ec.europa.eu/content/lucas-2009-topsoil-data with details of the larger European Soil Data Centre project at http://doi.org/10.17616/R34069. The additional MAOM and POM fractionation data for the 154 sites used in this analysis can also be found at European Soil Data Centre (ESDAC) of the European Commission Joint Research Centre (http://esdac.jrc.ec.europa.eu/). Access to model code is currently restricted to those directly collaborating with the MEMS development team. This is to ensure all bugs are caught and treated before release to the public. Detailed information and code relevant to specific questions can be provided upon request.

Supplementary materials

See separate attachments

Author Contribution

All authors contributed to the conceptualization of the MEMS model framework with MFC, KP and MDW formalizing the original foundational science. The *in-practice* model structure was then formalized by ADR, MFC, KP, SO and MWD. All model building, coding, statistical analyses and data analysis on the measured fractionation data and all model-measure comparisons was performed by ADR. Guidance on the optimisation procedures was provided by SO. The LUCAS database was provided by EL and all initial analysis and preparation of the data (e.g., refining bulk density estimates and NPP values for each site) was performed by EL. The project was overseen by all authors but primarily led by MFC. Funding was initially provided by MDW and later through grants awarded to MFC and KP. Developing, testing and evaluating the model was performed solely by ADR, as was all data presentation apart from the final conceptual diagram (Figure 1) which was outsourced (see acknowledgments). The manuscript was written and edited by ADR with comments and feedback from all co-authors.

Competing Interests

The authors declare that they have no conflict of interest.

Disclaimer

Acknowledgments

This research was supported by a National Science Foundation CAREER grant (number 255228) awarded to MDW, the US DOE Advanced Research Projects Agency-Energy program (ROOTS project; DE-FOA-00001565), the NSF-DEB Award #1743237 and the JRC (purchase order D.B720517). The authors like to thank Michelle Haddix for the soil organic matter fractionation work and Dr. Yao Zhang for help with regards to various parts of data generation

(e.g., climate inputs) and model development. The conceptual figure diagram was redrawn and stylized by Katie Burnet.

References

Aber, J. D., Melillo, J. M., & McClaugherty, C. A. (1990). Predicting long-term patterns of mass loss, nitrogen dynamics, and soil organic matter formation from initial fine litter chemistry in temperate forest ecosystems. *Canadian Journal of Botany*, 68(10), 2201-2208.

Abramoff, R., Xu, X., Hartman, M., O'Brien, S., Feng, W., Davidson, E., Finzi, A., Moorhead, D., Schimel, J., Torn, M. & Mayes, M. A. (2018). The Millennial model: in search of measurable pools and transformations for modeling soil carbon in the new century. *Biogeochemistry*, 137(1-2), 51-71.

Ahrens, B., Braakhekke, M. C., Guggenberger, G., Schrumpf, M., & Reichstein, M. (2015). Contribution of sorption, DOC transport and microbial interactions to the 14C age of a soil organic carbon profile: Insights from a calibrated process model. *Soil Biology and Biochemistry*, 88, 390-402.

Allison, S. D. (2012). A trait-based approach for modelling microbial litter decomposition. *Ecology letters*, 15(9), 1058-1070.

Allison, S. D., Wallenstein, M. D., & Bradford, M. A. (2010). Soil-carbon response to warming dependent on microbial physiology. *Nature Geoscience*, 3(5), 336.

Arora, V. K., Boer, G. J., Friedlingstein, P., Eby, M., Jones, C. D., Christian, J. R., Bonan, G., Bopp, L., Brovkin, V., Cadule, P., Hajima, T., Ilyini, T., Lindsay, K., Tjiputra, J.F. & Wu, T. (2013). Carbon–concentration and carbon–climate feedbacks in CMIP5 Earth system models. *Journal of Climate*, 26(15), 5289-5314.

Averill, C., & Waring, B. (2018). Nitrogen limitation of decomposition and decay: How can it occur?. *Global Change Biology*, 24(4), 1417-1427.

Beare, M. H., McNeill, S. J., Curtin, D., Parfitt, R. L., Jones, H. S., Dodd, M. B., & Sharp, J. (2014). Estimating the organic carbon stabilisation capacity and saturation deficit of soils: a New Zealand case study. *Biogeochemistry*, 120(1-3), 71-87.

Berg, B. (2000). Litter decomposition and organic matter turnover in northern forest soils. *Forest ecology and Management*, 133(1-2), 13-22.

Braakhekke, M. C., Beer, C., Hoosbeek, M. R., Reichstein, M., Kruijt, B., Schrumpf, M., & Kabat, P. (2011). SOMPROF: A vertically explicit soil organic matter model. *Ecological modelling,* 222(10), 1712-1730.

Bradford, M. A., Watts, B. W., & Davies, C. A. (2010). Thermal adaptation of heterotrophic soil respiration in laboratory microcosms. *Global Change Biology*, 16(5), 1576-1588.

Bu, R., Lu, J., Ren, T., Liu, B., Li, X., & Cong, R. (2015). Particulate organic matter affects soil nitrogen mineralization under two crop rotation systems. *PLoS One*, 10(12), e0143835.

Büks, F., & Kaupenjohann, M. (2016). Enzymatic biofilm digestion in soil aggregates facilitates the release of particulate organic matter by sonication. *Soil*, 2(4), 499-509.

Cambardella, C. A., & Elliott, E. T. (1992). Particulate soil organic-matter changes across a grassland cultivation sequence. *Soil science society of America journal*, 56(3), 777-783.

Campbell, E. E., & Paustian, K. (2015). Current developments in soil organic matter modeling and the expansion of model applications: a review. *Environmental Research Letters*, 10(12), 123004.

Campbell, E. E., Parton, W. J., Soong, J. L., Paustian, K., Hobbs, N. T., & Cotrufo, M. F. (2016). Using litter chemistry controls on microbial processes to partition litter carbon fluxes with the litter decomposition and leaching (LIDEL) model. *Soil Biology and Biochemistry*, 100, 160-174.

Canadell, J., Jackson, R. B., Ehleringer, J. B., Mooney, H. A., Sala, O. E., & Schulze, E. D. (1996). Maximum rooting depth of vegetation types at the global scale. *Oecologia*, 108(4), 583-595.

Carrington, E. M., Hernes, P. J., Dyda, R. Y., Plante, A. F., & Six, J. (2012). Biochemical changes across a carbon saturation gradient: lignin, cutin, and suberin decomposition and stabilization in fractionated carbon pools. *Soil Biology and Biochemistry*, 47, 179-190.

Castellano, M. J., Mueller, K. E., Olk, D. C., Sawyer, J. E., & Six, J. (2015). Integrating plant litter quality, soil organic matter stabilization, and the carbon saturation concept. *Global Change Biology*, 21(9), 3200-3209.

Christensen, B. T. (1992). Physical fractionation of soil and organic matter in primary particle size and density separates. In Advances in soil science (pp. 1-90). Springer, New York, NY.

Cotrufo, M. F., Soong, J. L., Horton, A. J., Campbell, E. E., Haddix, M. L., Wall, D. H., & Parton, W. J. (2015). Formation of soil organic matter via biochemical and physical pathways of litter mass loss. *Nature Geoscience*, 8(10), ngeo2520.

Cotrufo, M. F., Wallenstein, M. D., Boot, C. M., Denef, K., & Paul, E. (2013). The M icrobial E fficiency-M atrix S tabilization (MEMS) framework integrates plant litter decomposition with soil organic matter stabilization: do labile plant inputs form stable soil organic matter?. *Global Change Biology*, 19(4), 988-995.

~~Cotrufo, M.F., Ranalli, M.G., Haddix, M.L., Six, J. and Lugato, E., (2018). Drivers of soil C:N stoichiometry and implication for soil carbon accrual. *Science*, in review~~

Crow, S. E., Swanston, C. W., Lajtha, K., Brooks, J. R., & Keirstead, H. (2007). Density fractionation of forest soils: methodological questions and interpretation of incubation results and turnover time in an ecosystem context. *Biogeochemistry*, 85(1), 69-90.

DeGryze, S., Six, J., Paustian, K., Morris, S. J., Paul, E. A., & Merckx, R. (2004). Soil organic carbon pool changes following land-use conversions. *Global Change Biology*, 10(7), 1120-1132.

Dorodnikov, M., Blagodatskaya, E., Blagodatsky, S., Marhan, S., Fangmeier, A., & Kuzyakov, Y. (2009). Stimulation of microbial extracellular enzyme activities by elevated CO2 depends on soil aggregate size. *Global Change Biology*, 15(6), 1603-1614.

Dungait, J. A., Hopkins, D. W., Gregory, A. S., & Whitmore, A. P. (2012). Soil organic matter turnover is governed by accessibility not recalcitrance. *Global Change Biology*, 18(6), 1781-1796.

Dwivedi, D., Riley, W. J., Torn, M. S., Spycher, N., Maggi, F., & Tang, J. Y. (2017). Mineral properties, microbes, transport, and plant-input profiles control vertical distribution and age of soil carbon stocks. *Soil Biology and Biochemistry*, 107, 244-259.

Elliott, E. T., Paustian, K., & Frey, S. D. (1996). Modeling the measurable or measuring the modelable: A hierarchical approach to isolating meaningful soil organic matter fractionations. In Evaluation of soil organic matter models (pp. 161-179). Springer, Berlin, Heidelberg.

Feng, W. (2012). Testing the soil carbon saturation theory: maximal carbon stabilization and soil organic matter stability as a function of organic carbon inputs. PhD Thesis, University of Pennsylvania

Filley, T. R., Boutton, T. W., Liao, J. D., Jastrow, J. D., & Gamblin, D. E. (2008). Chemical changes to nonaggregated particulate soil organic matter following grassland-to-woodland transition in a subtropical savanna. *Journal of Geophysical Research: Biogeosciences*, 113(G3).

Frouz, J. (2018). Effects of soil macro-and mesofauna on litter decomposition and soil organic matter stabilization. *Geoderma*, 332, 161-172.

Gentile, R., Vanlauwe, B., & Six, J. (2011). Litter quality impacts short-but not long-term soil carbon dynamics in soil aggregate fractions. *Ecological Applications*, 21(3), 695-703.

Gulde, S., Chung, H., Amelung, W., Chang, C., & Six, J. (2008). Soil carbon saturation controls labile and stable carbon pool dynamics. *Soil Science Society of America Journal*, 72(3), 605-612.

Haddix, M. L., Paul, E. A., & Cotrufo, M. F. (2016). Dual, differential isotope labeling shows the preferential movement of labile plant constituents into mineral-bonded soil organic matter. *Global Change Biology*, 22(6), 2301-2312.

Harmon, M., and J. Domingo (2001), A User's Guide to STANDCARB Version 2.0: A Model to Simulate the Carbon Stores in Forest Stands, Dep. of For. Sci., Oreg. State Univ., Corvallis.

Heckman, K., Grandy, A. S., Gao, X., Keiluweit, M., Wickings, K., Carpenter, K., Chorover, J. & Rasmussen, C. (2013). Sorptive fractionation of organic matter and formation of organo-hydroxy-aluminum complexes during litter biodegradation in the presence of gibbsite. *Geochimica et Cosmochimica Acta*, 121, 667-683.

Huang, P. M., Wang, M. K., & Chiu, C. Y. (2005). Soil mineral–organic matter–microbe interactions: impacts on biogeochemical processes and biodiversity in soils. *Pedobiologia*, 49(6), 609-635.

Jackson, R. B., Canadell, J., Ehleringer, J. R., Mooney, H. A., Sala, O. E., & Schulze, E. D. (1996). A global analysis of root distributions for terrestrial biomes. *Oecologia*, 108(3), 389-411.

Jenkinson, D. S. (1977). Studies on the decomposition of plant material in soil. V. The effects of plant cover and soil type on the loss of carbon from14c labelled ryegrass decomposing under field conditions. *Journal of Soil Science*, 28(3), 424-434.

Jenkinson, D. S., & Rayner, J. H. (1977). The turnover of soil organic matter in some of the Rothamsted classical experiments. *Soil science*, 123(5), 298-305.

Jilling, A., Keiluweit, M., Contosta, A. R., Frey, S., Schimel, J., Schnecker, J., Smith, R. G., Tieman, L. & Grandy, A. S. Minerals in the rhizosphere: overlooked mediators of soil nitrogen availability to plants and microbes. *Biogeochemistry*, 1-20.

Jones, C., & Falloon, P. (2009). Sources of uncertainty in global modelling of future soil organic carbon storage. In Uncertainties in Environmental Modelling and Consequences for Policy Making (pp. 283-315). Springer, Dordrecht.

Kalbitz, K., Schwesig, D., Rethemeyer, J., & Matzner, E. (2005). Stabilization of dissolved organic matter by sorption to the mineral soil. *Soil Biology and Biochemistry*, 37(7), 1319-1331.

Kallenbach, C. M., Frey, S. D., & Grandy, A. S. (2016). Direct evidence for microbial-derived soil organic matter formation and its ecophysiological controls. *Nature communications*, 7, 13630.

Keiluweit, M., Nico, P. S., Kleber, M., & Fendorf, S. (2016). Are oxygen limitations under recognized regulators of organic carbon turnover in upland soils?. *Biogeochemistry*, *127*(2-3), 157-171.

Kindler, R., Siemens, J. A. N., Kaiser, K., Walmsley, D. C., Bernhofer, C., Buchmann, N., ... & Heim, A. (2011). Dissolved carbon leaching from soil is a crucial component of the net ecosystem carbon balance. *Global Change Biology*, 17(2), 1167-1185.

Kirschbaum, M. U., & Paul, K. I. (2002). Modelling C and N dynamics in forest soils with a modified version of the CENTURY model. *Soil Biology and Biochemistry*, 34(3), 341-354.

Kleber, M., Nico, P. S., Plante, A., Filley, T., Kramer, M., Swanston, C., & Sollins, P. (2011). Old and stable soil organic matter is not necessarily chemically recalcitrant: implications for modeling concepts and temperature sensitivity. *Global Change Biology*, 17(2), 1097-1107.

Klotzbücher, T., Kaiser, K., Guggenberger, G., Gatzek, C., & Kalbitz, K. (2011). A new conceptual model for the fate of lignin in decomposing plant litter. *Ecology*, 92(5), 1052-1062.

Kögel-Knabner, I., Guggenberger, G., Kleber, M., Kandeler, E., Kalbitz, K., Scheu, S., Eusterhues, K. & Leinweber, P. (2008). Organo-mineral associations in temperate soils: Integrating biology, mineralogy, and organic matter chemistry. *Journal of Plant Nutrition and Soil Science*, 171(1), 61-82.

Kolka, R., Weishampel, P., & Fröberg, M. (2008). Measurement and importance of dissolved organic carbon. In Field measurements for forest carbon monitoring (pp. 171-176). Springer, Dordrecht.

Kothawala, D. N., Moore, T. R., & Hendershot, W. H. (2008). Adsorption of dissolved organic carbon to mineral soils: A comparison of four isotherm approaches. *Geoderma*, 148(1), 43-50.

Kothawala, D. N., Moore, T. R., & Hendershot, W. H. (2009). Soil properties controlling the adsorption of dissolved organic carbon to mineral soils. *Soil Science Society of America Journal*, 73(6), 1831-1842.

Kothawala, D. N., Roehm, C., Blodau, C., & Moore, T. R. (2012). Selective adsorption of dissolved organic matter to mineral soils. *Geoderma*, 189, 334-342.

Kuhn, M., & Johnson, K. (2013). Applied predictive modeling (Vol. 26). New York: Springer.

Kuzyakov, Y. (2010). Priming effects: interactions between living and dead organic matter. *Soil Biology and Biochemistry*, 42(9), 1363-1371.

Lawrence, C. R., Neff, J. C., & Schimel, J. P. (2009). Does adding microbial mechanisms of decomposition improve soil organic matter models? A comparison of four models using data from a pulsed rewetting experiment. *Soil Biology and Biochemistry*, 41(9), 1923-1934.

Lehmann, J., & Kleber, M. (2015). The contentious nature of soil organic matter. *Nature*, 528(7580), 60.

Li, C., Frolking, S., & Frolking, T. A. (1992). A model of nitrous oxide evolution from soil driven by rainfall events: 1. Model structure and sensitivity. *Journal of Geophysical Research: Atmospheres*, 97(D9), 9759-9776.

Liang, C., Schimel, J. P., & Jastrow, J. D. (2017). The importance of anabolism in microbial control over soil carbon storage. *Nature microbiology*, 2(8), 17105.

Ludwig, M., Achtenhagen, J., Miltner, A., Eckhardt, K. U., Leinweber, P., Emmerling, C., & Thiele-Bruhn, S. (2015). Microbial contribution to SOM quantity and quality in density fractions of temperate arable soils. *Soil Biology and Biochemistry*, *81*, 311-322.

Luo, Y., Ahlström, A., Allison, S. D., Batjes, N. H., Brovkin, V., Carvalhais, N., ... & Georgiou, K. (2016). Toward more realistic projections of soil carbon dynamics by Earth system models. *Global Biogeochemical Cycles*, 30(1), 40-56.

Lützow, M. V., Kögel-Knabner, I., Ekschmitt, K., Matzner, E., Guggenberger, G., Marschner, B., & Flessa, H. (2006). Stabilization of organic matter in temperate soils: mechanisms and their relevance under different soil conditions–a review. *European Journal of Soil Science*, 57(4), 426-445.

Malamoud, K., McBratney, A. B., Minasny, B., & Field, D. J. (2009). Modelling how carbon affects soil structure. *Geoderma*, 149(1-2), 19-26.

Manzoni, S., Jackson, R. B., Trofymow, J. A., & Porporato, A. (2008). The global stoichiometry of litter nitrogen mineralization. Science, 321(5889), 684-686.

Manzoni, S., Moyano, F., Kätterer, T., & Schimel, J. (2016). Modeling coupled enzymatic and solute transport controls on decomposition in drying soils. *Soil Biology and Biochemistry*, 95, 275-287.

Marschner, B., Brodowski, S., Dreves, A., Gleixner, G., Gude, A., Grootes, P. M., ... & Kaiser, K. (2008). How relevant is recalcitrance for the stabilization of organic matter in soils?. *Journal of plant nutrition and soil science*, 171(1), 91-110.

Mayes, M. A., Heal, K. R., Brandt, C. C., Phillips, J. R., & Jardine, P. M. (2012). Relation between soil order and sorption of dissolved organic carbon in temperate subsoils. *Soil Science Society of America Journal*, 76(3), 1027-1037.

McGill, W.B., and C.V. Cole (1981) Comparative aspects of cycling of organic C, N, S and P through soil organic matter. *Geoderma* 26:267-286.

McGill W., Hunt H., Woodmansee R. and Reuss J. (1981). Phoenix, a model of the dynamics of carbon and nitrogen in grassland soils Terrestrial Nitrogen Cycles (Ecological Bulletins) (Stockholm, Sweden: Swedish Natural Science Research Council) pp 49–115

913 Miki, T., Ushio, M., Fukui, S., & Kondoh, M. (2010). Functional diversity of microbial decomposers facilitates plant
914 coexistence in a plant–microbe–soil feedback model. *Proceedings of the National Academy of Sciences*,
915 107(32), 14251-14256.
916 Mikutta, R., Kleber, M., Torn, M. S., & Jahn, R. (2006). Stabilization of soil organic matter: association with minerals
917 or chemical recalcitrance? *Biogeochemistry*, 77(1), 25-56.
918 Moorhead, D. L., Lashermes, G., Sinsabaugh, R. L., & Weintraub, M. N. (2013). Calculating co-metabolic costs of
919 lignin decay and their impacts on carbon use efficiency. *Soil Biology and Biochemistry*, 66, 17-19.
920 Moorhead, D., Lashermes, G., Recous, S., & Bertrand, I. (2014). Interacting microbe and litter quality controls on
921 litter decomposition: a modeling analysis. *PloS one*, 9(9), e108769.
922 NOAA (2018) CPC Global Temperature data provided by the NOAA/OAR/ESRL PSD, Boulder, Colorado, USA,
923 from their Web site at https://www.esrl.noaa.gov/psd/
924 ORNL DAAC (2009) MODIS and VIIRS Land Products Global Subsetting and Visualization Tool. ORNL DAAC,
925 Oak Ridge, Tennessee, USA. Accessed March 20, 2016. Subset obtained for MOD13Q1 product at various
926 sites in Spatial Range: N=70.00N, S=20.00N, E=35.00, W=-15.00W, time period: 2009 to 2009, and subset
927 size: 0.25 x 0.25 km.
928 Parton, W. J., Schimel, D. S., Cole, C. V., & Ojima, D. S. (1987). Analysis of factors controlling soil organic matter
929 levels in Great Plains Grasslands 1. *Soil Science Society of America Journal*, 51(5), 1173-1179.
930 Paton, T., Humphreys, G.S., Mitchell, P., 1995. Soils: A New Global View. Yale Univ. Press, New Haven [u.a.],
931 pp.33–67 (Chapter3.Bioturbation).
932 Paul, E. A. & van Veen, J. A. (1978). The use of tracers to determine the dynamic nature of organic matter. *Trans.*
933 *11th Int. Congress of Soil Science*, 3, 61-102.
934 Poeplau, C. (2016). Estimating root: shoot ratio and soil carbon inputs in temperate grasslands with the RothC model.
935 *Plant and soil*, 407(1-2), 293-305.
936 Poeplau, C., & Don, A. (2013). Sensitivity of soil organic carbon stocks and fractions to different land-use changes
937 across Europe. *Geoderma*, 192, 189-201.
938 Poeplau, C., Don, A., Six, J., Kaiser, M., Benbi, D., Chenu, C., ... & Gregorich, E. (2018). Isolating organic carbon
939 fractions with varying turnover rates in temperate agricultural soils–A comprehensive method comparison. *Soil*
940 *Biology and Biochemistry*, 125, 10-26.
941 Poeplau, C., Kätterer, T., Leblans, N. I., & Sigurdsson, B. D. (2017). Sensitivity of soil carbon fractions and their
942 specific stabilization mechanisms to extreme soil warming in a subarctic grassland. *Global Change Biology*,
943 23(3), 1316-1327.
944 R Core Team (2018). R: A language and environment for statistical computing. R Foundation for Statistical
945 Computing, Vienna, Austria. URL https://www.R-project.org/.
946 Saltelli, A., Ratto, M., Andres, T., Campolongo, F., Cariboni, J., Gatelli, D., ... & Tarantola, S. (2008). Global
947 sensitivity analysis: the primer. John Wiley & Sons.
948 Scheibe, A., & Gleixner, G. (2014). Influence of litter diversity on dissolved organic matter release and soil carbon
949 formation in a mixed beech forest. *PloS one*, 9(12), e114040.
950 Scheu, S., & Wolters, V. (1991). Influence of fragmentation and bioturbation on the decomposition of 14C-labelled
951 beech leaf litter. *Soil Biology and Biochemistry*, 23(11), 1029-1034.
952 Schmidt, M. W., Torn, M. S., Abiven, S., Dittmar, T., Guggenberger, G., Janssens, I. A., ... & Nannipieri, P. (2011).
953 Persistence of soil organic matter as an ecosystem property. *Nature*, 478(7367), 49.
954 Setia, R., Verma, S. L., & Marschner, P. (2012). Measuring microbial biomass carbon by direct extraction–
955 comparison with chloroform fumigation-extraction. *European journal of soil biology*, 53, 103-106.
956 Sierra, C. A., Malghani, S., & Müller, M. (2015). Model structure and parameter identification of soil organic matter
957 models. *Soil Biology and Biochemistry*, 90, 197-203.
958 Sima, N. Q., Harmel, R. D., Fang, Q. X., Ma, L., & Andales, A. A. (2018). A modified F-test for evaluating model
959 performance by including both experimental and simulation uncertainties. *Environmental Modelling &*
960 *Software*, 104, 236-248.
961 Sinsabaugh, R. L., Manzoni, S., Moorhead, D. L., & Richter, A. (2013). Carbon use efficiency of microbial
962 communities: stoichiometry, methodology and modelling. *Ecology letters*, 16(7), 930-939.
963 Six, J., Conant, R. T., Paul, E. A., & Paustian, K. (2002). Stabilization mechanisms of soil organic matter: implications
964 for C-saturation of soils. *Plant and soil*, 241(2), 155-176.
965 Smith, P., Smith, J. U., Powlson, D. S., McGill, W. B., Arah, J. R. M., Chertov, O. G., ... & Jensen, L. S. (1997). A
966 comparison of the performance of nine soil organic matter models using datasets from seven long-term
967 experiments. *Geoderma*, 81(1-2), 153-225.
968 Sobol, I. M. (2001). Global sensitivity indices for nonlinear mathematical models and their Monte Carlo estimates.
969 *Mathematics and computers in simulation*, 55(1-3), 271-280.
970 Soetaert, K., Petzoldt, T., & Setzer, R. W. (2010). Solving Differential Equations in R: Package deSolve. *Journal of*
971 *Statistical Software*, 33(9), 1—25

Soong, J. L., Parton, W. J., Calderon, F., Campbell, E. E., & Cotrufo, M. F. (2015). A new conceptual model on the fate and controls of fresh and pyrolized plant litter decomposition. *Biogeochemistry*, 124(1-3), 27-44.

Soong, J. L., Vandegehuchte, M. L., Horton, A. J., Nielsen, U. N., Denef, K., Shaw, E. A., de Tomasel, C. M., Parton, W., Wall, D. H. & Cotrufo, M. F. (2016). Soil microarthropods support ecosystem productivity and soil C accrual: evidence from a litter decomposition study in the tallgrass prairie. *Soil Biology and Biochemistry*, *92*, 230-238.

Sokol, N. W., Sanderman, J., & Bradford, M. A. (2018). Pathways of mineral-associated soil organic matter formation: Integrating the role of plant carbon source, chemistry, and point of entry. *Global change biology*. https://doi.org/10.1111/gcb.14482

Stewart, C. E., Paustian, K., Conant, R. T., Plante, A. F., & Six, J. (2007). Soil carbon saturation: concept, evidence and evaluation. *Biogeochemistry*, 86(1), 19-31.

Stewart, C. E., Plante, A. F., Paustian, K., Conant, R. T., & Six, J. (2008). Soil Carbon Saturation: Linking Concept and Measurable Carbon Pools. *Soil Science Society of America Journal*, 72(2), 379-392.

Stockmann, U., Adams, M. A., Crawford, J. W., Field, D. J., Henakaarchchi, N., Jenkins, M., ... & Wheeler, I. (2013). The knowns, known unknowns and unknowns of sequestration of soil organic carbon. *Agriculture, Ecosystems & Environment*, 164, 80-99.

Stout, J. D. & O'Brien, B. J. (1973). Factors affecting radiocarbon enrichment in soil and the turnover of soil organic matter. Proceedings of the 8th International Conference on Radiocarbon Dating, Vol. 2, pp. 394-407, Wellington, New Zealand.

Subke, J. A., Inglima, I., & Francesca Cotrufo, M. (2006). Trends and methodological impacts in soil CO2 efflux partitioning: a metaanalytical review. *Global Change Biology*, 12(6), 921-943.

Swift, M. J., Heal, O. W., Anderson, J. M., & Anderson, J. M. (1979). Decomposition in terrestrial ecosystems (Vol. 5). Univ of California Press.

Tan, Z., Lal, R., Owens, L., & Izaurralde, R. C. (2007). Distribution of light and heavy fractions of soil organic carbon as related to land use and tillage practice. *Soil and Tillage Research*, 92(1-2), 53-59.

Tappi (1981) Water solubility of wood and pulp. Test method T204 (or 207). Technical Association of the Pulp and Paper Industry, Atlanta

Toth G., Jones A., Montanarella L. (2013) LUCAS Topsoil Survey — methodology, data and results. In: JRC Technical Reports. European Union, Luxemburg.

Treseder, K. K., Balser, T. C., Bradford, M. A., Brodie, E. L., Dubinsky, E. A., Eviner, V. T., ... & Pett-Ridge, J. (2012). Integrating microbial ecology into ecosystem models: challenges and priorities. *Biogeochemistry*, 109(1-3), 7-18.

Trumbore, S. E., Schiff, S. L., Aravena, R., & Elgood, R. (1992). Sources and transformation of dissolved organic carbon in the Harp Lake forested catchment: the role of soils. *Radiocarbon*, 34(3), 626-635.

Van Soest PJ, Robertson JB, Lewis BA (1991) Methods for dietary fiber, neutral detergent fiber, and nonstarch polysaccharides in relation to animal nutrition. *Journal of Dairy Science*, 74(10):3583–3597.

Van Soest PJ, Wine RH (1968) Determination of lignin and cellulose in acid-detergent fiber with permanganate. *Journal of Associated Official Analytical Chemistry*, 51(4):780

Větrovský, T., Steffen, K. T., & Baldrian, P. (2014). Potential of cometabolic transformation of polysaccharides and lignin in lignocellulose by soil Actinobacteria. *PLoS One*, 9(2), e89108.

von Lützow, M., Kögel-Knabner, I., Ekschmitt, K., Flessa, H., Guggenberger, G., Matzner, E., & Marschner, B. (2007). SOM fractionation methods: relevance to functional pools and to stabilization mechanisms. *Soil Biology and Biochemistry*, 39(9), 2183-2207.

Wallenstein, M. D., & Hall, E. K. (2012). A trait-based framework for predicting when and where microbial adaptation to climate change will affect ecosystem functioning. *Biogeochemistry*, 109(1-3), 35-47.

Wander, M. (2004). Soil organic matter fractions and their relevance to soil function. Soil organic matter in sustainable agriculture. CRC Press, Boca Raton, FL, 67-102.

Wang, G., Post, W. M., & Mayes, M. A. (2013). Development of microbial-enzyme-mediated decomposition model parameters through steady-state and dynamic analyses. *Ecological Applications*, 23(1), 255-272.

Waring, B. G., Averill, C., & Hawkes, C. V. (2013). Differences in fungal and bacterial physiology alter soil carbon and nitrogen cycling: insights from meta-analysis and theoretical models. *Ecology letters*, 16(7), 887-894.

Wieder, W. R., Allison, S. D., Davidson, E. A., Georgiou, K., Hararuk, O., He, Y., ... & Todd-Brown, K. (2015). Explicitly representing soil microbial processes in Earth system models. *Global Biogeochemical Cycles*, 29(10), 1782-1800.

Wieder, W. R., Bonan, G. B., & Allison, S. D. (2013). Global soil carbon projections are improved by modelling microbial processes. *Nature Climate Change*, 3(10), 909.

Wieder, W. R., Grandy, A. S., Kallenbach, C. M., & Bonan, G. B. (2014). Integrating microbial physiology and physio-chemical principles in soils with the MIcrobial-MIneral Carbon Stabilization (MIMICS) model. *Biogeosciences*, 11(14), 3899-3917.

Williams, J. R., Jones, C. A., & Dyke, P. T. (1984). A modeling approach to determining the relationship between erosion and soil productivity. *Transactions of the ASAE*, 27(1), 129-0144.

Xu, X., Schimel, J. P., Thornton, P. E., Song, X., Yuan, F., & Goswami, S. (2014). Substrate and environmental controls on microbial assimilation of soil organic carbon: a framework for Earth system models. *Ecology Letters*, 17(5), 547-555.

Yoo, K., Ji, J., Aufdenkampe, A., & Klaminder, J. (2011). Rates of soil mixing and associated carbon fluxes in a forest versus tilled agricultural field: Implications for modeling the soil carbon cycle. Journal of Geophysical Research: *Biogeosciences*, 116(G1).

Zimmermann, M., Leifeld, J., Schmidt, M. W. I., Smith, P., & Fuhrer, J. (2007). Measured soil organic matter fractions can be related to pools in the RothC model. *European Journal of Soil Science*, 58(3), 658-667.

Figure legends

Figure 1 - Conceptual model diagram of MEMS v1.0 (see Table 1 for detailed information regarding each pool). Litter pools of MEMS v1.0 are defined as > 2mm particles and comprise of hot-water extractable (C1), acid-soluble (C2) and acid-insoluble (C3) fractions. A microbial pool (C4) and dissolved carbon pool (C6) are also part of the organic horizon and litter decomposition processes (see LIDEL for more information, Campbell et al., 2016). Soil organic matter (< 2mm particles belowground) comprises of a light particulate organic matter pool (light POM, C10) formed from the input through fragmentation and physical transfer of the structural litter residues (C2 and C3), a coarse heavy POM pool (C5) formed from both litter fragmentation and microbial residues coating sand-sized particles, a dissolved organic matter (DOM) pool (C8) formed from the decomposition of all other pools and receiving DOM from the organic soil layer, and a mineral-associated organic matter pool (MAOM C9), which exchanges C through sorption and desorption with the DOM. Arrows indicate the fluxes of carbon between the different pools. Carbon dioxide is produced from a number of these fluxes but for simplicity of graphical representation, these arrows are not linked to the carbon dioxide pool (C7). Deeper soil layers can be represented by the same structure, with or without root inputs depending on depth, but are not implemented in this inaugural version of MEMS v1.0.

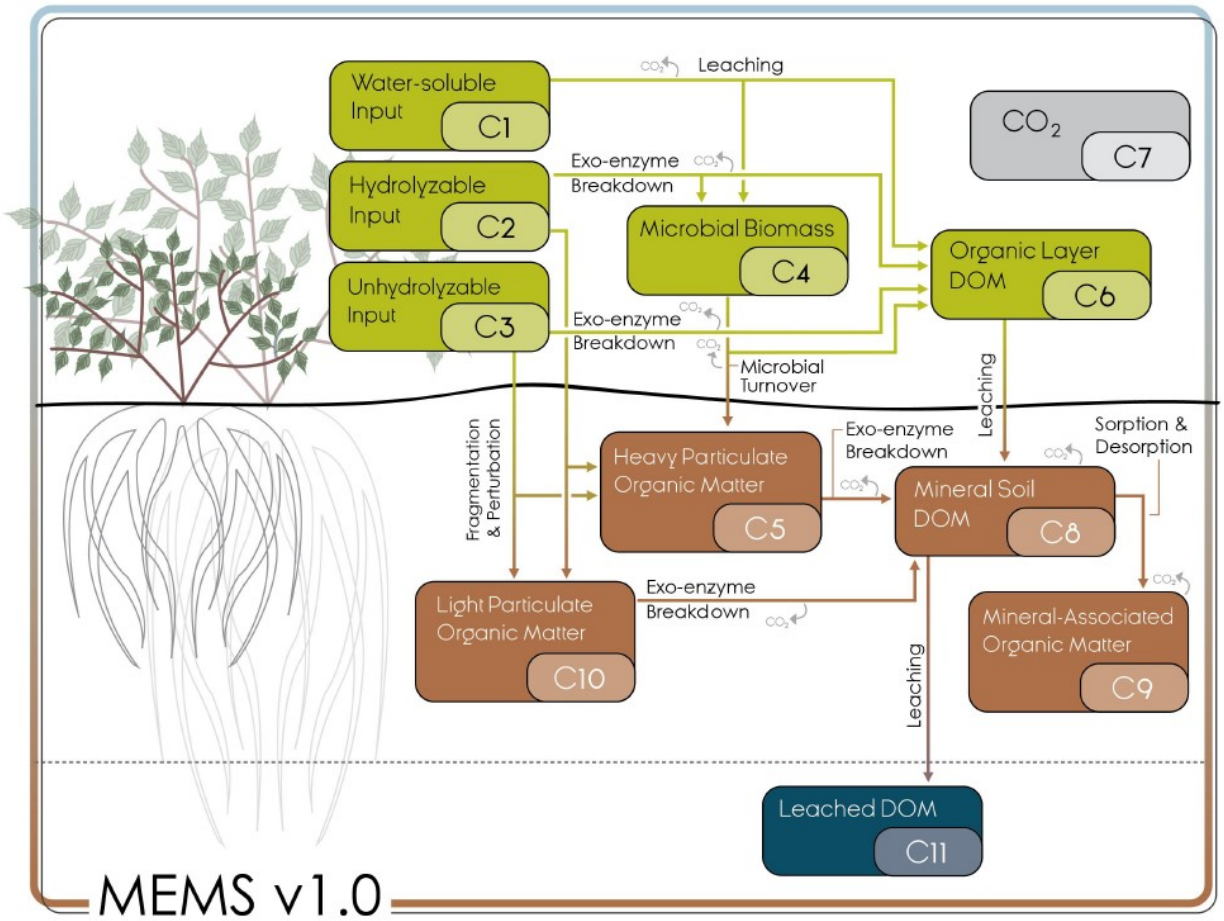

Figure 2 - Global sensitivity analysis results showing the relative contribution of each parameter to a change in carbon stock of each pool in MEMS v1.0 (leached carbon to deeper soil layers [pool C11] is omitted for clarity) after simulation to steady-state. Details of each parameter and the abbreviations used can be found in Table 2. The sensitivity analysis was repeated annually for simulation times between 1 and 100 years, every 10 years after that to 400-year simulations and every 100 years after that up to a 1000-year simulation. Results are presented on a log scale in years. The four parameters that were optimized in our analysis (Table S2) are coloured to highlight their importance in the different pools (mid-point of logistic curve where nitrogen content of input influences microbial carbon use efficiency, *Nmid*, red; maximum decay rate of heavy particulate organic matter, *k5*, orange; maximum decay rate of mineral-associated organic matter, *k9*, blue; maximum decay rate of light particulate organic matter, *k10*, green). ~~Parameters involved in different SOM formation processes are grouped by colour: yellows – parameters that define DOM leaching from the organic horizon to the soil layer; reds – parameters that affect microbial carbon use efficiency, purples – parameters that affect organic matter vertical transport to deeper layers, greens – maximum decay rates.~~A fully colourised version of these results can be in Figure S5.

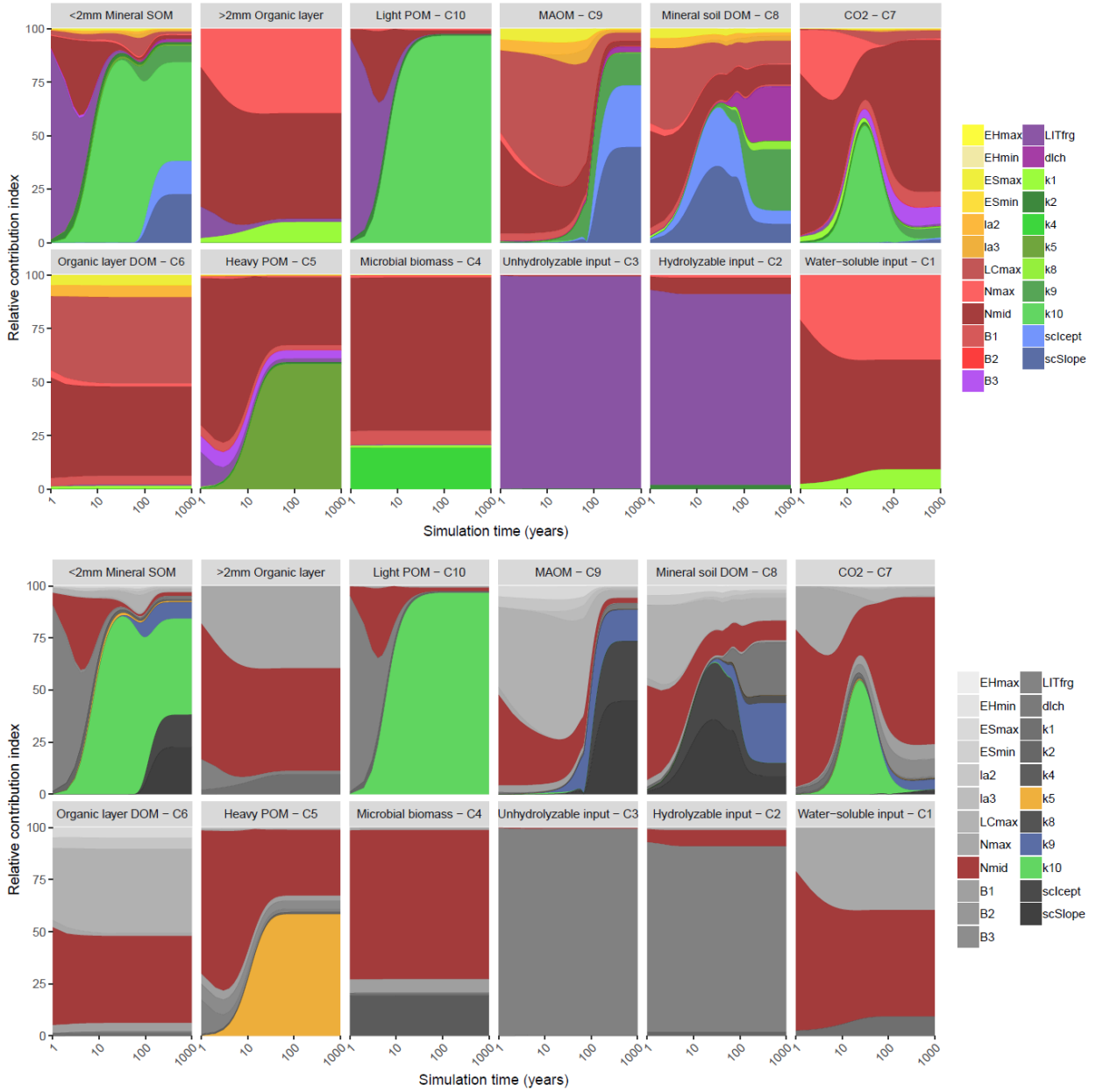

Figure 3 - The ratio between mineral-associated organic matter and total particulate organic matter (MAOM:POM) under steady-state input conditions in MEMS v1.0 as a response to the full, realistic range of driving variables. Note, total POM refers to the sum of pools C5 and C10. Each input was varied individually while all others remained fixed at baseline values (indicated by dashed lines) – mean, maximum and minimum values for litter chemistry driving variables (*LitN*, *fDOC*, *fLIG* and *fSOL*) were derived from Campbell *et al.* (2016) and edaphic, climatic and C input driving variables (soil bulk density, sand content, soil pH, mean annual temperature and annual net primary productivity) were derived from the LUCAS dataset (Toth *et al.*, 2013).

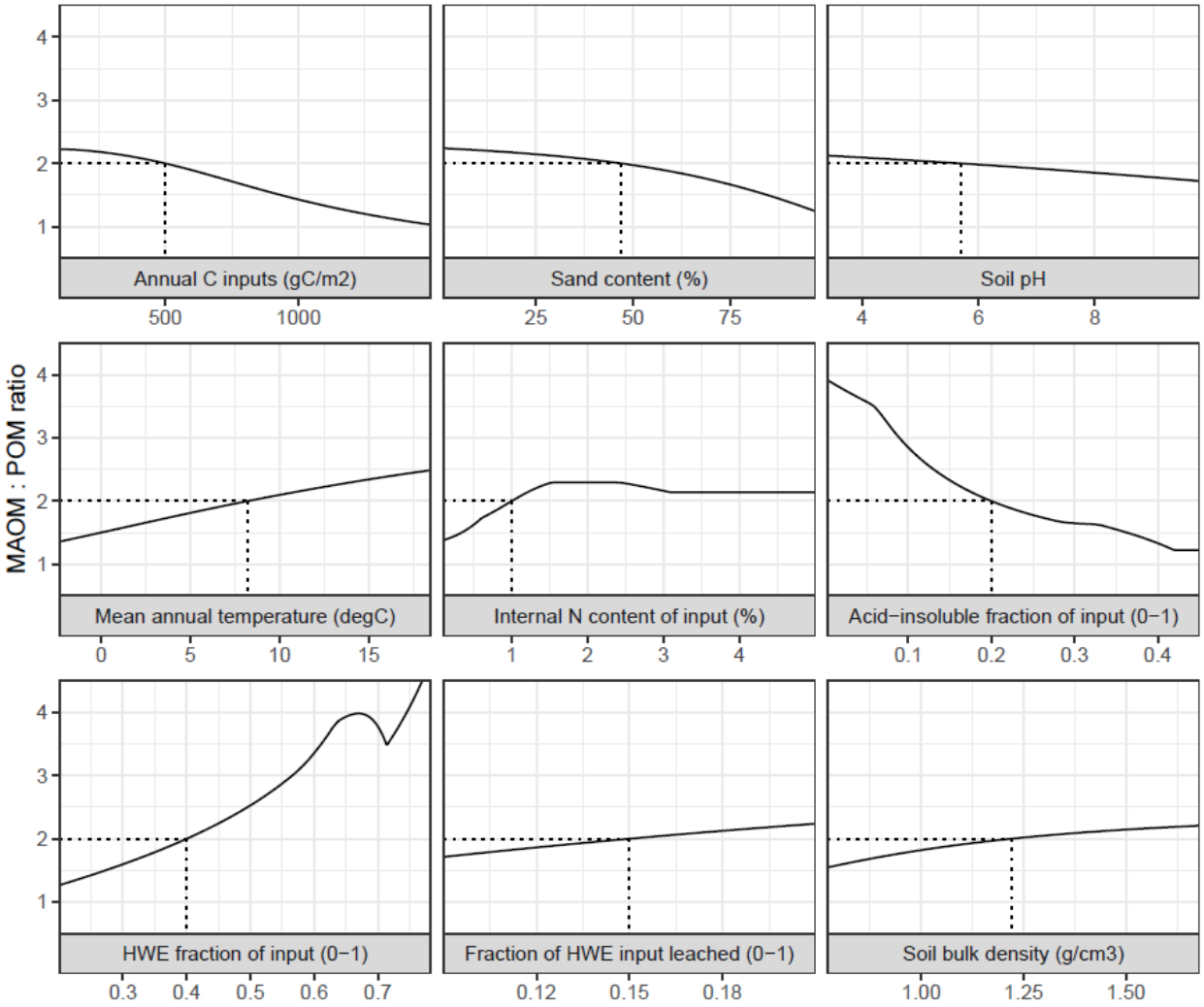

Figure 4 - Mineral-associated organic matter (MAOM) stock response to different levels of input litter quality and quantity, compared for edaphic conditions which equate to different MAOM sorption relationships in MEMS v1.0. Formatting adopted from Castellano *et al*. (2015) to aid comparison between the hypothetical relationship postulated and the actual response simulated by MEMS v1.0 here.

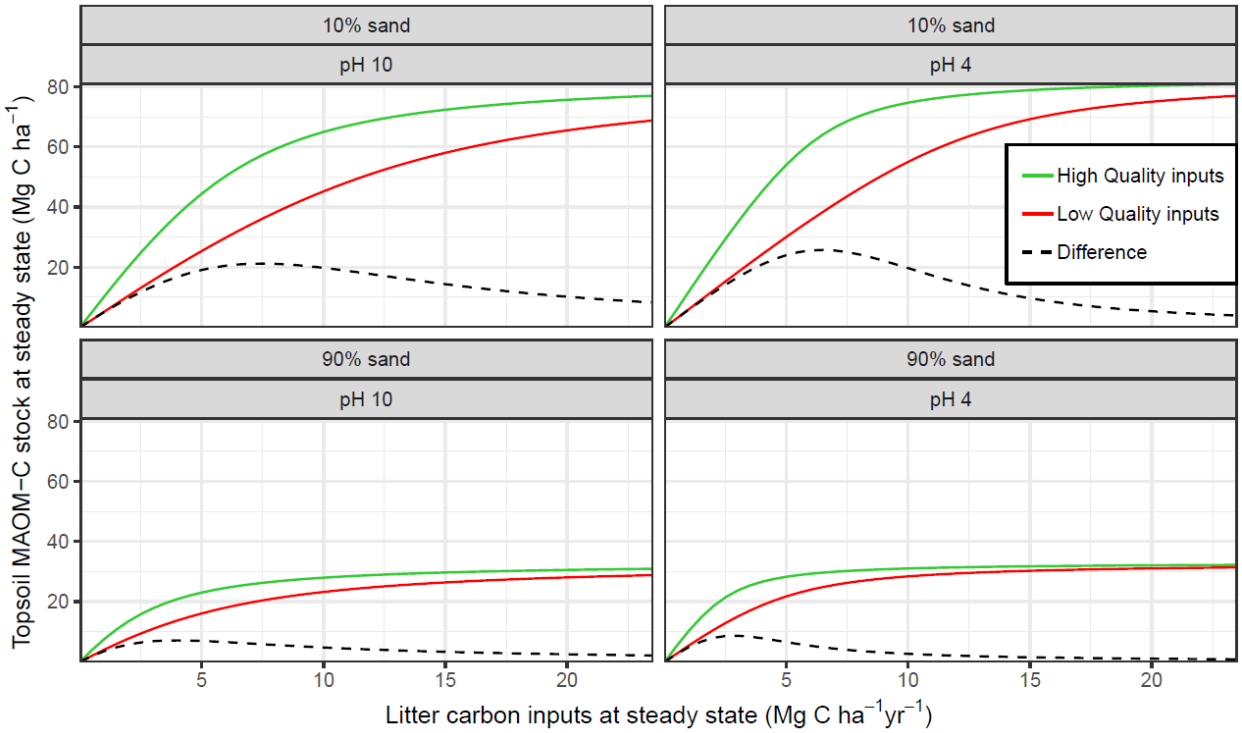

Figure 5 - Measured and modelled soil C stocks (split into mineral-associated organic matter, MAOM, total particulate organic matter, POM, and total soil organic carbon, SOC) for the forest and grassland land-use classes of the fractionated sites from the LUCAS dataset (*n* = 154). Note that the MAOM:POM ratio facet is unitless, not as shown by the y-axis label. Also note the free y-axis scales and that total POM is a sum of both light and heavy fractions.

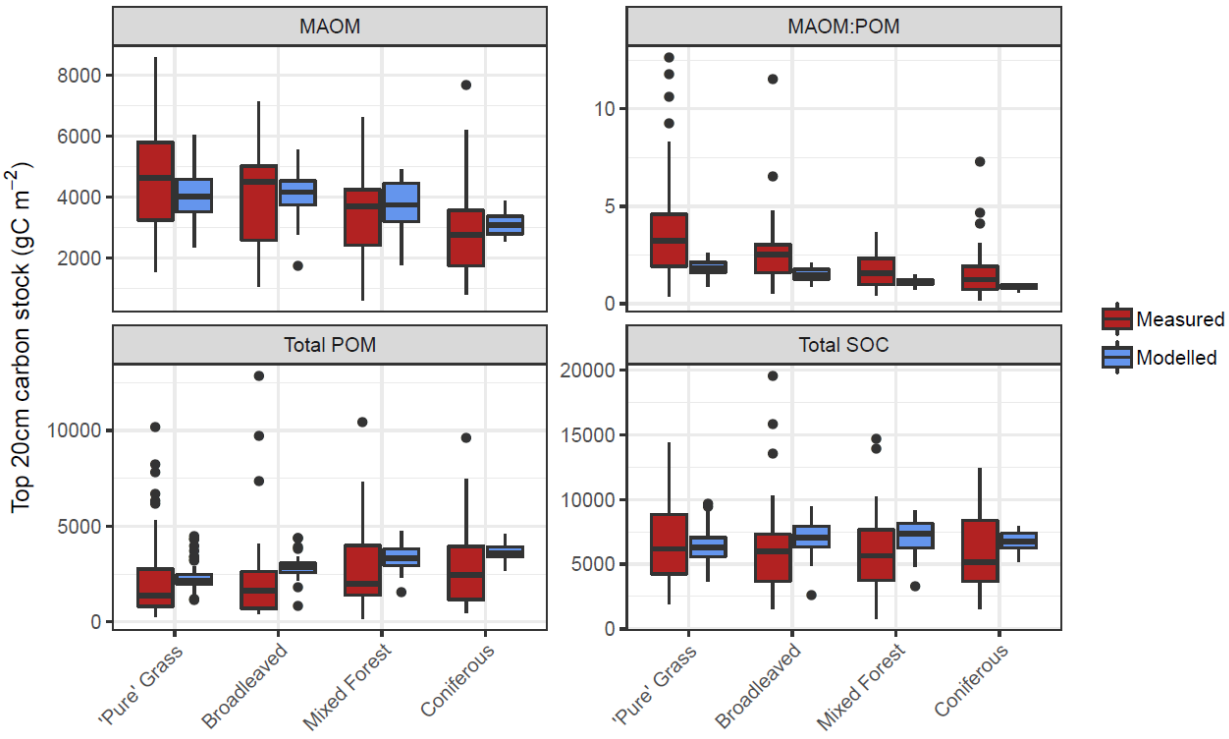

Figure 6 - Comparisons between average (± 1 standard error) measured (red) and modelled (blue) bulk SOC stocks for 8192 forestry and grassland sites over a climatic and edaphic gradient across Europe. Each comparison is partitioned into high and low groups of mean annual precipitation, MAP (top *vs* bottom panels), mean annual temperature, MAT (left *vs* right panels) and soil texture (alternating panels left to right). ANOVA comparisons of means is performed to show significant differences (* p < 0.001, ** p < 0.01, * p < 0.05). Number of samples for each land use and division is shown at the base of each bar.**

Figure 7 - Model residuals of topsoil (0-20 cm) C stocks (Mg C ha^{-1}) for 8192 sites (3487 grasslands, 1713 coniferous forests, 1590 broadleaved forests and 1402 'mixed' forests) across Europe, comparing measured values from the LUCAS database (Toth *et al*., 2013) to simulated steady-state estimates from the MEMS v1.0 model. All land uses are grouped for averages. Residuals are averaged across all sites within each NUTS2 region (populations between 800,000 and 3 million) and coloured accordingly. Measured site C stocks were subtracted from modelled values, meaning the model underestimates SOC stocks in positive (blue) regions and overestimates SOC stocks in negative (red) regions. Residuals average to within 10 Mg C ha^{-1} in areas with the lightest yellow colour. The size of circles within each region represents the number of sites simulated. Grey regions included no sites.

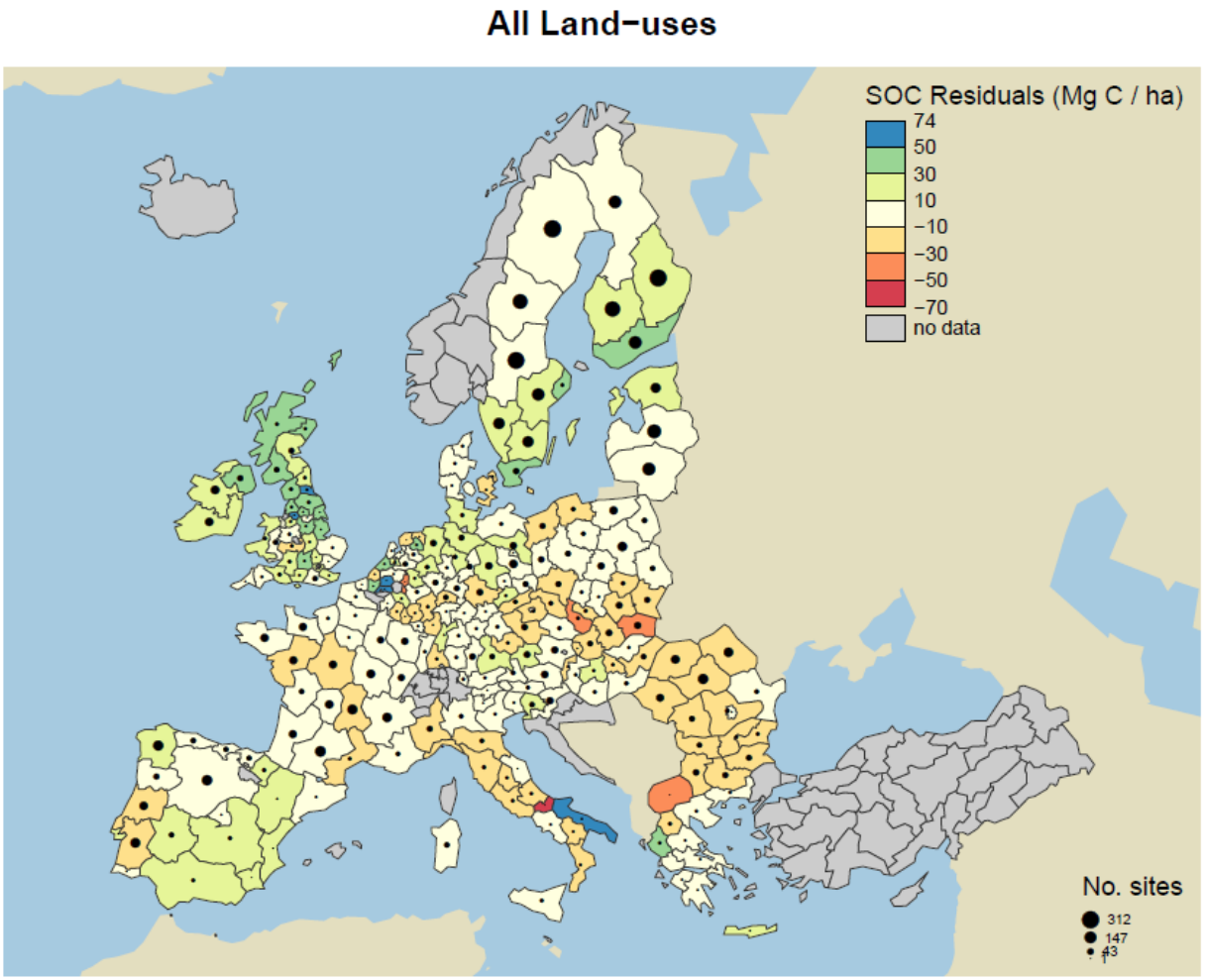

Tables

Table 1 - State variables of MEMS v1.0 and fractionation definitions (measurement proxy and protocol) for isolating each pool. C1 to C4, and C6, refer to the litter layer, while C5 and C8 to C10 refer to the mineral soil. POM, Particulate organic matter; DOM, Dissolved organic matter; OM, Organic Matter. All SOM fractions are primary fractions obtained after dispersion to break up aggregates. For detail on a fractionation scheme to quantify each pool of the MEMS model please refer Table S1.

State variable	Pool description	Measurement proxy	Method reference
C1	Water soluble litter	Hot-water extractable C	Tappi (1981)
C2	Acid-soluble litter	Hydrolyzable fraction	Van Soest and Wine (1968); Van Soest *et al*. (1991)
C3	Acid-insoluble litter	Unhydrolyzable fraction	
C4	Microbial biomass	Direct extraction	Various (e.g., Setia *et al*., 2012)
C5	Coarse, heavy POM	> 1.8 g cm^{-3} and > 53 µm C	Christensen, 1992
C6	Litter layer DOM	< 0.45 µm extractable C	Kolka *et al*., 2008
C7	Emitted CO_2	Heterotrophic soil respiration	See Subke *et al*., 2006
C8	Soil layer DOM	< 0.45 µm extractable C	Kolka *et al*., 2008
C9	Mineral-associated OM	> 1.8 g cm^{-3} and < 53 µm C	Christensen, 1992
C10	Light POM	< 1.8 g cm^{-3}	Christensen, 1992
C11	Leached DOM	Suction cups / pans etc.	See Kindler *et al*., 2011

Table 2 - Description and default values of all parameters used with MEMS v1.0. Where possible, notation has been used to remain consistent with further details in the supplementary information. Driving variables are reported in Table 3. Ranges are indicative of those observed in literature. Refer to Materials and Methods and Table S2 for details of the optimized parameter ranges.

Parameter	Parameter definition	Default value (range)	Units	Reference(s)
$B1$	Maximum growth efficiency of microbial use of water-soluble litter carbon (C1)	0.6 (0.4 – 0.7)	g microbial biomass C/g decayed	Sinsabaugh *et al*., 2013
$B2$	Maximum growth efficiency of microbial use of acid-soluble structural litter carbon (C2)	0.5 (0.3 – 0.6)	g microbial biomass C/g decayed	Sinsabaugh *et al*., 2013
$B3$	Heavy, coarse particulate organic matter (C5) generation from microbial biomass carbon (C4) decay	0.33 (0.028 – 0.79)	g microbial products C/g decayed C	Campbell *et al*., 2016
LIT_{frg}	Carbon in structural litter inputs (C2 and C3) transported to soil particulate organic matter (C5 and C10) each time step	0.006 ($1{\cdot}10^{-5}$ – $2{\cdot}10^{-3}$)	g C/g C decayed	-
POM_{split}	Fraction of fragmented litter inputs that form heavy particulate organic matter (C5)	0.30 (0.07 – 0.83)	0-1 scaling	Poeplau and Don, 2013; Soong *et al*., 2016
DOC_{frg}	Carbon in litter layer DOM (C6) transported to soil DOM (C8) each time step	0.8 (0.2 – 0.99)	g DOM-C/g DOM-C	-
DOC_{lch}	Maximum specific rate of leaching to represent vertical transport of carbon in DOM through the soil profile	0.00438 ($1{\cdot}10^{-5}$ – 0.02)	g C day^{-1}	Trumbore *et al*. 1992
EH_{max}	Maximum amount of carbon leached from decayed acid-soluble litter carbon (C2) to litter layer DOM (C6)	0.15	g DOM-C/g decayed C	Campbell *et al*., 2016

EH_{min}	Minimum amount of carbon leached from decayed acid-soluble litter carbon (C2) to litter layer DOM (C6)	0.005	g DOM-C/g decayed C	Campbell *et al*., 2016
ES_{max}	Maximum amount of carbon leached from decayed water-soluble litter carbon (C1) to litter layer DOM (C6)	0.15	g DOM-C g decayed C^{-1}	Campbell *et al*., 2016
ES_{min}	Minimum amount of carbon leached from decayed water-soluble litter carbon (C1) to litter layer DOM (C6)	0.005	g DOM-C g decayed C^{-1}	Campbell *et al*., 2016
k_1	Maximum decay rate of water-soluble litter carbon (C1)	0.37 (0.16 – 0.70)	~~g C~~ day^{-1}	Campbell *et al*., 2016
k_2	Maximum decay rate of acid-soluble litter carbon (C2)	0.009 (0.0011–0.0200)	~~g C~~ day^{-1}	Campbell *et al*., 2016
k_3 *	Maximum decay rate of acid-insoluble litter carbon (C3)	0.0002 ($2{\cdot}10^{-5}$– $1{\cdot}10^{-3}$)	~~g C~~ day^{-1}	Moorhead *et al*., 2013
k_4	Maximum decay rate of microbial biomass carbon (C4)	0.57 (0.11-0.97)	~~g C~~ day^{-1}	Campbell *et al*., 2016
k_5	Maximum decay rate of heavy, coarse particulate soil organic matter (C5)	0.0005 ($6{\cdot}10^{-5}$– $1{\cdot}10^{-3}$)	~~g C~~ day^{-1}	Campbell *et al*., 2016; Del Galdo *et al*., 2003
k_8	Maximum decay rate of soil DOM (C8)	0.00144	~~g C~~ day^{-1}	Kalbitz *et al*., 2005
k_9	Maximum decay rate of mineral-associated soil organic matter (C9)	$2.2{\cdot}10^{-5}$ ($1{\cdot}10^{-5}$– $4{\cdot}10^{-5}$)	~~g C~~ day^{-1}	Del Galdo *et al*., 2003
k_{10}	Maximum decay rate of light particulate soil organic matter (C10)	$2.96{\cdot}10^{-4}$ ($4{\cdot}10^{-3}$–$1{\cdot}10^{-4}$)	~~g C~~ day^{-1}	Del Galdo *et al*., 2003
la_2	Carbon leached from decayed microbial biomass carbon (C4)	0.19 (0.022 – 0.42)	g DOM-C g decayed C^{-1}	Campbell *et al*., 2016

la_3	Carbon leached from acid-insoluble litter carbon and heavy, coarse particulate organic matter carbon (C3 and C5)	0.038 (0.014 – 0.050)	g DOM-C g decayed C^{-1}	Campbell *et al*., 2016; Soong *et al*., 2015
LCI_{max}	Maximum lignocellulosic index that influences DOM generation from litter decay	0.51	-	Campbell *et al*., 2016; Soong *et al*., 2015
N_{max}	Maximum N content that influences rates (above this, there is no limit) of DOM generation and microbial carbon assimilation	3	%	Sinsabaugh *et al*., 2013
N_{mid}	Mid-point of logistic function that describes N limitation	1.75	%	Campbell *et al*., 2016; Soong *et al*., 2015
T_{opt}	Optimum temperature at which decay rates are highest	45	°C	Harmon and Domingo, 2001
T_{Q10}	Rate at which the decomposition rate increases with a 10 °C increase in soil temperature	2	-	Harmon and Domingo, 2001
T_{ref}	The reference temperature of estimated maximum decay rates (i.e., parameters k_x)	13.5	°C	Del Galdo *et al*., 2003
T_{shp}	Shape of the excessive temperature limitation for temperature modifier on decay rates beyond optimum temperature	15	-	Harmon and Domingo, 2001
T_{lag}	Difference from optimum temperature to the decline above that threshold applying to the temperature modifier on decay rates	4	°C	Harmon and Domingo, 2001
T_{range}	Difference between the maximum and minimum soil temperature values over a given year (*unused when temperature inputs are available*)	24	°C	Toth *et al*., 2013
SC_{icept}	Intercept coefficient used for the linear regression that estimates the maximum sorption capacity (parameter Q_{max}) of a soil	11.08	g C in < 53 µm fraction kg $soil^{-1}$	Six *et al*., 2002

SC_{slope}	Slope coefficient used for the linear regression that estimates the maximum sorption capacity (parameter Q_{max}) of a soil	0.2613	-	Six *et al*., 2002
${}^{L}k_{lm}$ *	Binding affinity for carbon in soil DOM (C8) sorption to mineral surfaces (C9) of the soil layer L	0.25	gC day^{-1}	Mayes *et al*., 2012; Abramoff *et al*., 2017
${}^{L}Q_{max}$ *	Maximum sorption capacity of mineral-associated soil organic matter carbon (C9) of soil layer L	-	gC m^{-2} depth^{-1}	Six *et al*., 2002

* These parameters are calculated as functions of others. For example, Q_{max} is a function of sand content, soil bulk density, rock fraction, SC_{icept} and SC_{slope}. More details can be found in the supplementary materials.

Table 3 - List of required driving variables for the MEMS v1.0 model. Baseline values represent mean values as reported in the LUCAS database (Toth *et al*., 2013) of 8192 forest and grassland sites across Europe and were used for all qualitative testing and sensitivity analyses.

Driving variable	Symbol	Units	Baseline value	Land-use specific values				Reference
				Grassland	Broadleaf forest	Mixed forest	Coniferous forest	
Site condition variables								
Annual net primary productivity	*annNPP*	g C m^{-2} yr^{-1}	681	Site-specific values required				ORNL DAAC, 2009
Sand content of soil layer	*Sand*	%	47.8					
Bulk density of soil layer	*BD*	g cm^{-3}	1.21					Toth *et al*., 2013
Rock fraction of soil layer	*Rock*	%	7.62					
Soil pH of layer	*pH*	-	5.58					
* Daily total carbon input	*CT*	g C m^{-2} day^{-1}	1.30					-
* Mean daily soil temperature	*soilT*	ºC	8.28					NOAA, 2018
Litter chemistry variables								
Hot-water extractable fraction	*fSOL*	0-1	0.45	0.35	0.40	0.38	0.35	
Acid-insoluble fraction	*fLIG*	0-1	0.20	0.15	0.27	0.30	0.32	Campbell *et al*., 2016
Internal nitrogen content	*LitN*	%	1.00	1.10	1.32	0.87	0.41	
Root distribution variables								
Maximum rooting depth	*Rdepmx*	cm	300	260	290	340	390	Canadell *et al*., 1996
Depth to which 50% of root mass is distributed	*Rdep50*	cm	20	15	25	27.5	30	Jackson *et al*., 1996
Root to shoot ratio	*RtoS*	-	1.00	3.70	0.23	0.21	0.18	Jackson *et al*., 1996

* - When daily measurements are not available annual values can be used to interpolate daily estimates. For more information please refer to the supplementary materials.

Table 4 - Evaluation results of comparisons between measured and modelled topsoil (0-20 cm) C stock for 8192 grassland and forest sites across Europe (see Figure 7 for geographic distribution of residuals). Mean absolute error (MAE) and mean bias error (MBE) describe the overall difference and directional difference between measured and modelled values, respectively. The model is deemed to describe the trend of the measured data better than the mean of the measurements when the modelling efficiency (EF) is positive, or when the Coefficient of Determination (CofD) is above 1. Each is a discrete evaluation metric. Divisions of high/low site conditions (mean annual temperature, mean annual precipitation, annual C inputs, sand content) were used to derive statistical significance (root mean square error, RMSE, and *F*-statistic) of differences between measured and modelled values while accounting for measurement variance within these divisions. An RMSE value below $RMSE_{95}$ indicates that simulated C stocks fall within the 95 % confidence interval of the measurements. An F-statistic below 0.05 also shows that simulated values are not significantly different to measurements at a 95 % confidence level.

		Evaluation metrics for individual site performance						Evaluation metrics using site condition *divisions* to include variance		
Land use	*n*	Mean ± 1 S.E. (Mg C ha^{-1})		MAE (Mg C ha^{-1})	MBE (Mg C ha^{-1})	EF	CofD	RMSE (Mg C ha^{-1})	$RMSE_{95}$ (Mg C ha^{-1})	*F*-statistic
		Observed	Predicted							
Pure grass	3487	65.9 ± 0.5	66.3 ± 0.3	24.7	-0.4	-0.047	4.52	13.0	10.3	0.009
Broadleaved	1590	71.2 ± 1.0	73.8 ± 0.4	31.0	-2.5	-0.062	5.54	19.0	14.7	0.052
Mixed Forest	1402	82.3 ± 1.1	75.2 ± 0.3	35.4	7	-0.173	8.36	12.9	19.2	0.042
Coniferous	1713	79.0 ± 1.1	76.3 ± 0.3	36.1	2.7	-0.057	10.35	13.5	18.7	0.006
* All	8192	72.5 ± 0.4	71.4 ± 0.2	30.2	1.1	-0.048	6.32	14.9	15.7	0.020

* All sites use 64 divisions (high/low site conditions and land use type)

12

MARKED-UP SUPPLEMENTARY MATERIAL BELOW THIS POINT

15

SUPPLEMENTARY MATERIALS FOR:

Unifying soil organic matter formation and persistence frameworks: the MEMS model

Full model description of MEMS v1.0

Mathematical representation of MEMS v1.0

Below are the differential equations for dynamics through time as calculated by MEMS v1.0. For simplicity, many of the individual fluxes are summarized by single names (e.g., $C1_{in}^{i}$ to represent total inputs to the C1 pool from litter material *i*, instead of including the separate calculation). Please refer to the equations provided in this Supplementary Materials. Parameter descriptions can be found in Table 2 of the main manuscript. Please note that the below list equations are fully representative of the carbon dynamics of MEMS v1.0 but are layer- and time-specific. However, for simplicity are presented in a generalized form.

$$\frac{dC1}{dt} = C1_{in}^{i} - (uk * C1 * k_1) \quad (1)$$

$$\frac{dC2}{dt} = C2_{in}^{i} - (uk * C2 * k_2) - (C2 * LIT_{frg}) \quad (2)$$

$$\frac{dC3}{dt} = C3_{in}^{i} - (C3 * k_3) - (C3 * LIT_{frg}) \quad (3)$$

$$\frac{dC4}{dt} = C4_{ass}^{C1} + C4_{ass}^{C2} - (C4 * k_4) \quad (4)$$

$$\frac{dC5}{dt} = C5_{gen}^{C4} + C5_{frg}^{C2} + C5_{frg}^{C3} - (C5 * k_5) \quad (5)$$

$$\frac{dC6}{dt} = C6_{in}^{i} + C6_{in}^{C1} + C6_{in}^{C2} + C6_{in}^{C3} + C6_{in}^{C4} - C8_{in}^{C6} \quad (6)$$

$$\frac{dC7}{dt} = C1_{co2} + C2_{co2} + C3_{co2} + C4_{co2} + C5_{co2} + C8_{co2} + C9_{co2} + C10_{co2} \quad (7)$$

$$\frac{dC8}{dt} = C8_{in}^{C5} + C8_{in}^{C6} + C8_{in}^{C10} - sorption - (C8 * DOC_{lch}) - (C8 * k_8) \quad (8)$$

$$\frac{dC9}{dt} = sorption - (C9 * k_9) \quad (9)$$

$$\frac{dC10}{dt} = C10_{frg}^{C2} + C10_{frg}^{C3} - (C10 * k_{10}) \quad (10)$$

$$\frac{dC11}{dt} = (C8 * DOC_{lch}) \quad (11)$$

Carbon inputs from external sources

In MEMS v1.0 the above- and below-ground plant residue inputs are combined and input to the system on a daily timestep. These total inputs are partitioned between C1, C2, C3 and C6 as a function of the external source (*i*) input properties (Eqs. 12-15): the cold water extractable fraction of the hot-water extractable litter input (f_{DOC}^{i}), the hot water extractable fraction of the litter input (f_{SOL}^{i}) and acid-insoluble fraction of the litter input (f_{LIG}^{i}).

$$_{j}^{L}C1_{in}^{i} = (_{j}^{L}CT^{i} * f_{SOL}^{i}) - (_{j}^{L}CT^{i} * f_{SOL}^{i} * f_{DOC}^{i}) \quad (12)$$

$$_{j}^{L}C2_{in}^{i} = {}_{j}^{L}CT^{i} - \left(_{j}^{L}CT^{i} * (f_{SOL}^{i} + f_{LIG}^{i})\right) \quad (13)$$

$$_{j}^{L}C3_{in}^{i} = (_{j}^{L}CT^{i} * f_{LIG}^{i}) \quad (14)$$

$$ {}_{j}^{L}C6_{in}^{i} = {}_{j}^{L}CT^{i} * f_{SOL}^{i} * f_{DOC}^{i} \quad (15) $$

Where ${}_{j}^{L}X_{in}^{i}$ is refers to the daily carbon input to pool X from external source i ~~for layer L~~ on day j, and ${}_{j}^{L}CT^{i}$ is the total daily carbon input from external source i ~~for layer L~~ on day j. For MEMS v1.0 the layer is fixed to the aboveground litter layer only, allowing for use of the same functions as those presenting in the LIDEL model (Campbell *et al*., 2016). However, future versions may incorporate the same structure for different points of entry for C inputs (e.g., root death and the rhizosphere).

Once allocated to their initial pools, the carbon is susceptible to assimilation in microbial biomass if it is water-soluble (C1) or acid-soluble (C2) but only co-metabolized if it is acid-insoluble (C3). The contents of these pools represent compounds of increasing chemical complexity (e.g., C1, mostly soluble carbohydrates, phenols and amino acids; C2, mostly cellulose, xylans and other hemicelluloses; C3, mostly lignin aboveground and suberin/cutin belowground) and are associated with decreasing microbial use efficiency.

Microbial assimilation from litter pools

Many of the biogeochemical processes represented by MEMS are assumed to be microbially mediated, and therefore are associated with C-mineralization and the resulting carbon dioxide (CO_2) emissions from microbial respiration. The primary carbon losses ~~to CO_2~~ result from the metabolic processes of bacteria and fungi within the soil and are aligned with the mathematical representations as described by Campbell *et al*. (2016) and, in part, summarise the findings of Sinsabaugh *et al*. (2013), Moorhead *et al*. (2013) and Soong *et al*. (2015). In addition, carbon assimilation ~~of~~ by microbial biomass (C4) in the litter layer results from the balance between anabolic and catabolic processes and thus, as biomass is formed, dissolved organic matter (DOM) and CO_2 are also produced ~~there is also CO_2 as well as carbon in dissolved organic matter (DOM) production~~. Microbial assimilation is a function of nitrogen content and lignocellulosic index (Eq. 16) of the structural litter pools (C2 and C3; organic matter > 2 mm) ~~in each layer~~ and controlled by maximum decomposition rates for C1 (k_1) and C2 (k_2) that assume first-order decay.

$$ {}_{j}^{L}LCI_{lit} = \frac{{}_{j}^{L}C3}{\left({}_{j}^{L}C2 + {}_{j}^{L}C3\right)} \quad (16) $$

$$ {}_{j}^{L}C4_{ass}^{C1} = uB * B_1 * (1 - la_4) * uk * k_1 * {}_{j}^{L}C1 \quad (17) $$

$$ {}_{j}^{L}C4_{ass}^{C2} = uB * B_2 * (1 - la_1) * uk * k_2 * {}_{j}^{L}C2 \quad (18) $$

Where ${}_{j}^{L}C4_{ass}^{C1}$ and ${}_{j}^{L}C4_{ass}^{C2}$ refer to the fraction of the given litter pool (i.e., C1 or C2) that is microbially assimilated to pool C4 ~~of layer L~~ on day j from pool C1 or C2, respectively. Note that these functions are make microbial assimilation explicit in this ~~specific to a single~~ aboveground litter layer. In the soil itself, microbial assimilation of organic matter is still occurring but assumed to be implicit and incorporated in the carbon mineralization rates for each of the soil pools (e.g., C5, C8, C9 and C10). In future versions of the model, the same general structure can apply, with an explicit microbial component at the different ~~(aboveground litter in MEMS v1.0)~~points of entry (i.e.,

rhizospheric inputs vs aboveground litter) but ~~and~~ parameter values may differ between layers, when more are added. Detail about the concepts behind this approach can be found in Sokol *et al*., 2018.

More information of the parameters uB, uk, B_x, la_x and k_x can be found in Campbell *et al*. (2016) and in the equations below~~Table 2 in the main manuscript~~, but briefly:

- ${}^{L}_{j}uB$ and ${}^{L}_{j}uk$ are rate modifiers to represent the litter chemistry controls (LCI and available nitrogen) on microbial use efficiency, ~~for layer L~~ on day j.

$$ {}^{L}_{j}\boldsymbol{uB} = \boldsymbol{min}\left(\left(\frac{1}{1+e^{-N_{max}\left(N_{lit}-N_{mid}\right)}}\right),\left(1-e^{-0.7\left(\left|{}^{L}_{j}LCI_{lit}-0.7\right|*10\right)}\right)\right) \quad \textbf{(19)} $$

$$ {}^{L}_{j}\boldsymbol{uk} = \boldsymbol{min}\left(\left(\frac{1}{1+e^{-N_{max}\left(N_{lit}-N_{mid}\right)}}\right),\left(e^{-3*{}^{L}_{j}LCI_{lit}}\right)\right) \quad \textbf{(20)} $$

Where N_{max} and N_{mid} are maximum and mid points of litter nitrogen content having an impact on microbial use efficiencies, using a logistic curve (see Figure S~~6~~7). N_{lit} and ${}^{L}_{j}LCI_{lit}$ are the input material nitrogen content and LCI ~~of layer L~~ being simulated on day j.

IMPORTANT NOTE – In MEMS v1.0 there is no nitrogen cycling and therefore the N_{lit} value is not dynamic, as it likely should be. Consequently, MEMS v1.0 uses the nitrogen content of the input material, and therefore N_{lit} is a constant through time and across layers. This constant nitrogen value is consistent with the approach used by the LIDEL model (Campbell *et al*., 2016) however it is expected that a dynamic nitrogen (i.e. be ${}^{L}_{j}N_{lit}$ – as equivalent to ${}^{L}_{j}LCI_{lit}$) content would more likely reflect real-world conditions, especially in extended periods without litter input.

- B_1 and B_2 are maximum growth efficiencies associated with the water-soluble and acid-soluble litter pools (C1 and C2), respectively (See Table 2 in the main manuscript).
- la_1 and la_4 are estimates of carbon in DOM generation from leaching the decayed litter pools ~~of layer L~~ on day j.

$$ {}^{L}_{j}\boldsymbol{la_1} = \boldsymbol{min}\left(\left(E_{Hmax}-\frac{\left(E_{Hmax}-E_{Hmin}\right)}{LCI_{max}}*{}^{L}_{j}LCI_{lit}\right),\left(E_{Hmax}-\frac{\left(E_{Hmax}-E_{Hmin}\right)}{N_{max}}*N_{lit}\right)\right) \quad \textbf{(21)} $$

$$ {}^{L}_{j}\boldsymbol{la_4} = \boldsymbol{min}\left(\left(E_{Smax}-\frac{\left(E_{Smax}-E_{Smin}\right)}{LCI_{max}}*{}^{L}_{j}LCI_{lit}\right),\left(E_{Smax}-\frac{\left(E_{Smax}-E_{Smin}\right)}{N_{max}}*N_{lit}\right)\right) \quad \textbf{(22)} $$

Where E_{Hmax} and E_{Hmin} are the maximum and minimum amount of DOM leached from decay of acid-soluble litter (C2), and E_{Smax} and E_{Smin} are the maximum and minimum amount of DOM leached from decay of water-soluble litter (C1). LCI_{max} refers to the maximum lignocellulosic index that can have an impact on these rates. As noted above, N_{lit} and ${}^{L}_{j}LCI_{lit}$ are the nitrogen content of input material and LCI ~~of layer L~~ being simulated on day j.

- k_1 and k_2 are the maximum decay rates of water-soluble (C1) and acid-soluble (C2) litter pools, respectively (See Table 2 in the main manuscript).

Microbial mortality and necromass production

After carbon is metabolized by microbes and incorporated in pool C4, the death and products of microbial activity result in the compounds that form the coarse, heavy particulate SOM (C5) that is often found coating sand particles in the > 53 µm soil fraction (Ludwig *et al.*, 2015). In the aboveground litter layer simulated by MEMS v1.0, this process of microbial biomass decay results in loss to DOC (C6) and CO_2 (C7), in addition to the C5 pool belowground.

$$ {}^{L}_{j}C5^{C4}_{gen} = B_3 * (1 - la_2) * k_4 * {}^{L}_{j}C4 \quad (23) $$

Where ${}^{L}_{j}C5^{C4}_{gen}$ refers to the fraction of carbon that is transferred from C4 to C5 (i.e., microbial products transported belowground when physical and hydrological processes mix between the input layer [aboveground litter only in MEMS v1.0] and soil layer) ~~with structural litter fragmentation and bioturbation or advection and leaching of DOC for layer L~~ on day j. ~~Belowground, this flux does not move vertically between layers but is transferred from C4 to C5 within the same soil layer.~~ The flux from the aboveground microbial biomass pool (C4) is assumed to move belowground, to the first soil layer (see Figure 1 in the main manuscript). More information of the parameters B_3, la_2 and k_4 can be found in Table 2 in the main manuscript, but briefly, B_3 refers to a maximum rate of microbial product (C5) generation per unit of microbial biomass (C4) decayed, la_2 refers to the maximum amount of DOM produced per unit of microbial biomass (C4) decayed and k_4 refers to the maximum rate of microbial biomass (C4) decay.

Fragmentation and perturbation

To quantify the transfer of carbon from large (> 2 mm) particulates to small particulates belowground, simple parameter values have been allocated to represent first-order rates of transfer from both structural litter pools (C2 and C3). As model development continues, these rates will be improved to provide more mechanistic relationships with site conditions (see Braakehekke *et al.*, 2011). See Table 2 for information about the parameter used in MEMS v1.0 (LIT_{frg}). The amount of litter C fragmented and transferred vertically from structural litter pools to the belowground POM pools (C5 and C10) is also governed by the POM_{split} parameter that defines how much of the total is allocated to C5.

$$ {}^{L}_{j}C5^{C2}_{frg} = POM_{split} * LIT_{frg} * {}^{L}_{j}C2 \quad (24) $$

$$ {}^{L}_{j}C5^{C3}_{frg} = POM_{split} * LIT_{frg} * {}^{L}_{j}C3 \quad (25) $$

$$ {}^{L}_{j}C10^{C2}_{frg} = (1 - POM_{split}) * LIT_{frg} * {}^{L}_{j}C2 \quad (26) $$

$$ {}^{L}_{j}C10^{C3}_{frg} = (1 - POM_{split}) * LIT_{frg} * {}^{L}_{j}C3 \quad (27) $$

Where ${}^{L}_{j}CX^{CY}_{frg}$ refers to the amount of carbon that is transferred from pool CY to pool CX ~~for layer L~~ on day j.

Dissolved organic matter production

Dissolved organic matter plays a major role in the MEMS model as it is the only way in which carbon can sorb to mineral surfaces in the soil, meaning that if there is limited DOM there will also be limited stabilization in MAOM (C9). Consequently, DOM production from all model pools is simulated explicitly according to the formulae provided by the LIDEL model (Campbell *et al*., 2016) and based on empirical data in Soong *et al*. (2015). Each timestep, the aboveground litter layer DOM (C6) receives a fraction of inputs from external sources directly (Eq. 15; ${}_{j}^{L}C6_{in}^{i}$), from all litter layer pools (${}_{j}^{L}C6_{in}^{C1}$, ${}_{j}^{L}C6_{in}^{C2}$, ${}_{j}^{L}C6_{in}^{C3}$) and from microbial biomass (${}_{j}^{L}C6_{in}^{C4}$).

$$ {}_{j}^{L}C6_{in}^{C1} = la_4 * uk * k_1 * {}_{j}^{L}C1 \quad (28) $$

$$ {}_{j}^{L}C6_{in}^{C2} = la_1 * uk * k_2 * {}_{j}^{L}C2 \quad (29) $$

$$ {}_{j}^{L}C6_{in}^{C3} = la_3 * k_3 * {}_{j}^{L}C3 \quad (30) $$

$$ {}_{j}^{L}C6_{in}^{C4} = la_2 * k_4 * {}_{j}^{L}C4 \quad (31) $$

Where ${}_{j}^{L}Cx_{in}^{Cy}$ refers to DOM leaching from pool *y* to pool *x* ~~of layer *L*~~ on day *j*. The parameters used are detailed in Table 2 in the main manuscript, and/or defined in previous equation in this section. Note that pool C6 is not the DOM consumed by microbial biomass but rather the amount leftover after microbial activity. In this initial model version, the litter layer only refers to the aboveground component, but the same structure can equally apply to belowground C inputs such as root death. ~~only exists in the aboveground litter layer and therefore in the above equations *L* is always the aboveground layer.~~ However, measurably, the DOM in the C6 pool ~~aboveground litter layer DOM~~ is directly equivalent to the belowground soil DOM (C8). In MEMS v1.0, DOM enters the soil through the C6 pool only. ~~However, w~~When explicit inputs from belowground litter (e.g., roots) are simulated in future versions Eqs. 28-31 can apply for each soil layer adding the DOM that is in excess of microbial activity directly to pool C8 instead of the 'C6' shown in the equations above.~~, s~~Similarly, root exudates can be simulated as direct addition to the C8 pool of any specific soil layer. Hence, just as the litter layer DOM (C6) receives inputs from the aboveground litter layer pools, the soil DOM (C8) would receive inputs from the belowground pools (e.g., decomposing root matter and root exudation). In addition, the soil DOM pool receives inputs from the POM and MAOM pools (${}_{j}^{L}C8_{in}^{C5}$, ${}_{j}^{L}sorption$, ${}_{j}^{L}C8_{in}^{C10}$) as well as from leached litter DOM (C6). Here, the $sorption$ flux represents the net carbon exchange between soil DOM (C8) and MAOM (C9).

$$ {}_{j}^{L}C8_{in}^{C5} = la_3 * k_5 * {}_{j}^{L}C5 \quad (32) $$

$$ {}_{j}^{L}C8_{in}^{C6} = DOC_{frg} * {}_{j}^{L}C6 \quad (33) $$

$$ {}_{j}^{L}C8_{in}^{C10} = la_3 * k_{10} * {}_{j}^{L}C10 \quad (34) $$

The parameter values are defined in Table 2 in the main manuscript. As with the LIT_{frg} parameter, the DOC_{frg} value in MEMS v1.0 is set as a tuning parameter and simply assumes first-order rates to allocate a given proportion of the carbon in litter layer DOM pool (C6) to the soil DOM pool (C8) each timestep. As noted earlier, these functions are

layer-specific and therefore in a multi-layer version of MEMS, there would be vertical leaching of DOM between C8 pool of different layers, instead of from the aboveground C6 pool alone (i.e., to replace Eq. 33).

Sorption and desorption

The formation of organo-mineral complexes in MEMS v1.0 is represented by a net sorption-desorption process that uses the amount of soil DOM (C8) to estimate adsorption rates based on a Langmuir isotherm (Kothawala *et al.*, 2008). The key elements of this isotherm are the 'binding affinity' (K_{lm}) – see Eq. 35 – and maximum sorption capacity (Q_{max}) – see Eq. 36 – which are controlled by site-specific conditions (soil pH and soil texture, respectively). It is worth noting that each of these site-specific conditions are provided as driving variables to the model, and are constants that represent the site at time-zero (i.e., soil pH is not simulated to change through time). The net sorption rate ($sorption$) aims to account for several different sorption mechanisms (e.g., cation bridging, surface complexation, etc.) to retain parsimony. A more accurate net flux may simulate the different mechanisms individually to allow for more detailed representation of different mineralogies as per Six *et al.* (2002) (e.g., dominated by 2:1 clays *vs* 1:1 clays). Future development of MEMS may adopt these changes.

$$ {}^{L}K_{lm} = 10^{(-0.186\ {}^{L}soilpH - 0.216)} \quad (35) $$

Where ${}^{L}soilpH$ refers to the 'native' soil pH of the simulated soil ~~layer *L*~~. The soil pH, as used in Eq 35, acts as a proxy for mineralogical differences between soils, with higher native soil pH being equated with weaker chemical bonding. This tenet is adopted from the regression provided in Mayes *et al.* (2012) and results in K_{lm} being estimated as in the MILLENNIAL model (Abramoff *et al.*, 2017). However, the MEMS v1.0 estimate of Q_{max} does not follow the MILLENNIAL model and instead calculates a general relationship between maximum soil carbon capacity and soil texture using the entire dataset of Six *et al.* (2002). This takes a simple linear regression approach using the soil layer's percent silt and clay content (i.e., $100 - sand$)

$$ {}^{L}Q_{max} = {}^{L}\rho * (0.26126 * (100 - {}^{L}sand) + 11.07820) * (1 - {}^{L}rock) \quad (36) $$

Where ${}^{L}\rho$ refers to the bulk density of the soil ~~layer *L*~~ at the site being simulated. Note that the bulk density is a conversion specific to the depth of the soil layer that converts a concentration from the regression of Six *et al.* (2002) to carbon density (e.g., gC m^{-2} layer $depth^{-1}$) and therefore the equations shown here assume a 1 meter deep layer for simplification. Both the sand content (${}^{L}sand$) and rock fraction (${}^{L}rock$) are expressed in percent (i.e., 0-100) ~~and specific to layer *L*~~. The resulting equation to represent net sorption is controlled by a Langmuir saturation function, using the amount of soil DOC (C8) available for sorption as well as the saturation deficit of MAOM (C9). Note, all coefficients in the equation below are layer- and timestep-specific.

$$ {}^{L}_{j}sorption = {}^{L}_{j}C8 * \frac{\left(\left(\frac{({}^{L}K_{lm} * {}^{L}Q_{max} * {}^{L}_{j}C8)}{1+({}^{L}_{j}K_{lm} * {}^{L}_{j}C8)}\right) - {}^{L}_{j}C9\right)}{{}^{L}Q_{max}} \quad (37) $$

Where ~~$_{L}$~~$_{j}sorption$ is a net exchange of carbon between the soil DOM (C8) and MAOM (C9) pools ~~of layer L~~ given their size on day j. Since K_{lm} and Q_{max} are site-specific parameters, and the pool sizes (C8 and C9) are dynamic through time, there are interactions between these factors which mean sorption rates are not necessarily comparable between sites. This sorption process is assumed to be abiotic in that it results in no CO_2 emitted. As a net rate, sorption and desorption are not simulated individually which may make it difficult to represent potential priming effects on organo-mineral associations (e.g., Keiluweit *et al.*, 2015). Future MEMS model version will explore these feedbacks further.

Decomposition and pool decay rates

Apart from the litter layer DOM (C6), each of the state variables in MEMS v1.0 decay directly with unique decay rates informed by literature values (see Table 2). This decay results in CO_2 emissions which continually accumulate in the sink C7. The amount of CO_2 associated with each microbial process is equivalent to the amount of carbon leftover after losses to DOM are calculated so the decay rate constants for pool x (k_x) also embody explicit DOM generation and not just CO_2 emissions, as is more common in traditional SOM models (e.g., CENTURY or RothC). As with earlier equations, these below ~~are~~ can be layer- and time-specific but for simplicity are presented in a generalized form.

$$\boldsymbol{C1_{co2} = \left(\left(1 - (uB * B_1)\right) * (1 - la_4)\right) * uk * k_1 * C1} \quad \textbf{(38)}$$

$$\boldsymbol{C2_{co2} = \left(\left(1 - (uB * B_2)\right) * (1 - la_1)\right) * uk * k_2 * C2} \quad \textbf{(39)}$$

$$\boldsymbol{C3_{co2} = (1 - la_3) * k_3 * C3} \quad \textbf{(40)}$$

$$\boldsymbol{C4_{co2} = \left((1 - B_3) * (1 - la_2)\right) * k_4 * C4} \quad \textbf{(41)}$$

$$\boldsymbol{C5_{co2} = (1 - la_3) * k_5 * C5} \quad \textbf{(42)}$$

$$\boldsymbol{C8_{co2} = k_8 * C8} \quad \textbf{(43)}$$

$$\boldsymbol{C9_{co2} = k_9 * C9} \quad \textbf{(44)}$$

$$\boldsymbol{C10_{co2} = (1 - la_3) * k_3 * C10} \quad \textbf{(45)}$$

Where all parameters are defined in Table 2 in the main manuscript and earlier in this section. While the maximum decay rates (k_x) for most pools are fixed constants, Campbell *et al.* (2016) suggested that k_3 ~~and k_5 were~~is best estimated in relation to the maximum decay rate of the microbially-accessible litter (C2) pool (k_2).

$$\boldsymbol{{}_{\cancel{L}}{}_{j}k_3 = k_2 * \left(\frac{0.2}{1 + \frac{200}{e^{8.15 * {}_{\cancel{L}}{}_{j}LCI_{lit}}}}\right)} \quad \textbf{(46)}$$

$$\boldsymbol{k_8 = \frac{\left(\left((0.000099) * \left(\frac{1}{100}\right)\right) + \left((0.000855) * \left(\frac{1}{42}\right)\right) + \left((0.001796) * \left(\frac{1}{13}\right)\right)\right)}{sum\left(\left(\frac{1}{100}\right), \left(\frac{1}{42}\right), \left(\frac{1}{13}\right)\right)}} \quad \textbf{(47)}$$

Note that when k_2 is a fixed value, k_3 only fluctuates with changes in the LCI of the litter layer. ~~At present, CO_2 emitted from soil DOM (determined by the maximum decay rate, k_8) is associated with the values presented in Kalbitz *et al.* (2005).~~ Also note that because the maximum decay rate of acid-insoluble litter (k_3) is determined relative to the LCI of all litter pools ~~in a given layer (L)~~ on a given day (j) the parameter itself can~~is~~ also be layer- and time-specific. At present, CO_2 emitted from soil DOM (determined by the maximum decay rate, k_8) is associated with the values presented in Kalbitz *et al.* (2005).

$$k_8 = \frac{\left(\left((0.000099)*\left(\frac{1}{100}\right)\right)+\left((0.000855)*\left(\frac{1}{42}\right)\right)+\left((0.001796)*\left(\frac{1}{13}\right)\right)\right)}{sum\left(\left(\frac{1}{100}\right),\left(\frac{1}{42}\right),\left(\frac{1}{13}\right)\right)} \quad (47)$$

Decay rate modifiers

Soil temperature is simulated to have a polynomial relationship with decomposition, modifying each pool's decay rate according to the mean soil temperature of that layer on that day. The rationale behind this is to attempt to capture microbial processes and equate with realistic changes in enzymatic activity to be consistent with Michaelis-Menten kinetics. This follows the same function that is used by the STANDCARB 2.0 model (Harmon and Domingo, 2001) and produces a multiplier based on provided coefficients of optimum decomposition temperature (T_{opt}), the rate at which the decomposition rate increases with a 10 °C increase (T_{Q10}), the reference temperature at which that Q_{10} value was derived (T_{ref}), the shape of the excessive temperature limitation (T_{shp}) and the difference between optimum temperature and the decline above that threshold (T_{lag}).

$$~~{}^{L}_{j}~~T_{mod} = e^{\left(-\left(\frac{~~{}^{L}_{j}~~soilT}{T_{opt}+T_{lag}}\right)\right)^{T_{shp}}} * T_{Q10}^{\frac{~~{}^{L}_{j}~~soilT-T_{ref}}{T_{ref}}} \quad (48)$$

Where ~~${}^{L}_{j}$~~T_{mod} is the temperature multiplier applied to decomposition of pools ~~in layer L~~ on day j, given the soil temperature ~~of that layer~~ on that day (~~${}^{L}_{j}$~~$soilT$). An initial MEMS v1.0 evaluation (prior to use with the LUCAS sites reported in the main manuscript), indicated the model consistently overestimated decomposition due to the temperature modifier effect. Consequently, the coefficients reported in Harmon and Domingo (2001) were revised down from those reported in Table 2 of the main manuscript (T_{opt} reduced to 35 °C, T_{shp} reduced to 3, T_{lag} increased to 7 °C and T_{Q10} increased to 3). In MEMS v1.0 this single function is used for all pools and over the single soil layer, however, it is also sufficiently generalizable to represent varying temperature sensitivities of the different pools (i.e., through the T_{Q10} coefficient) and of different layers. In which case, the temperature modifier would be specific to pool x ~~of layer L~~ on day j – e.g. ~~${}^{L}_{j}$~~T^{x}_{mod}. Furthermore, in future versions of the MEMS model, we expect more explicit and complex relationships to temperature and moisture.

DOM transfer through soil layers

MEMS v1.0 does not have an explicit hydrological model, however this is likely needed for MEMS outputs to be reliably compared with empirical data at most sites (soil moisture often has a considerable influence on SOM formation and decomposition rates). Consequently, this is one of the first developments intended for MEMS. As a placeholder, leaching is assumed to be a unidirectional process with DOM lost to deeper soil layers (in the single-layer version) at a given maximum rate. This follows a first order rate of loss and simply assumes half the highest literature value found when performing a search of relevant studies.

Driving variables and initializing MEMS v1.0

Site inputs and interpolating daily values from annual measurements

Driving variables of MEMS v1.0 can be either provided manually if they are known, or interpolated/estimated using basic site information. The format of this input information is typically in comma separated values (CSV) or any other ASCII text format and in R (R Core Team, 2018) is stored as a dataframe. As a single-layer, carbon model that only simulates litter and soil components of a site, MEMS v1.0 includes only a few *essential* driving variables. These fall into three major categories (climatic, edaphic and land use). For convenience, a summary of these essential inputs is provided in Table 3 of the main manuscript. The model operates on the assumption that a user must have measurements of soil pH, soil bulk density, annual NPP, sand content and rock fraction in order to simulate the site. Additionally, if daily temperature data are not known, the maximum, minimum and mean annual temperature can be used to interpolate daily values.

At the time of writing, daily soil temperature is the only climatic variable simulated in MEMS v1.0. The model can either be initialized using real, site-specific temperature data (if available), or daily values can be roughly estimated using a simple sine function related to the mean annual temperature (MAT) of the site (Eq. 49). This sine function provides 365 days of temperature values that are normally distributed around the MAT (therefore ensuring that the average from these daily values will also equal the MAT provided), with the peak of this sine on Julian day 182 (July 1st). This assumes the site is in the northern hemisphere but simulating a site in the southern hemisphere simply requires changing the sign of the 1.5 coefficient in Equation 49 below.

$$~^{L}_{j}soilT = \frac{T_{range}}{2} * sin\left((2 * PIseq) - 1.5\right) + MAT \quad (49)$$

Where $~^{L}_{j}soilT$ is the soil temperature in degrees Celsius ~~for soil layer L~~ on day j, T_{range} is the difference between the maximum daily soil temperature and minimum daily soil temperature measured over a year in degrees Celsius, PIseq is a sequence of 365 values evenly distributed from 0 to pi (≈ 3.14159), and MAT is the mean annual temperature in degrees Celsius of the site in question. While this approximation provides more realistic inputs than a constant temperature for each day, where possible, real, measured values should be imported separately as a list of average daily soil temperature values.

It should be noted that this sine function (with an intra-annual variation of T_{range} degrees Celsius) may not work well for sites near the equator where reduced seasonal dynamics mean that a smoothed sine curve does not represent reality. The T_{range} coefficient in Equation 49 is ideally calculated from estimates/measurements of a site's maximum and minimum soil temperatures of an average year, included alongside the MAT as inputs. However, these are optional and instead, a constant T_{range} value (i.e., the same range at all sites simulated) can be set as a global parameter as shown in Table 2 in the main manuscript. This should be chosen carefully by the model user to best represent their site(s). It should also be noted that when simulating deeper soil layers they are also less likely to see large fluctuations in soil temperature and this should be considered when the user initializes multi-layer versions of the MEMS model.

Land use and management conditions

As with the sine function estimate soil temperature, the daily carbon inputs ($_jCT^i$) can also be estimated crudely according to a simplistic relationship with annual net primary productivity (NPP) – Equation 50).

$$_{\boldsymbol{j}}\boldsymbol{CT^i} = \boldsymbol{dnorm(seqDAY, peakDAY, sdNPP)} * \boldsymbol{annNPP} \quad \textbf{(50)}$$

Where $_jCT^i$ are the daily total carbon inputs from material *i* on day *j*, $seqDAY$ is a list of 365 integers that represent each day of the year, $peakDAY$ is a parameter value to specify the julian day of year when inputs peak (around which a normal distribution is generated) and $sdNPP$ is the 'width' of the distribution around the peak value. The $annNPP$ value is the site-specific annual NPP value in gC m^{-2} yr^{-1}. The $sdNPP$ parameter (specified as a global parameter) can be modified to represent different intra-annual distributions of the total carbon inputs. Specifically, this can change how 'quickly' the inputs are added to the soil (is the whole carbon input added within a few days or is it spread out over months?). For different land uses, $sdNPP$ may change according to the trends in plant growth at a given site. However, when simulating an equilibrium scenario where steady-state inputs are assumed, this has little or no effect over long simulations (i.e., 500+ years).

In most systems the total annual NPP is not directly equivalent to the total carbon inputs to the topsoil layer. Consequently, MEMS v1.0 reduces the annual amount based on how much of the total can be realistically expected to be input to the specific layer given that site's land use. For example, Bolinder *et al*. (2007) suggest that, in arable sites where all residues are returned to soil, the proportion of annual NPP that is input to all soil varies between 55% and 78%. Whereas when all residues are removed, the proportion input can be as little as 21%. Furthermore, not all of this will be input to the topsoil layer simulated by MEMS v1.0. Consequently, before the daily inputs are interpolated from an annual value using Equation 50, the total is reduced based on best estimates for the land use and management routines of the site simulated.

$$_{\boldsymbol{j}}\boldsymbol{aCT^i} = {}_{\boldsymbol{j}}\boldsymbol{CT^i} * \left(\frac{\mathbf{1}}{\boldsymbol{RtoS^i}+\mathbf{1}}\right) * (\mathbf{1} - {}_{\boldsymbol{j}}\boldsymbol{aHARV^i}) \quad (51)$$

$$_{\boldsymbol{j}}\boldsymbol{bCT^i} = {}_{\boldsymbol{j}}\boldsymbol{CT^i} * \left(\frac{\boldsymbol{RtoS^i}}{\boldsymbol{RtoS^i}+\mathbf{1}}\right) * (\mathbf{1} - {}^{\boldsymbol{L}}_{\boldsymbol{j}}\boldsymbol{bHARV^i}) \quad (52)$$

Where ${}_jaCT^i$ and ${}_jbCT^i$ are the aboveground and belowground carbon inputs of material *i* on day *j*. The aboveground and belowground split is achieved by use of a land-use specific root to shoot ratio of material *i* ($RtoS^i$) which are then reduced by fixed fractions (i.e., 0-1) to represent any losses through harvesting. Another parameter to describe natural losses due to weather (e.g., high winds) is also possible and resides as a placeholder in the general crop parameters file of MEMS v1.0. After the realistic aboveground fraction of NPP is derived, it can then replace the ${}_jCT^i$ term in Equation 50 and be used to interpolate daily inputs. However, the belowground fractions of NPP also includes inputs that are likely allocated to deeper soil layers than the topsoil simulated by MEMS v1.0. Consequently, the ${}_jbCT^i$ as calculated in Equation 52 is reduced by use of a Michaelis-Menten style function (see Kätterer *et al.*, 2011) to proportion roots to the simulated soil layer.

$$ {}^{L}_{j}\boldsymbol{bCT^i} = {}_{j}\boldsymbol{bCT^i} * \left(\frac{{}^{L}\boldsymbol{depth}*(\boldsymbol{Rdep_{50}}+\boldsymbol{Rdep_{max}})}{\boldsymbol{Rdep_{max}}*(\boldsymbol{Rdep_{50}}+{}^{L}\boldsymbol{depth})}\right) \quad (53) $$

Where ${}^{L}_{j}bCT^i$ is the belowground carbon input of material *i* ~~to soil layer *L*~~ on day *j*, ${}^{L}depth$ is the depth of the soil ~~layer *L*~~ in centimetres, $Rdep_{50}$ is the soil depth from the surface at which 50 % of the root biomass is proportioned in centimeters, and $Rdep_{max}$ is the maximum rooting depth in centimeters. These last two parameters are site specific but can be generalized according to different land-uses, reducing the number of inputs required by the model user. For information regarding these generalized parameters, see Canadell *et al.* (1996) and Jackson *et al.* (1996). For an example implementation of Equation 53 for the purpose of simulating SOM dynamics, see Poeplau (2016).

As with the interpolation of daily soil temperature from MAT, estimating daily values of carbon input are less precise than using real measured data. When possible, empirical data should be preferred and can be input along with daily climate data.

Supplementary Figures

(see attached files for high-resolution versions)

Figure S1 – Site information of all 8192 forest and grassland sites of the LUCAS dataset (Toth *et al*., 2013) used for validation of the MEMS v1.0 soil organic matter model. Different shapes represent different land use classes and all are overlaid over each other (grass = circles, n = 3487; broadleaved forests = triangle, n = 1590; mixed forest = crosses, n = 1402; coniferous forest = squares, n = 1713).

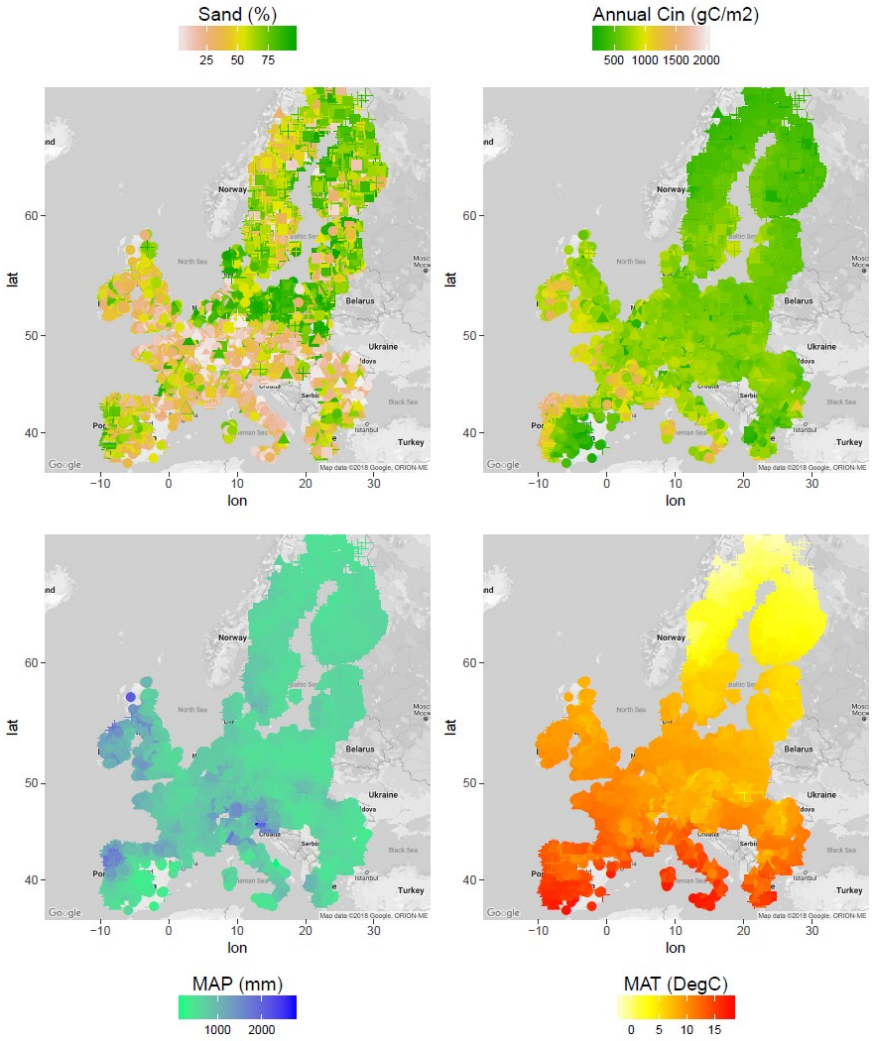

Figure S2 - Geographical distribution of 154 grassland and forest sites chosen for fractionation (a representative subsample of the total LUCAS database, see Toth *et al*., 2013). Reported mean annual temperature, mean annual precipitation and sand content are indicated for each site along with Net Primary Productivity (NPP) in 2009 derived from MODIS. Symbols indicate the land

use division within grassland and forest. Cin is the C input, MAP is the mean annual precipitation and MAT is the mean annual temperature.

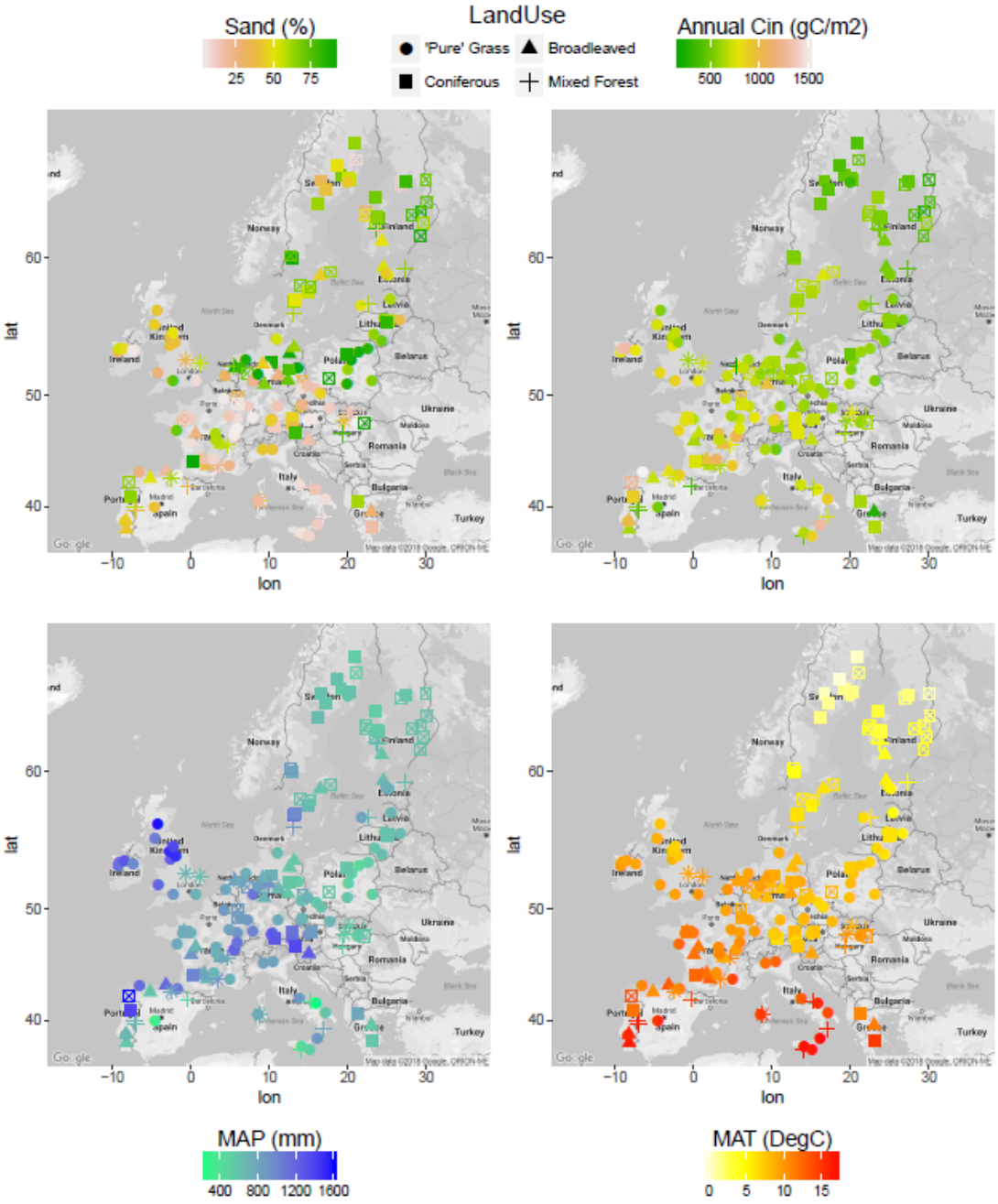

Figure S3 - Summary statistics of the site information and soil C stocks for four land use classes (Grassland, n=78; Broadleaved forest, n=25; Coniferous forest, n=27; Mixed forest, n=24) across Europe. Boxplots indicate the median, first and third quartiles with the box and maximum and minimum at the extent of the whiskers. Outliers beyond the 95% are shown by individual points. MAT = Mean Annual Temperature; MAP = Mean Annual Precipitation; NPP = Net Primary Productivity; SOC = Soil Organic Carbon; POM = Particulate Organic Matter; MAOM = Mineral-Associated Organic Matter.

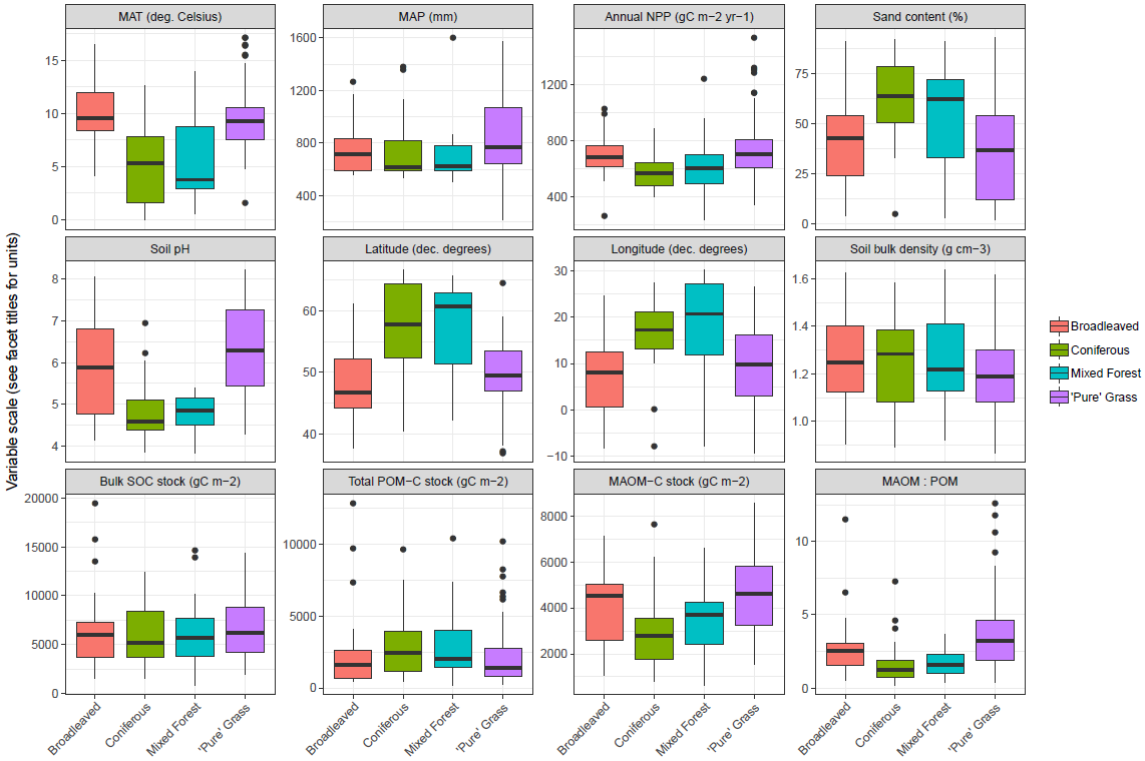

Figure S4 - One-way ANOVA results with pairwise comparisons for each measured fractionation data (bulk soil C stock, mineral-associated organic matter (MAOM) C stock, particulate organic matter (POM) C stock, and the MAOM:POM ratio) between the four land use classes (Grassland, n=78; Broadleaved forest, n=25; Coniferous forest, n=27; Mixed forest, n=24) of topsoils (0-20 cm) from 154 sites across Europe.

Significant differences indicated by p-values for each pair ($p < 0.001$, red; $p < 0.01$, orange; $p < 0.05$, yellow; $p < 0.1$, green; $p > 0.1$, blue). NPP = Net Primary Productivity.

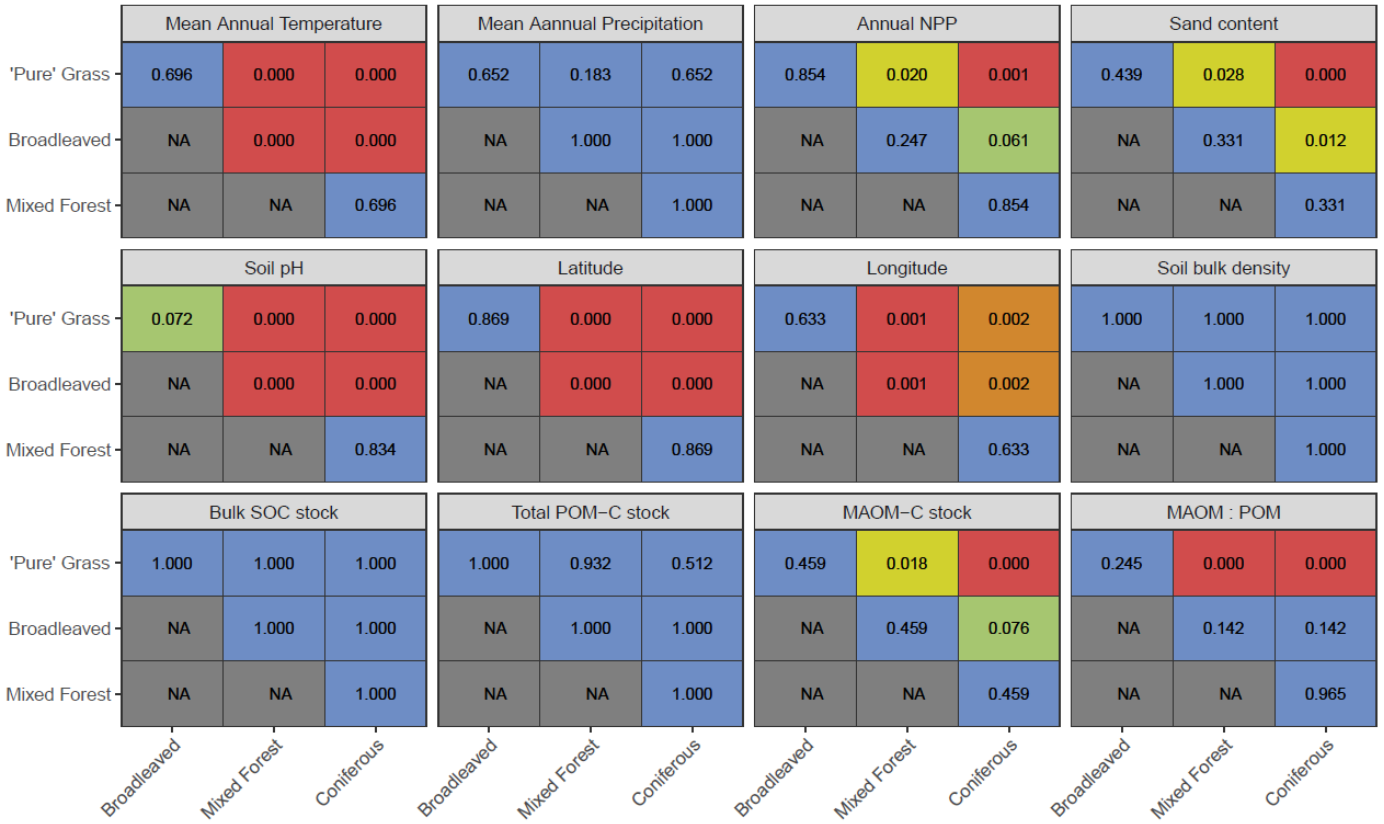

Figure S5 – Fully-colourised version of main text Figure 2. Global sensitivity analysis results showing the relative contribution of each parameter to a change in carbon stock of each pool in MEMS v1.0 (leached carbon to deeper soil layers [pool C11] is omitted for clarity). Details of each parameter and the abbreviations used can be found in Table 2. The sensitivity analysis was repeated annually for simulation times between 1 and 100 years, every 10 years after that to 400-year simulations and every 100 years after that up to a 1000-year simulation. Results are presented on a log scale in years. Parameters involved in different SOM formation processes are grouped by colour: yellows – parameters that define DOM

leaching from the organic horizon to the soil layer; reds – parameters that affect microbial carbon use efficiency, purples – parameters that affect organic matter vertical transport to deeper layers, greens – maximum decay rates.

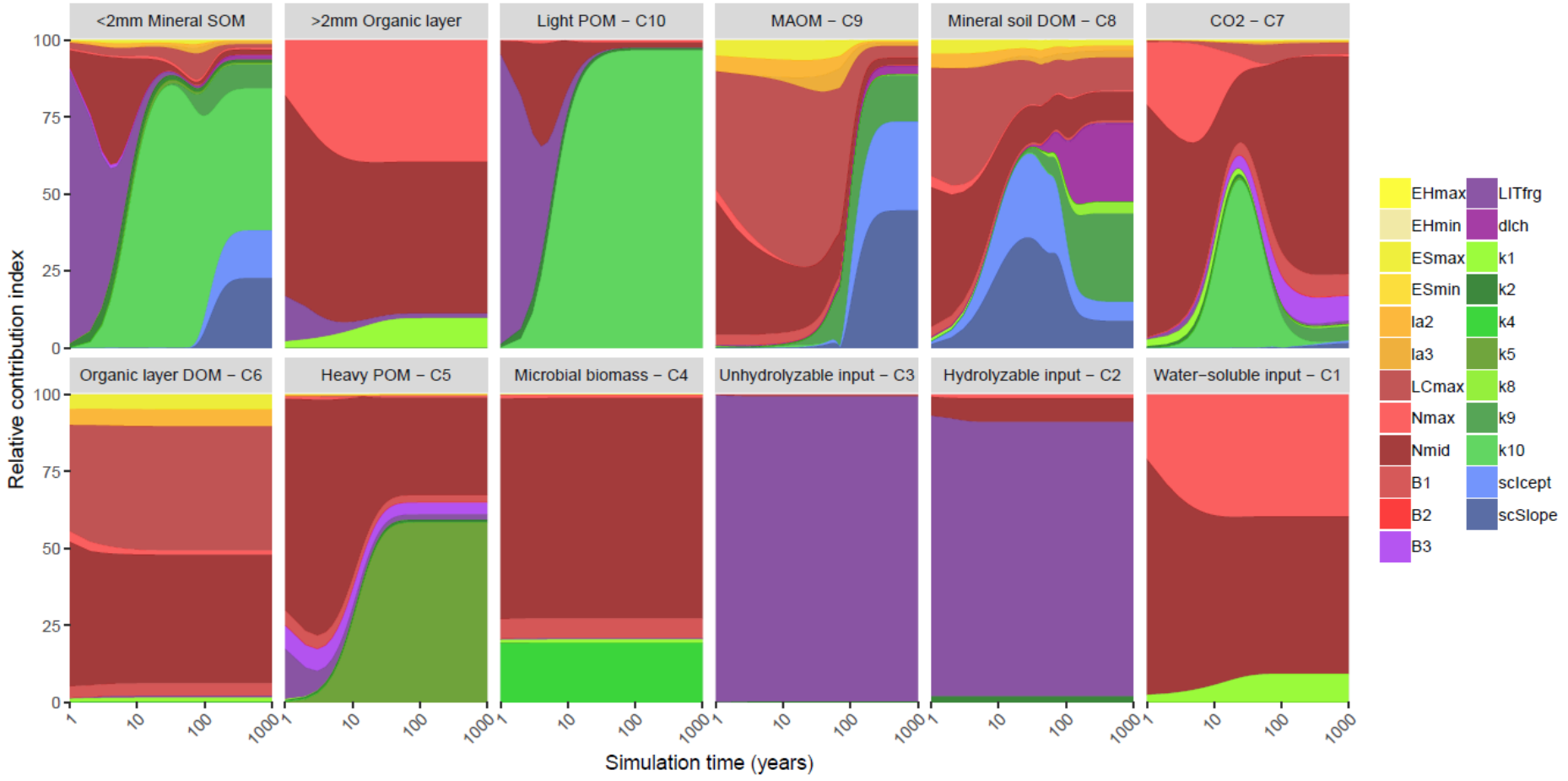

Figure S6 – Variability in model-data residuals compared with mean annual temperature for 8192 forest and grassland sites of the LUCAS dataset (Toth *et al*., 2013) simulated with the MEMS v1.0 soil organic matter model. Residuals indicate the modelled minus measured total topsoil (0-20 cm) organic carbon stock in MgC ha^{-1} for each of four land-use classes (Grassland, red; Broadleaved forest, blue; Coniferous forest, purple; Mixed forest, green). Sites are divided into high and low groups of mean annual precipitation, MAP (top *vs* bottom panels), soil texture (left *vs* right panels) and annual carbon inputs (provided by net primary productivity, NPP) (alternating panels left to right).

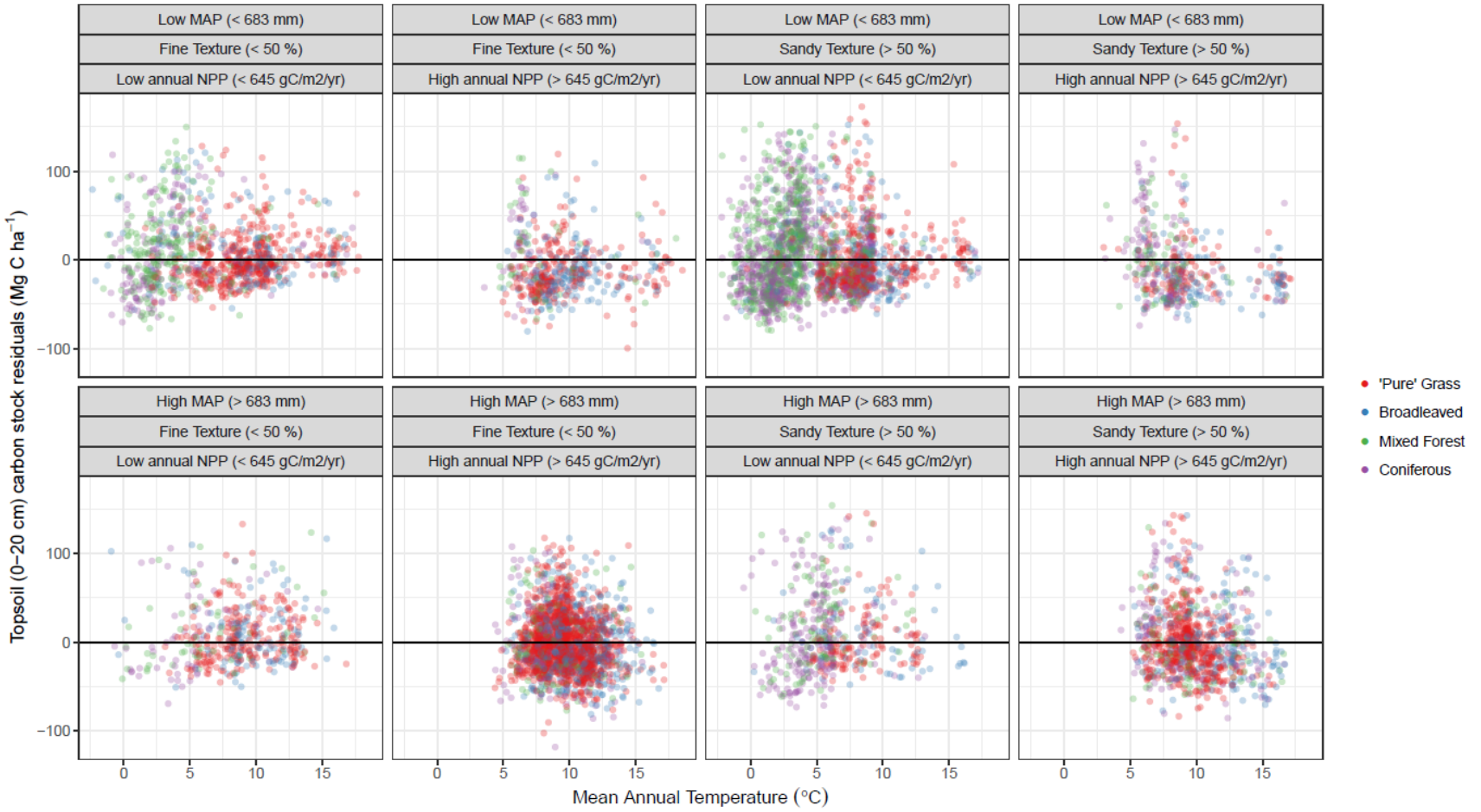

Figure S75 - Modifiers for microbial carbon use efficiency and rates of water-soluble and acid-soluble litter fractions decay by lignocellulosic index (A and B) and initial litter percent nitrogen (C). Reproduced with permission from Campbell *et al*., 2016.

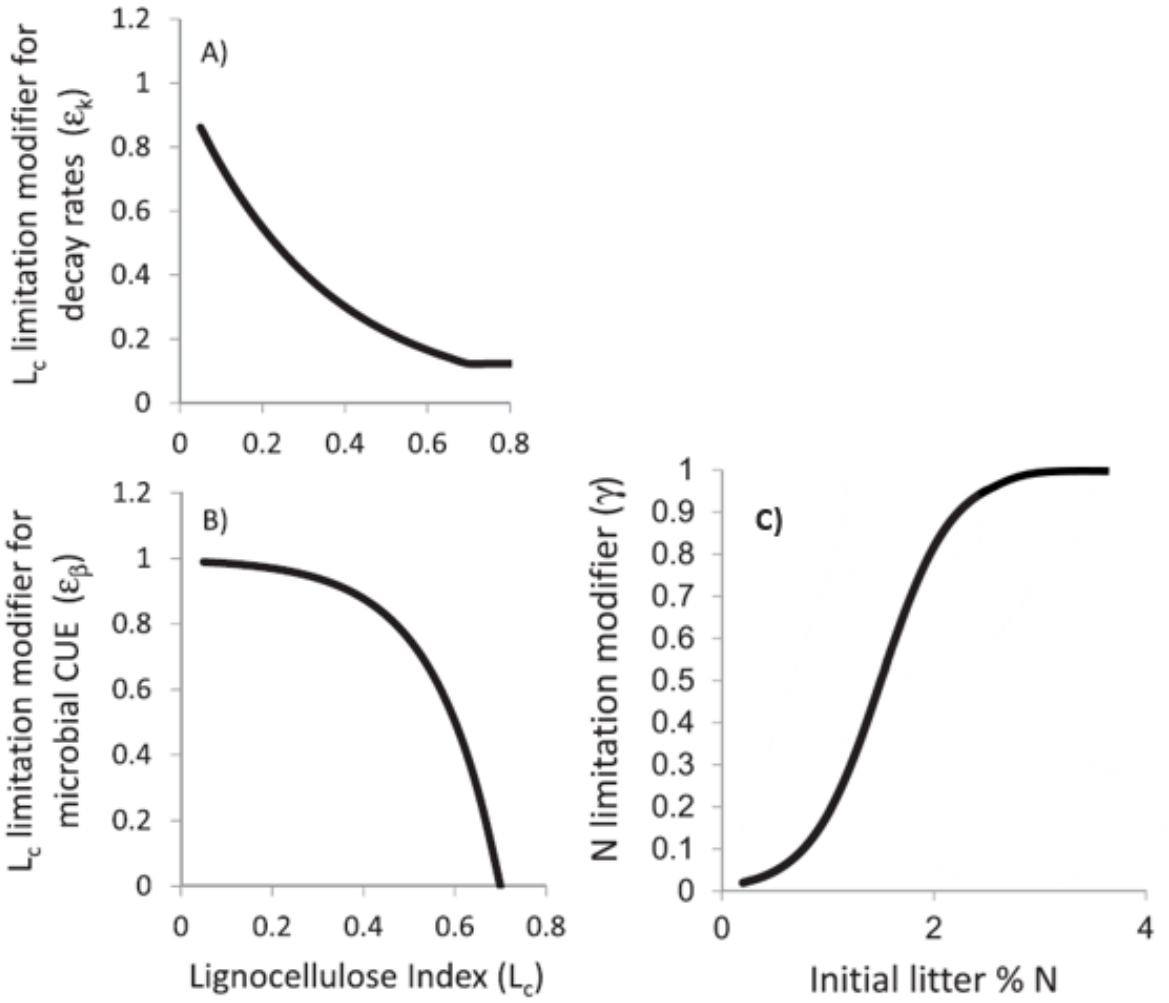

Supplementary Tables

Table S1 - Fractionation scheme to measure each OM pool of MEMS v1.0. Physical particle size is given sequentially from top to bottom (i.e. C9 pools are between 0.45 µm and 53 µm in size). Soil particles (< 2mm) are primary particles obtained after soil aggregates dispersion. All SOM fractions can be separated sequentially on one soil sample by first isolating the DOM through centrifugation, separating the solid subnatant into a light POM and a heavy fraction by density (at 1.8 g/cm^3) and the latter into a heavy POM and a MAOM by wet sieving (at 53µm). NDF – Neutral detergent fibre; ADF – Acid detergent fibre; HWE – Hot-water extractable.

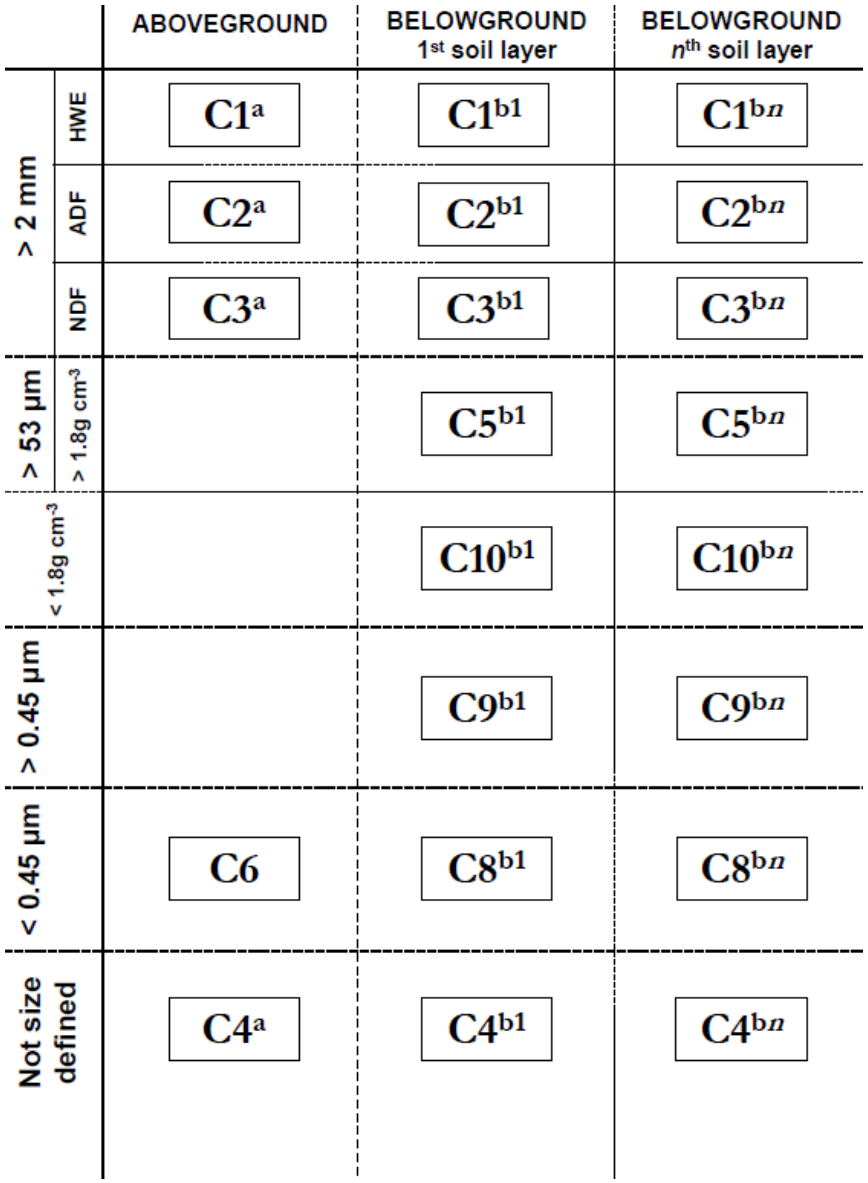

Table S2 - Optimized parameter values for the mid-point of the nitrogen modifier (*Nmid*), maximum decay rate for coarse, heavy particulate organic matter (*k5*), maximum decay rate for mineral-associated organic matter (*k9*) and maximum decay rate for light particulate organic matter (*k10*). Depending on what fraction was match (measured-modelled comparisons), different parameter values were derived. Root mean square error (RMSE) was minimised for each unique parameter set and assessed for each fraction (Mineral-Associated Organic Matter, MAOM; total Particulate Organic Matter, POM; bulk soil Soil Organic Carbon, SOC). Note that total POM refers to the composite of light and heavy POM measurements and the sum of the C5 and C10 pools). Analysis was performed on 154 forest and grassland sites from the LUCAS database – see Figure S2 and Figure S3 for more information.

Parameter	**Default (Initial optimized range)**	**Optimized for POM**	**Optimized for MAOM**	**Optimized for total SOC**
Nmid	1.750 (0.875 – 2.625)	1.617~~03~~	0.923~~12~~	2.45~~48~~~~0~~
k5	5.00^{-4} (6.0^{-5} – 1.0^{-3})	5.~~7~~66~~1~~$^{-4}$	2.37~~6~~$^{-4}$	2.51~~3~~$^{-4}$
k9	2.19^{-5} (1.0^{-5} – 4.0^{-5})	2.33~~7~~$^{-5}$	2.98~~7~~$^{-5}$	3.97^{-5}
k10	2.96^{-4} (1.0^{-4} – 1.0^{-3})	4.31~~0~~$^{-4}$	2.94~~3~~$^{-4}$	3.01~~2~~$^{-4}$
RMSE between measured and modelled C stocks for 154 sites (Mg C ha^{-1})				
Total SOC	35.5	35.9~~7~~	35.2~~1~~	33.5~~7~~
POM-C	23.4	23.5~~4~~	23.1	25.5~~3~~
MAOM-C	17.9	17.8~~7~~	17.5	20.2

Supplementary References

Abramoff, R., Xu, X., Hartman, M., O'Brien, S., Feng, W., Davidson, E., Finzi, A., Moorhead, D., Schimel, J., Torn, M. & Mayes, M. A. (2018). The Millennial model: in search of measurable pools and transformations for modeling soil carbon in the new century. *Biogeochemistry*, 137(1-2), 51-71.

Bolinder, M. A., Janzen, H. H., Gregorich, E. G., Angers, D. A., & VandenBygaart, A. J. (2007). An approach for estimating net primary productivity and annual carbon inputs to soil for common agricultural crops in Canada. *Agriculture, Ecosystems & Environment*, *118*(1-4), 29-42.

Braakhekke, M. C., Beer, C., Hoosbeek, M. R., Reichstein, M., Kruijt, B., Schrumpf, M., & Kabat, P. (2011). SOMPROF: A vertically explicit soil organic matter model. *Ecological modelling,* 222(10), 1712-1730.

Campbell, E. E., Parton, W. J., Soong, J. L., Paustian, K., Hobbs, N. T., & Cotrufo, M. F. (2016). Using litter chemistry controls on microbial processes to partition litter carbon fluxes with the litter decomposition and leaching (LIDEL) model. *Soil Biology and Biochemistry*, 100, 160-174.

Canadell, J., Jackson, R. B., Ehleringer, J. B., Mooney, H. A., Sala, O. E., & Schulze, E. D. (1996). Maximum rooting depth of vegetation types at the global scale. *Oecologia*, 108(4), 583-595.

Harmon, M., and J. Domingo (2001), A User's Guide to STANDCARB Version 2.0: A Model to Simulate the Carbon Stores in Forest Stands, Dep. of For. Sci., Oreg. State Univ., Corvallis.

Jackson, R. B., Canadell, J., Ehleringer, J. R., Mooney, H. A., Sala, O. E., & Schulze, E. D. (1996). A global analysis of root distributions for terrestrial biomes. *Oecologia*, 108(3), 389-411.

Kalbitz, K., Schwesig, D., Rethemeyer, J., & Matzner, E. (2005). Stabilization of dissolved organic matter by sorption to the mineral soil. *Soil Biology and Biochemistry*, 37(7), 1319-1331.

Kätterer, T., Bolinder, M. A., Andrén, O., Kirchmann, H., Menichetti, L. (2011) Roots contribute more to refractory soil organic matter than aboveground crop residues, as revealed by a long-term field experiment. *Agriculture Ecosystems and Environment*, 141(1-2), 184–192.

Keiluweit, M., Bougoure, J. J., Nico, P. S., Pett-Ridge, J., Weber, P. K., & Kleber, M. (2015). Mineral protection of soil carbon counteracted by root exudates. *Nature Climate Change*, *5*(6), 588.

Kothawala, D. N., Moore, T. R., & Hendershot, W. H. (2008). Adsorption of dissolved organic carbon to mineral soils: A comparison of four isotherm approaches. *Geoderma*, 148(1), 43-50.

Ludwig, M., Achtenhagen, J., Miltner, A., Eckhardt, K. U., Leinweber, P., Emmerling, C., & Thiele-Bruhn, S. (2015). Microbial contribution to SOM quantity and quality in density fractions of temperate arable soils. *Soil Biology and Biochemistry*, *81*, 311-322.

Mayes, M. A., Heal, K. R., Brandt, C. C., Phillips, J. R., & Jardine, P. M. (2012). Relation between soil order and sorption of dissolved organic carbon in temperate subsoils. *Soil Science Society of America Journal*, 76(3), 1027-1037.

Moorhead, D. L., Lashermes, G., Sinsabaugh, R. L., & Weintraub, M. N. (2013). Calculating co-metabolic costs of lignin decay and their impacts on carbon use efficiency. *Soil Biology and Biochemistry*, 66, 17-19.

Poeplau, C. (2016). Estimating root: shoot ratio and soil carbon inputs in temperate grasslands with the RothC model. *Plant and soil*, 407(1-2), 293-305.

R Core Team (2018). R: A language and environment for statistical computing. R Foundation for Statistical Computing, Vienna, Austria. URL https://www.R-project.org/.

Sinsabaugh, R. L., Manzoni, S., Moorhead, D. L., & Richter, A. (2013). Carbon use efficiency of microbial communities: stoichiometry, methodology and modelling. *Ecology letters*, 16(7), 930-939.

Six, J., Conant, R. T., Paul, E. A., & Paustian, K. (2002). Stabilization mechanisms of soil organic matter: implications for C-saturation of soils. *Plant and soil*, 241(2), 155-176.

Sokol, N. W., Sanderman, J., & Bradford, M. A. (2018). Pathways of mineral-associated soil organic matter formation: Integrating the role of plant carbon source, chemistry, and point of entry. *Global change biology*. https://doi.org/10.1111/gcb.14482

Soong, J. L., Parton, W. J., Calderon, F., Campbell, E. E., & Cotrufo, M. F. (2015). A new conceptual model on the fate and controls of fresh and pyrolized plant litter decomposition. *Biogeochemistry*, 124(1-3), 27-44.

Toth G., Jones A., Montanarella L. (2013) LUCAS Topsoil Survey — methodology, data and results. In: JRC Technical Reports. European Union, Luxemburg.